WELL TEST ANALYSIS IN THE PRESENCE OF CARBON DIOXIDE IN FRACTURED RESERVOIRS

A THESIS SUBMITTED TO
THE GRADUATE SCHOOL OF NATURAL AND APPLIED SCIENCES
OF
MIDDLE EAST TECHNICAL UNIVERSITY

BY

TUĞÇE BAYRAM

IN PARTIAL FULFILLMENT OF THE REQUIREMENTS
FOR
THE DEGREE MASTER OF SCIENCE
IN
PETROLEUM AND NATURAL GAS ENGINEERING

MAY 2011

Approval of the thesis:

WELL TEST ANALYSIS IN THE PRESENCE OF CARBONDIOXIDE IN FRACTURED RESERVOIRS

submitted by **TUĞÇE BAYRAM** in partial fulfillment of the requirements for the degree of **Master of Science in Petroleum and Natural Gas Engineering Department, Middle East Technical University** by,

Prof. Dr. Canan Özgen _____
Dean, Graduate School of **Natural and Applied Sciences**

Prof. Dr. Mahmut Parlaktuna _____
Head of Department, **Petroleum and Natural Gas Engineering**

Prof. Dr. Serhat Akın _____
Supervisor, **Petroleum and Natural Gas Engineering Dept., METU**

Examining Committee Members

Prof. Dr. Mahmut Parlaktuna _____
Petroleum and Natural Gas Engineering Dept., METU

Prof. Dr. Serhat Akın _____
Petroleum and Natural Gas Engineering Dept., METU

Prof. Dr. Mustafa Verşan Kök _____
Petroleum and Natural Gas Engineering Dept., METU

Mustafa Yılmaz, MSc. _____
TPAO, ANKARA

Ülker Kalfa, MSc., _____
TPAO, ANKARA

Date: 16/05/2011

I hereby declare that all information in this document has been obtained and presented in accordance with academic rules and ethical conduct. I also declare that, as required by these rules and conduct, I have fully cited and referenced all material and results that are not original to this work.

Name, Last name : Tuğçe BAYRAM

Signature :

ABSTRACT

WELL TEST ANALYSIS IN THE PRESENCE OF CARBON DIOXIDE IN FRACTURED RESERVOIRS

Bayram, Tuğçe

M.Sc., Department of Petroleum and Natural Gas Engineering

Supervisor: Prof. Dr. Serhat Akın

May 2011, 137 pages

The application of carbon-dioxide injection for enhanced oil recovery and/or sequestration purposes has gained impetus in the last decade. It is known that well test analysis plays a crucial role on getting information about reservoir properties, boundary conditions, etc. Although there are some studies related to the well test analysis in the fractured reservoirs, most of them are not focused on the carbon dioxide injection into the reservoir.

Naturally fractured reservoirs (NFR) represent an important percentage of the worldwide hydrocarbon reserves and current production. Reservoir simulation is a fundamental technique in characterizing this type of reservoirs. Fracture

properties are often not clear due to difficulty to characterize the fracture systems.

On the other hand, well test analysis is a well known and widely applied reservoir characterization technique. Well testing in NFR provides two significant characteristic parameters, storativity ratio (ω) and interporosity flow coefficient (λ). The storativity ratio is related to fracture porosity. The interporosity flow coefficient can be linked to the shape factor which is a function of fracture spacing.

In this study, the effects of fracture and fluid flow factors (geometry, orientation and flow properties) on pressure and pressure derivative behavior are studied by applying a reservoir simulation model. Model is utilized mainly for the observation of multiphase flow effects in CO_2 flooded fractured reservoirs. Several runs are conducted for various ranges of the aforementioned properties in the CO_2 flooded reservoir. Results of well test analysis are compared to the input data of simulation models on a parameter basis.

Keywords: well test analysis, fractured reservoirs, carbon dioxide injection, carbonate reservoirs.

ÖZ

ÇATLAKLI REZERVUARLARDA KARBONDİOKSİT VARLIĞINDA KUYU TESTİ ANALİZLERİ

Bayram,Tuğçe

Yüksek Lisans, Petrol ve Doğal Gaz Mühendisliği Bölümü

Tez Yöneticisi: Prof. Dr. Serhat Akın

Mayıs 2011, 137 sayfa

Son yıllarda, karbondioksit enjeksiyon uygulaması geliştirilmiş petrol kazanımı ve/veya depolama açısından ivme kazanmıştır. Bilindiği üzere, kuyu testi analizleri rezervuar özellikleri ve sınır koşulları hakkında bilgi edinmekte ciddi rol oynar. Çatlaklı rezervuarlarda kuyu testi analiziyle ilgili çeşitli çalışmalar var olsa da, bu çalışmaların birçoğu rezervuara karbon dioksit enjeksiyonu üzerine yoğunlaşmamıştır.

Doğal çatlaklı rezervuarlar hidrokarbon rezervlerinin ve bugünkü üretiminin önemli bir yüzdesini temsil eder. Rezervuar simülasyonları, bu tip rezervuarları tanımlayabilen temel bir yöntemdir. Çatlak sistemlerinin tanımlaması zor oluğundan dolayı çoğu zaman çatlaklara ait özellikler net değillerdir.

Öte yandan, kuyu testi analizleri bilindik ve sıkça uygulanan rezervuar tanımlama tekniğidir. Doğal çatlaklı rezervuarlarda kuyu testi analizi iki önemli tanımlama parametresine ulaşılmasını sağlar; depolama katsayı oranı ve interporozite akış katsayısı. Depolama katsayı oranı (ω) çatlak gözenekliliğiyle ilgilidir. Interporozite akış katsayısı (λ) çatlak aralığının bir fonksiyonu olan şekil faktörüne bağlıdır.

Bu çalışmada, çatlak ve akışkan akım faktörlerinin (geometri, oryantasyon, akım özellikleri) basınç ve basıncın türevi üzerindeki etkileri bir rezervuar simülasyon modeli aracılığıyla incelenmiştir. CO_2 enjeksiyonu yapılmış rezervuarlarda, yukarıda bahsedilen özellikler farklı değer aralıklarında değiştirilerek çeşitli simülasyonlar yürütülmüştür. Kuyu testi analizi sonuçları simulasyon programında kullanılan girdilerle karşılaştırılmıştır.

Anahtar Sözcükler: kuyu testi analizleri, çatlaklı rezervuarlar, karbondioksit enjeksiyonu, karbonat rezervuarlar.

To My Family

ACKNOWLEDGMENTS

I wish to express my deepest gratitude to my supervisor Prof. Dr. Serhat Akın for his guidance, advice, criticism and encouragements throughout the research.

I would like to thank to my parents Gülsen and Ali, my sister Meltem for their endless support, trust, love and understanding in every stage of my life, which has been my source of strength and inspiration.

Moreover, I wish to thank to my friends and colleagues especially to Mehmet Cihan ERTÜRK for his patience, suggestions, support and encouragement throughout this study.

My thanks also go to Berkay GÜRBÜZ and S. Aslı GÜNDOĞAR for their moral support, enthusiasm and contribution whenever I need.

Lastly, I want to express my thanks to all Petroleum and Natural Gas Engineering Department coworkers for their kind company during my thesis study period.

TABLE OF CONTENTS

LIST OF FIGURES

FIGURES

LIST OF TABLES

TABLES

NOMENCLATURE

A = Arithmetic average

c = Total system compressibility, 1/psi

e = Fracture width, in, cm

D=Fracture Spacing, cm

dP/dl= pressure gradient in flow direction, atm/cm

G = Geometric average

g=Gravitational constant, m/s^2

H = Harmonic average

k = Permeability, md

L = Fracture spacing, ft

r_i = Radius of investigation, ft

r_w = Wellbore radius, ft

Ø = Porosity

μ = Viscosity, cp

ρ = Fluid density, lbm/ft^3

σ = Shape factor, ft^{-2}

v=Apparent flow velocity, cm/sec

ω = Storativity ratio

λ = Interporosity flow coefficient

rk: rate of reaction k

r_{rk}: constant part of rk

E_{ak}: temperature dependence of rk

R: gas constant

T: temperature

C_i: concentration of component i in void volume

t_D=Dimensionless time

C_D=Dimensionless wellbore storage coefficient

C=Wellbore storage coefficient, cu ft/psi (m^3/kPa)

P_D=Dimensionless pressure

S= Skin factor

Subscripts

e = effective

m = matrix

f = fracture

CHAPTER 1

INTRODUCTION

Naturally fractured reservoirs (NFR) are those reservoirs that contain natural fractures that may or may not have an effect, either positive or negative, on fluid flow. NFR have two different porous media; the matrix, which has high storage but low flow capacity and the fractures which provide high flow path but low storage capacity. A significant percentage of oil and gas reserves are trapped in the fractured carbonate reservoirs. One of the methods of producing the remaining oil from the naturally fractured reservoirs is applying an enhanced oil recovery method. Carbon dioxide flooding is one of the commonly used methods.

A number of authors have developed different models for interpreting the pressure response in fractured reservoirs considering, among others, the characteristics of flow from matrix to fractures, fracture orientation, and block-size distribution. In general, pressure-transient tests in NFR show a behavior consistent with the Warren and Root model.[1] The characteristic behavior of pressure response can be described with two dimensionless parameters, namely storativity ratio (ω) and interporosity flow coefficient (λ).

Standard simulation models for NFR are based on the same principle of two porous media, where the simulation model is divided into two superimposed grids; one grid for matrix and another for fractures. Fluid flow from matrix to fractures is represented by transfer function.

Success of a simulation model in depicting observed behavior and predicting the future performance depends highly on the accuracy of reservoir description. In NFR, knowing how fractures are distributed and interconnected is one of the most important points. Information from different sources is incorporated during the process of understanding the fractured system, but there is no documented evidence that ω and λ, the two parameters obtained from well test in NFR, had been used as input data in building simulation models.

Well test analysis is a well known and widely used reservoir management tool. Besides its usage for short term usage like damage identification, well optimization and stimulation evaluation; well test results are essential for incorporating into other reservoir management process such as numerical simulation.

Effective permeability and average reservoir pressure are two parameters commonly estimated from well test and later incorporated into simulation models as input data. Well test has also been used as a calibration tool in building simulation models by comparing pressure response from the model with actual data.

In NFR, there are two characteristic parameters, ω and λ, which are related to fracture porosity and shape factor, respectively. Fracture porosity and shape factor (expressed in terms of fracture spacing) are required as input data to build dual-porosity simulation models.
In this study, the effects of carbon dioxide flooding in well test analysis in the naturally fractured reservoirs are examined. Two characteristic parameters of

naturally fractured reservoirs are estimated and compared with the actual data.

CHAPTER 2

LITERATURE REVIEW

2.1. USE OF WELL TEST ANALYSIS IN PETROLEUM ENGINEERING

Accurate information about reservoir conditions is significant for many aspects of petroleum engineering calculations. For reservoir performance analysis and future prediction under various operations, reservoir engineers must have adequate information about the in-situ reservoir conditions. Not only reservoir engineers but also the production engineers must have sufficient information about the reservoir to get the best performance from the reservoir. Most of this vital information can be attained from well test. [2]

Since well test analysis play an important role in order to estimate future potentials of wells and characterize the reservoir, most of the wells are subjected to well test analysis from their exploration to abandoned time. By giving transient response due to change in well flow rate, evaluation and enhancing of well performance are carried out.

Satter et al.[2] defined objectives of the well test briefly in three key statements:

1. Know the well.
2. Know the reservoir.

3. Integrate the results of well test interpretation with information obtained from other sources in order to manage well and the reservoir.

To assess the reservoir productivity and reservoir viability, a well test study needs to be conducted in a newly drilled well. For an exploratory well drilled in a newly discovered reservoir, it is vital to decide the viability of the reservoir.

In closely monitor oil and gas fields, well tests are conducted at regular intervals to evaluate the performance of producers and injectors. Since the absolute permeability around the wellbore may change during the production in CO_2 flooded reservoirs, by conducting a well test productivity of the well can be identified; hence a decision to make any correction for the well can be considered such as well stimulation, recompletion, or horizontal drilling for the problematic wells.

For the reservoirs which have relatively low productivity due to low permeability or skin damage wells are stimulated. For the evaluation of the success of the stimulation a well test study is done in order to show the enhancement in the productivity.

Well tests supply information about the reservoir properties such as permeability, transmissibility, and reservoir heterogeneity which gives reservoir characteristics within in the radius of investigation.

A well test which has sufficient length of time can provide the delineation of the reservoir, i.e. reservoir boundary, which leads to calculation of hydrocarbon in place. Moreover geologic boundaries (whether in the form of

facies or faults) and type of the boundary (no flow or constant pressure boundary) can be identified and located.

Estimation of average and/or initial reservoir pressure and subsequent changes in these pressures in several stages of reservoir life can be attained by conducting well tests.

Beside this specific information well test analyses can provide information about interwell characterization, gas well deliverability, and aid to develop reservoir simulation models, and field exploration strategies.

2.2. TYPES OF TRANSIENT WELL TEST

Well tests are dependent on the principle of step change in the well flow rate and the response of the pressure in the reservoir.

2.2.1 PRESSURE BUILD UP TEST

Pressure build up test is the one of the most common methods to test the well. The method begins with producing the well at a constant rate for a sufficient time length. The production stage is followed by shutting the well (usually at the surface), allowing the pressure build up in the wellbore, and recording the pressure (usually at the down hole) in the wellbore as a function of time. The buildup duration changes from the reservoir to reservoir depending on the characteristics and the test aim. From the pressure data one can estimate the formation permeability, reservoir heterogeneity and presence of boundaries, current drainage-area pressure and characterize wellbore damage or stimulation.

A typical pressure build up response is given in the Figure 2.1. The highest pressure build up rate can be observed at the very initial part of the shut in period, and then it decelerates gradually until the stabilization is achieved. Reservoir rock and fluid properties highly influence the pressure response.

One of limitations of the build up test is the cut in the production process and the resulting loss in revenue.

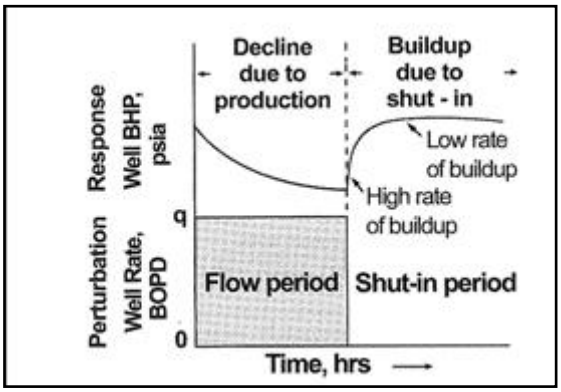

Figure 2- 1- Pressure Build Up Test [2]

2.2.2 DRAWDOWN TEST

Once the static pressure is reached in shut in well, it may be started to produce at a constant rate. As a result of the production period the pressure declines. As shown in the Figure 2.2 in the beginning period of the test the rate of decline is higher than that of the later period of the drawdown.

Drawdown test may have an advantage when compared with build up test such that the production is not impaired for an extended period.

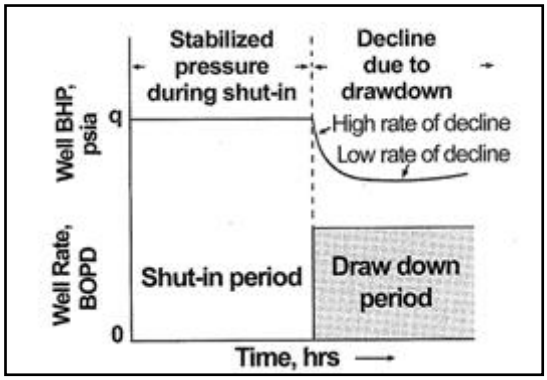

Figure 2- 2– Drawdown Test [2]

2.2.3 FALLOFF TEST

This test is conducted in fluid injection wells which are mostly used for pressure maintenance or enhanced oil recovery purposes. To stabilize the injection pressure, well is injected at constant rate and then it is shut. As a result bottomhole pressure of the well begins to decline, i.e. fall off, as shown in the Figure 2.3. This pressure is recorded as a function of time and analyzed. A falloff test can be used to find the leading edge of the injected fluid bank in water injection wells, as long as test is run for sufficiently long period. It can be understood from the recognizable change in pressure response at the fluid phase boundary between the injected water phase and the in-situ oil phase. The test may provide information about reservoir and completion characteristics such as transmissibility, skin factor, bottomhole injection pressure, reservoir static pressure, and geologic boundaries. [3]

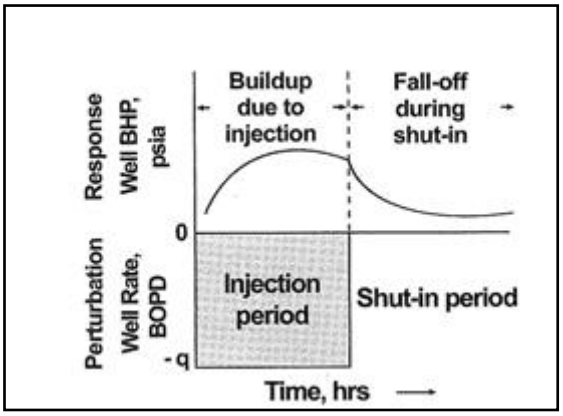

Figure 2- 3- Falloff Test [2]

2.2.4 STEP-RATE TEST

In step-rate test series of injection rates are applied increasingly to an injection well to identify the fracture pressure and fracture gradient of the formation. As different rate applied the injection pressure is recorded. The fracture pressure of the formation is threshold pressure at which subsurface formation is fractured. In artificially fractured wells, the increase in pressure as a result of the increase in injection rate becomes clearly less. In some cases, data observed from step-rate test can be used to get information about some reservoir properties, such as formation skin and transmissibility.

2.2.5 MULTIRATE TEST

Multirate test is used mostly in gas reservoirs in order to estimate the reservoir performance and well potential. Most common types of the multirate test are; flow-after-flow test and isochronal test.

In **flow-after-flow test**, different flow rates are applied to the well and the bottomhole pressure is recorded. Test usually includes four different

stabilized flowrates in increasing order as shown in the Figure 2.4. This test is also known as gas deliverability test and four point test.

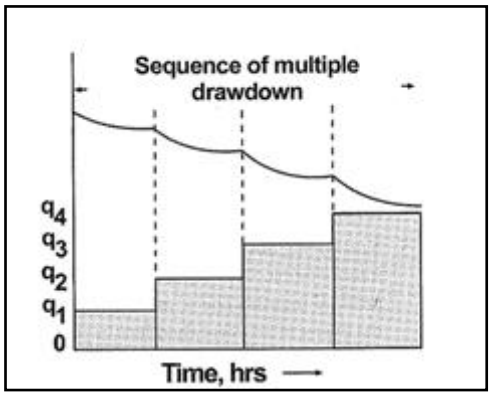

Figure 2- 4- Flow-after-flow Test Based on Multirate Drawdown [2]

Isochronal test, the multirate test is designed as a series of drawdown and build up periods at different drawdown flowrates, with each drawdown of the same duration and each build up reaching stabilization at the same pressure as at the start of the test. The aim of the test is to get well deliverability of gas well.

In tight reservoirs time for the pressure stabilization can be very long. As a result of that modified isochronal tests are designed to minimize the time loss for production which build up periods are equal to the drawdown periods, as shown in the Figure 2.5.

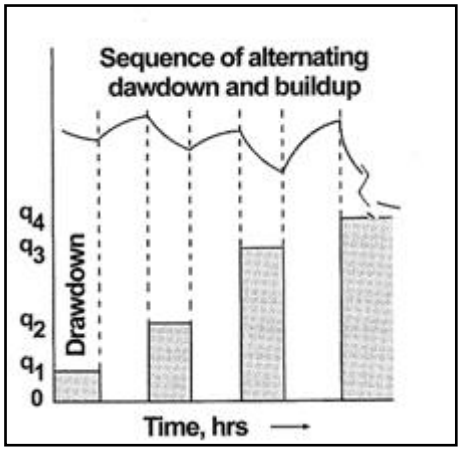

Figure 2- 5- Modified Isochronal Test [2]

2.2.6 INTERFERENCE TEST

Interference test is used to determine whether two or more wells have pressure communication or not and if the communication exists, some parameters may be estimated such as permeability, porosity, and compressibility. There are at least two wells, one of them is called as active well which is producing or injecting in changing rates. The other well is called the observation well which the pressure response is observed. The interference leads to changing pressure response in both wells.

2.2.7 PULSE TEST

Pulse test has the same objectives with the interference test. The technique uses sequences of short rate pulses at active well. At the observation well, pressure responses to the pulses are measured. The pulse series are created by producing or injecting from active well, after that shut-in and repeating the same procedures in a regular arrangement as shown in the Figure 2.6. In order to measure the pressure response exposed to short duration pulse, highly sensitive pressure gauges are used.

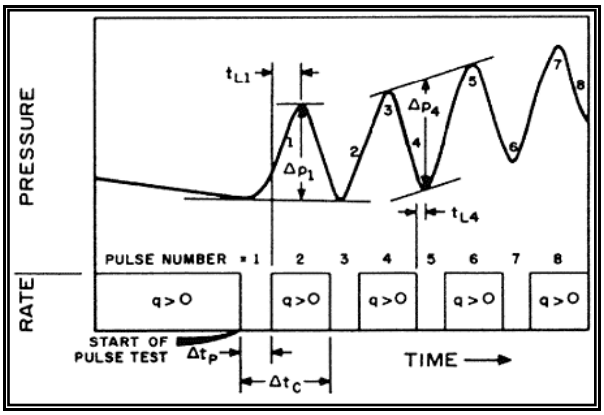

Figure 2- 6– Pulse Test [2]

2.2.8 DRILL STEM TESTING

Drill stem test (DST) is conducted before the completion of the well, to determine the feasibility and potential of the well. The main aim is to estimate formation and fluid properties of the reservoir. A DST consists of short series of multiple flow and shut-in periods. Firstly, for 5 to 20 minutes well is flowed and then shut in for an hour to determine the initial reservoir pressure. Secondly, a flow period for 4 to 24 hours is established to attain the stabilized flow to the surface. Lastly, well is shut in again and permeability thickness product and flow potential can be estimate from build-up period. At the same time, fluid which is obtained from the tested formation can be analyzed for different purposes. [4]

2.3 NATURALLY FRACTURED RESERVOIRS

A fractured reservoir is a system formed by intercommunicating pores and channels, where the pores form "matrix system" and channels form the "fracture system". The characterization of the naturally fractured reservoirs (NFR) has been a challenge for geologists and engineers for a long time. Although initially most of the reservoirs are considered as classical matrix reservoirs, which results in significant losses on recoverable reserves, later on they were identified as fractured reservoirs after studies about characterizing fractured reservoirs. (5)

It is essential to characterize fractures network at the very beginning of the reservoir life to manage the reservoir adequately.

Compared to the conventional reservoirs, fractured reservoirs are more complicated and difficult to evaluate. Therefore, analysis of the fractured reservoir must follow a special pattern that begins with the characterization of single fracture then study of multi fracture system. Single fracture parameters refer to the intrinsic characteristics, such as width, size and nature of fracture. Another characteristic of the single fracture that exists in the reservoir is the orientation of the fracture. Multi fracture parameters refer to geometry that creates the bulk unit, i.e. matrix block. The distribution and the density of the fractures depend on the number of the fractures and their orientation. Parameters for single and multi fractures and relationships are shown in the Figure 2.7. (5)

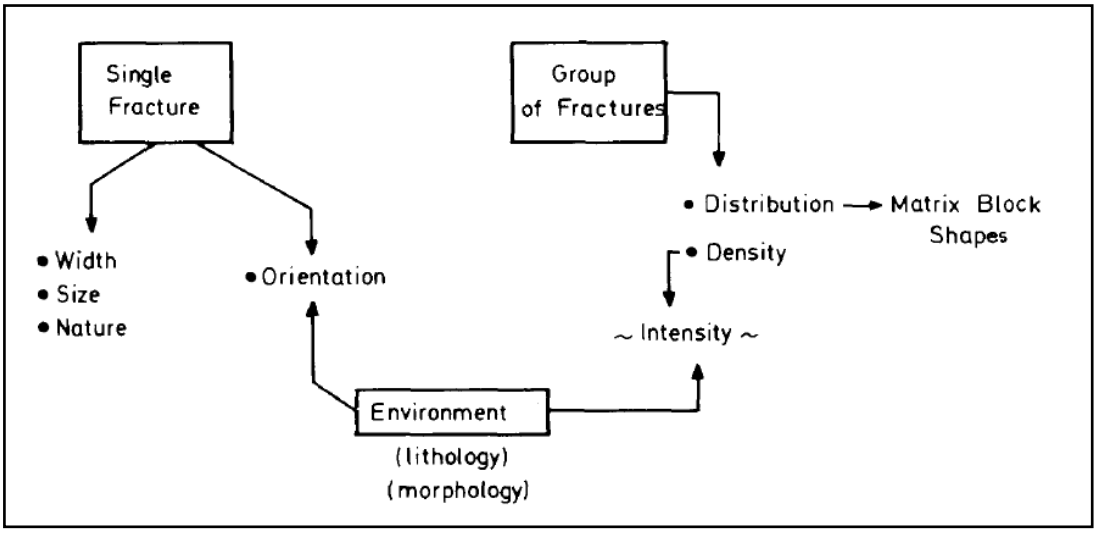

Figure 2- 7 – Fracture Parameters [5]

Basic production characteristics of the naturally fractured reservoirs can be:

1. High well productivity indices
2. Rapid decline in oil production
3. Fast water (gas) breakthrough
4. High vertical/horizontal permeability ratio
5. Permeability anisotropy (existence of directional permeability and permeability difference both horizontally and vertically)

Fractures can be detected from logs (Formation Imaging Logs, GR, Porosity logs and Resistivity), core, well tests-transient pressure analysis, drilling records (fluid losses, changes in rate of penetration) and outcrop analogies.

2.3.1 FRACTURE PROPERTIES

After the detection of the origin of the fracture system in the reservoir, petrophysical properties of the rock-fracture system must be examined. These consist of the study of physical morphology, distribution, and estimation of reservoir properties such as permeability and porosity.

In fracture networks, there are two major factors that govern the porosity and permeability of the fracture, width and spacing of fracture. Fracture width (fracture opening, e) is the distance between the fracture walls. In the reservoir environment, it depends on the depth, pore pressure and lithological-petrographic characteristics of the rock and nature of stresses. Fracture spacing (fracture density, D) is the average distance between parallel regularly spaced fractures. [5]

As Nelson [6] emphasized, there are four major properties of the fractures which are fracture porosity, fracture permeability, fluid saturations within the fractures and expected recovery factor, which are in order of increasing difficulty to determine.

2.3.1.1 FRACTURE POROSITY

In fractured reservoirs there are two porosity systems. First one is called primary porosity (Figure 2.8) which is formed by void spaces between the rock grains. [5]

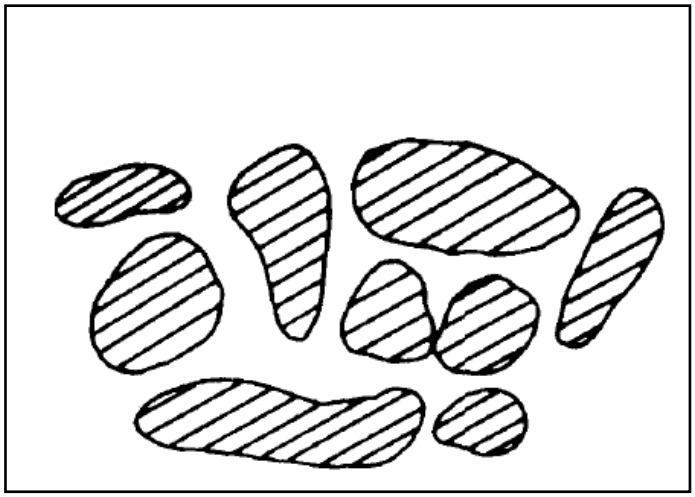

Figure 2- 8– Consolidated Grain Volume Space (matrix) [5]

The second type is formed by void spaces between fractures and vugs and it is called secondary porosity (Figure 2.9). For fractures or vugs instead of secondary porosity, vugular porosity or fracture porosity is used.

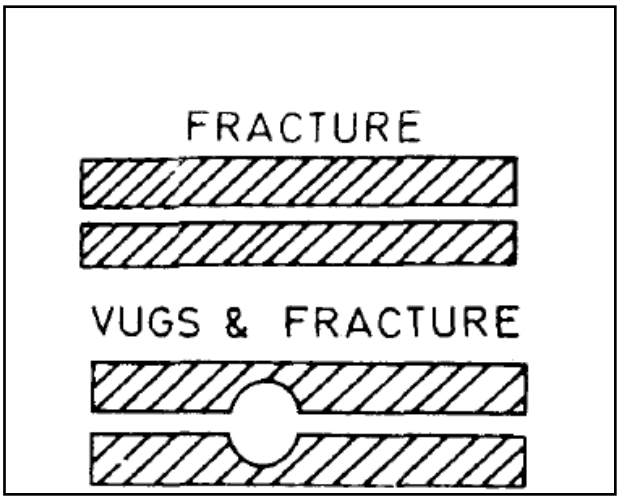

Figure 2- 9– Simplified representations of vugs and fracture void space [5]

Secondary porosity mostly exist in the brittle and compact rock formation that has relatively low intergranular porosity, such as compact limestones shales, shaly sandstones, siltstones, schists, etc. Rock fracturing, jointing and dissolution can result in secondary porosity in formation. Generally secondary porosity decreases with time, because void spaces are filled with minerals younger than those of which the matrix is composed. These younger minerals are formed by dissolution and precipitation in the reservoir. In carbonate formations, weathering or burial in the sedimentary basin causes solution channels or vugs. Most of the fractures or joints can be formed by tectonic or overburden stresses that decrease rock cohesion.

Fracture porosity can be defined as a percentage the void spaces in fractures to the total volume of the system. The following expression is used to calculate the fracture porosity: [6]

$$\emptyset_f = \left(\frac{e}{D+e}\right) \times \mathbf{100} \qquad (2.1)$$

Where:
e= fracture width
D= fracture spacing

It can be understood from the expression that the fracture porosity ($Ø_f$) is very scale dependent. According to Nelson [6], fracture porosity is always less than 2%, most of the case it is even less than 1% with a general value of less than 0.5%. However in the vuggy fractures porosity can be between 0 to a very large value.

Although the determination of the fracture porosity is difficult, there are several ways to estimate. It can be estimated from core analysis, porosity-permeability relationships, field/lab determination, logs, and multiple-well tests.

The type of the fractured reservoir defines the importance of the fracture porosity's impact on reservoir performance. If matrix porosity isn't providing the essential porosity and permeability to the system, the fracture porosity becomes a crucial parameter to determine in the early stages of the development. However, in reservoirs where fracture porosity is several orders of magnitude smaller than matrix porosity, the estimation of this parameter in early stages is not that crucial. [6]

Total porosity ($Ø_t$) in the fractured reservoirs is simply sum of the primary porosity and secondary porosity:

$$Ø_t = Ø_1 + Ø_2 \quad (2.2)$$

This total porosity is equivalent to the static definition of rock storage or total void space.

The two porosities can be expressed by the definitions which are dependent to total bulk volume (Matrix + Fracture):

$$Ø_1 = matrix\ void\ volume/total\ bulk\ volume \quad (2.3)$$
$$Ø_2 = fracture\ void\ volume/total\ bulk\ volume \quad (2.4)$$

In matrix porosity expression ($Ø_m$), it seems that it is relative only to matrix bulk:

$$Ø_m = \frac{volume\ void\ of\ the\ matrix}{matrix\ bulk\ volume} \quad (2.5)$$

Fracture porosity can be considered as;

$$\emptyset_2 \approx \emptyset_f \tag{2.6}$$

In this case primary porosity can be written as a function of matrix porosity:

$$\emptyset_1 = (1 - \emptyset_2)\emptyset_m \tag{2.7}$$

And effective porosity, containing oil phase, can be expressed as:

$$\emptyset_{1,eff} = (1 - \emptyset_2)\emptyset_m(1 - S_{wi}) \tag{2.8}$$

As seen in the Figure 2.10, unit of bulk is scaled in the upper part where the matrix bulk unit is scaled in the lower part. In the matrix porosity, one part is saturated with water and one with oil, and each is written as a percentage of matrix bulk units.

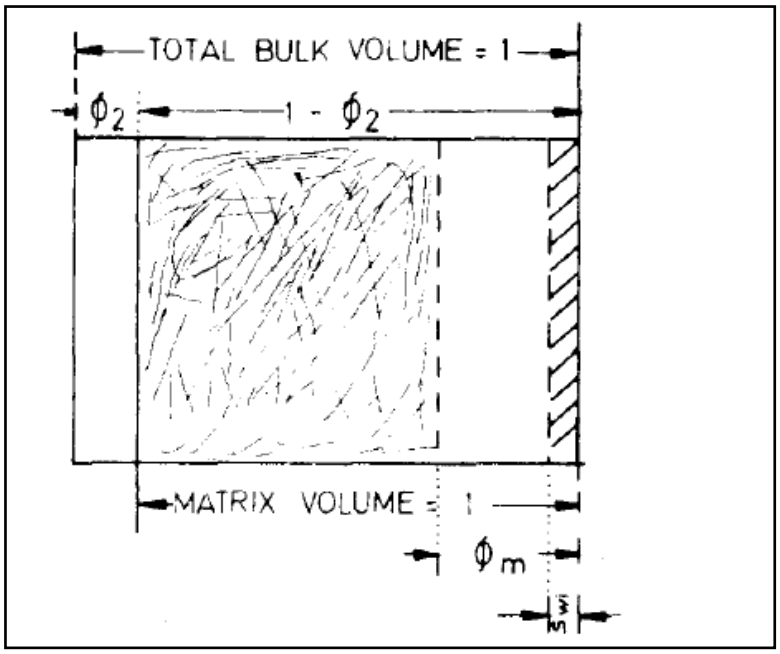

Figure 2- 10-Schematization of double-porosity [6]

2.3.1.2 FRACTURE PERMEABILITY

Permeability is a measure of ability of porous medium to transmit fluids. Fracture permeability is a significant factor that designates the reservoir productivity, since existence of the open fractures has a big influence in reservoir flow capacity.

A reservoir can have primary permeability, which is also referred as matrix permeability and secondary permeability that is by fractures or vugs. Matrix permeability can be evaluated by using Darcy's law:

$$v = -\frac{k}{\mu} \times \frac{dP}{dl} \qquad (2.9)$$

Where:

v= apparent flow velocity, cm/sec
μ= viscosity of flowing fluid, cp
dP/dl= pressure gradient in flow direction, atm/cm
k= permeability of the rock, Darcys

Fracture permeability can be estimated by using parallel plate theory which is based on fracture width and spacing concepts. Nelson [6] combined the model for fracture and matrix fluid flow and get an expression for the fracture permeability:

$$k_f = \frac{e^2}{12} \times \frac{\rho g}{\mu} \qquad (2.10)$$

This equation can be applied in following conditions: (1) laminar flow, (2) smooth-non moving parallel plates and (3) homogeneous fractures with respect to orientation, width and spacing.

In some cases, fractures do not advance the fluid flow in reservoir. Full or partially filled fractures can act as flow barriers. Morphology and orientation are the determined factors for the effect of the fractures on permeability.

It is hard to estimate the permeability from direct sources like core analysis or laboratory tests, so that well test analysis is the most common way to determine the fracture permeability. [7]

2.3.2 CLASSIFICATION OF FRACTURED RESERVOIRS

After reservoir properties of fractured system was defined and flow interaction between the fractures and matrix has been examined, classification of the reservoir which is based on the effects of the fracture system on the reservoir, must be done. Nelson [6] proposed the classification of the fractured reservoirs according to effect of the fractures on reservoir performance:

Type 1: Fractures provide essential reservoir porosity and permeability.
Type 2: Fractures provide the essential reservoir permeability.
Type 3: Fractures assist permeability in an already producible reservoir.
Type 4: Fractures provide no additional porosity or permeability but create significant reservoir anisotropy, such as barriers to flow.

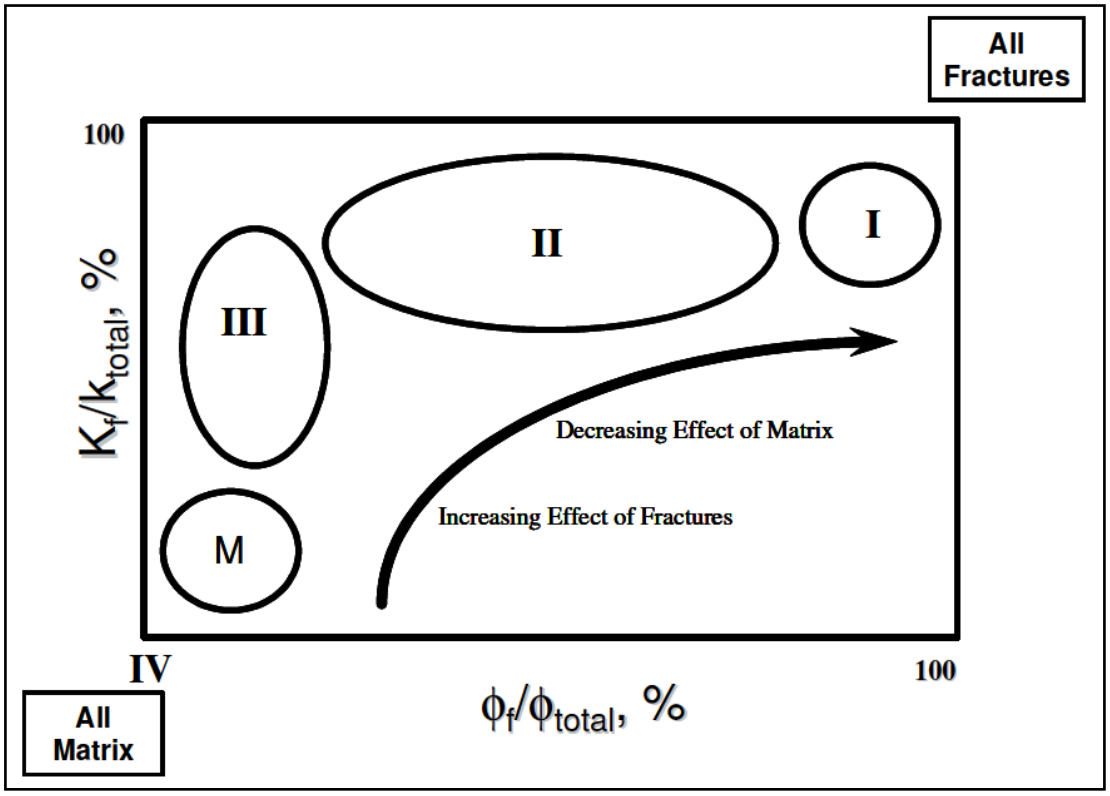

Figure 2- 11-Schematic plot of fracture porosity and permeability percentage for the four fractured reservoir types. (After Nelson) [6]

As seen in Figure 2.11, effect of the fractures is of dominant for Type 1 reservoirs, decreases for Type 2 and so on. Positive attributes of the first three types to reservoir can be detected from the graph. In the same way, the importance of proper characterization of porosity and permeability changes with reservoir type. Type M in the Figure 2.11 is representing the conventional matrix reservoir and conventional matrix reservoir characteristics can be seen in the Type 4 reservoir where fractures act as heterogeneities.

In Type 1 naturally fractured reservoirs early calculation of fracture porosity and permeability is essential to determine the total reserves obtained per well and to predict if initially high flow rates will be kept or decline rapidly in time. In these reservoirs few wells are needed which have large drainage

areas for development and it is easy to identify well locations. The problems associated with such reservoirs are rapid decline, possible early water encroachment, difficulties in determination of the size or shape of the drainage area. Moreover, reserve estimations are difficult compared the other fractured reservoir types.

In Type 2 naturally fractured reservoirs where fractures provide essential permeability; well rates are higher than expected. Characteristics of Type 2 reservoirs are: they can develop low permeability rocks and large storage volume associated with matrix porosity. Problems associated with these reservoirs are they have poor fracture matrix communication and poor performance on secondary recovery. Also recovery factor estimation can be variable and difficult. Possible water encroachment can be encountered.

In Type 3 naturally fractured reservoirs matrix properties dominate reserves and compared to other types reserve distribution is fairly homogeneous. Type 3 reservoirs have high sustained well rates and good reservoir continuity. Potential problems of Type 3 relate to the absence of recognition of fracture system, especially in secondary recovery process. Often rapid decline curve, early water encroachment, size and shape determination of drainage area, and difficulties in reserve estimation can happen. Additional wells for development add rate but not additional reserves.

In Type 4 reservoirs where fractures create flow barriers, permeability anisotropy may be unlike that in adjacent fractured reservoirs with different fracture style. Generally compartmentalization is seen. Wells underperform compared to matrix capabilities and recovery factor highly variable across the field are the problems involved in fractured reservoir type 4. [6]

2.4. WELL TEST ANALYSIS IN NATURALLY FRACTURED RESERVOIRS

One of the early studies about NFR was documented by Pollard [8] in 1959, who developed a method for evaluating acid treatments. He considered the reservoir in three regions: one around the wellbore, one in the fractured system, and one in the matrix. Appropriately, he divided the pressure differential in three parts: (1) pressure differential across skin near the wall of the well, (2) pressure differential due to flow resistance in the coarse communicating fissures, and (3) pressure differential between the fine voids and the coarse fissures. After that Pirson and Pirson [9] extended Pollard's study and they estimate the matrix pore volume (V_b). Pollard's graphic method and Pirson-Pirson formulas to interpret wellbore pressure data have had somewhat of a success. Warren-Root [1] and Kazemi [10] showed it has some inaccuracies.

Warren and Root had developed an idealized model to examine the fluid flow in naturally fractured reservoirs. In the naturally fractured reservoirs both primary and secondary porosity exist and an independent system of secondary porosity is superimposed on the primary porosity. The ideal model composed of discrete volumetric elements which represent matrix with primary porosity and space between the rectangular elements that represent fractures, as shown in Figure 2.12. The model is based on the following assumptions:

1. Matrix system primary porosity is assigned as homogenous and isotropic. A systematic array of identical, rectangular parallelepipeds is used for this purpose.

2. Secondary porosities are defined within an orthogonal system of continuous, uniform fractures. They are oriented as a way that each fracture is parallel to one of the principle axes and are uniformly spaced with a constant width.
3. The primary porosity and secondary porosity system are assigned as the flow is allowed only from matrix to fracture and fracture to well. Consequently flow through primary porosity elements cannot occur.

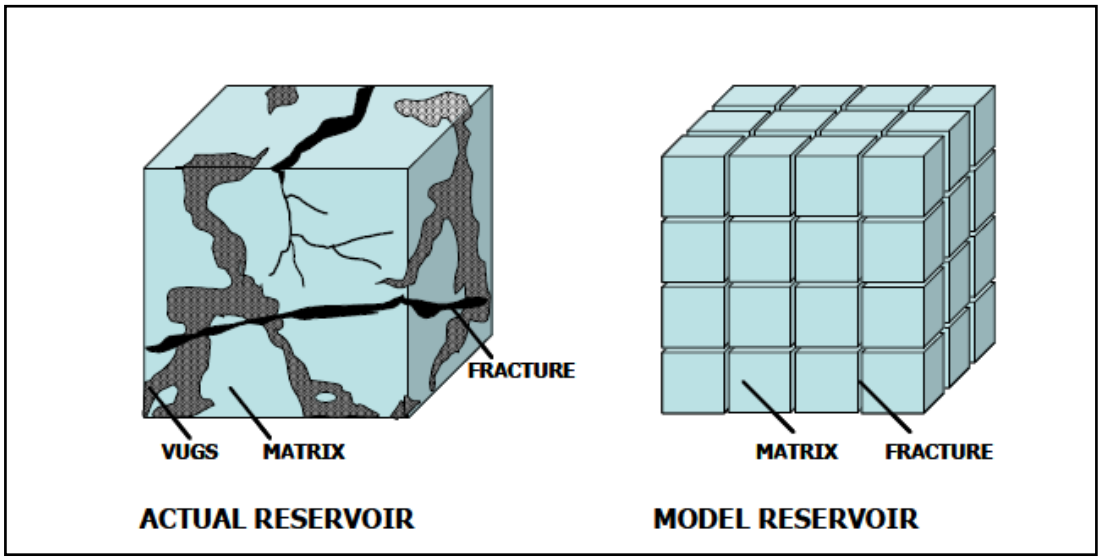

Figure 2- 12-Ideal model for a natural fractured reservoir (after Warren and Root) [1]

Warren and Root made an analytical examination of the unsteady-state flow in the model. They found two parallel straight lines in conventional buildup test plot as shown in the Figure 2.13. The vertical separation of the two lines depends on the storage capacity of the fractures. Straight line in the upper part corresponds to the flow in fractured media and the lower one corresponds to the flow in total system. Slope of the straight lines related to the flow capacity of the formation. To characterize the behavior of the naturally fractured reservoirs, they defined two parameters. Storativity ratio

(ω) represents the fluid capacity and it is the ratio of fracture storage capacity to the total storage capacity of the system. Other parameter is interporosity flow (λ) coefficient which governs the flow from matrix to fracture and it depends on the degree of heterogeneity of the system. Later Warren and Root model has been extended by Mavor and Cinco [11] by considering the wellbore storage and skin.

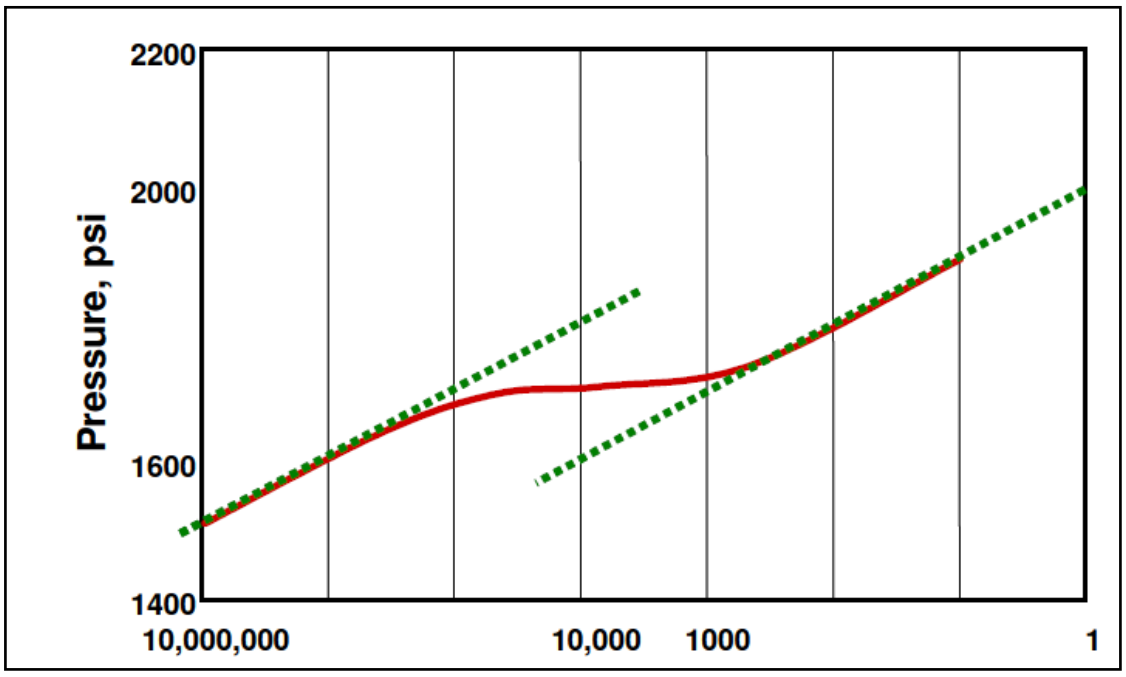

Figure 2- 13-Pressure response of build up plot on semi log of NFR (1)

Kazemi [10] developed a different model which consisted of a finite circular reservoir with a well located in the center and two distinct porous regions, referred to as matrix and fractures, as shown in the Figure 2.14. His model is based on the following assumptions:

1. Single-phase, unsteady state flow that occurs in radial and vertical direction.
2. The matrix has high storage capacity, but low flow capacity. The fracture has low storage capacity, but high flow capacity.

3. Occurrence of fluid flow is from matrix to fracture and from fracture to the wellbore.
4. Both matrix and fractures are horizontal, homogeneous and isotropic.
5. The well is in the center of a finite circular reservoir.

Kazemi studied hypothetical thesis and concluded there are three semi-log straight lines. The first and the last lines have the same explanations as in the Warren and Roots model. The second line related to the transition regime from fracture dominated flow to total system flow. Kazemi concluded that Warren and Root model for fractured reservoirs is valid for unsteady-state flow, and the value of interporosity flow coefficient depends on matrix-to-fracture flow regime.

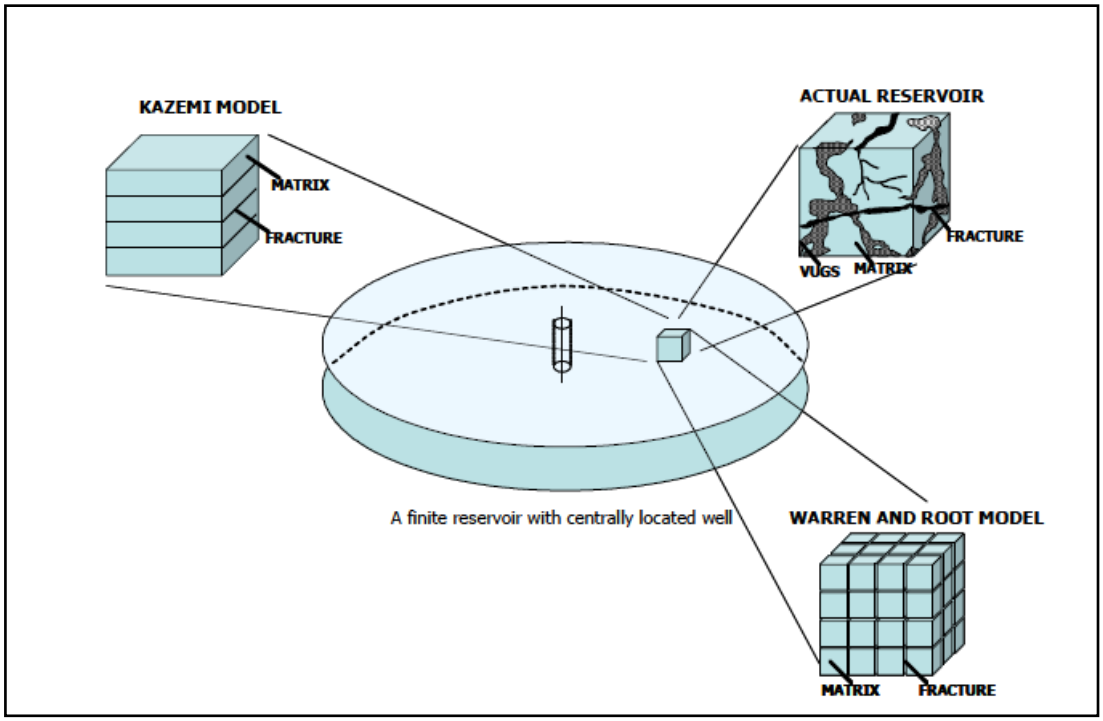

Figure 2- 14- Idealizatrion of NFR after Kazemi study [10]

De Swaan [12] demonstrated an analytical approach for interporosity transient flow for different geometries than those used by Kazemi. Results of the De Swann are close to Kazemi and showed similar semilog straight lines. Najurieta [13] included the transition period to De Swaan's theory and Moench [14] extended the theory by adding the effect of pseudo steady state skin between matrix and fracture system.

Cinco et al. [15] developed a mathematical model to examine the transient flow behavior for a well near an infinite conductivity vertical, non-intersecting, natural fracture in an infinite slab reservoir, shown in the Figure 2.15. The theory was valid if reservoir is isotropic and horizontal; a slightly compressible fluid has constant viscosity and compressibility, and with constant production rate fully penetrating.

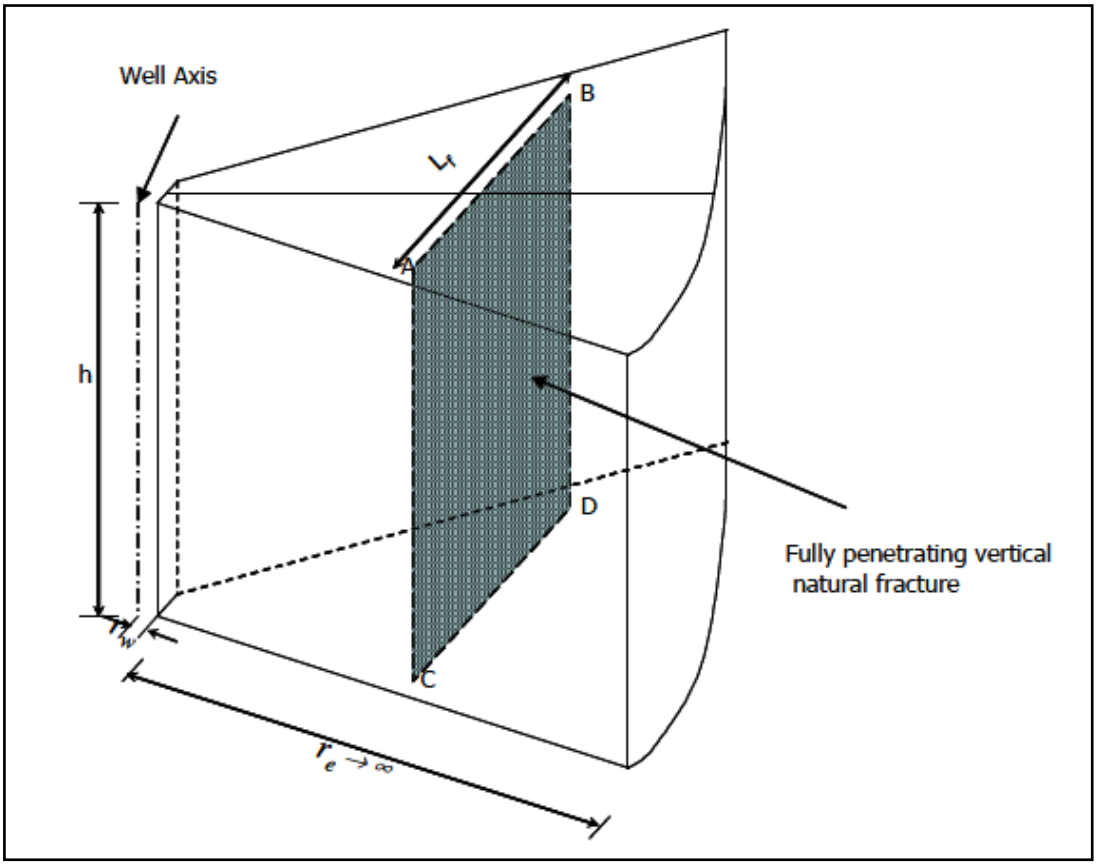

Figure 2- 15-Model of Nonintersecting Verticle Fracture (After Cinco et al.) [15]

Although Cinco et al. assumed of one fracture, the results showed a similar response with uniformly fractured reservoir with three semilog straight lines: fracture, transition, and total-system flow periods. Fracture orientation effect on the pressure response was considered and they concluded that the straight lines in semilog plot exist in all cases with the transition period varying as a function of fracture orientation.

A new set of pressure -derivative type curves was introduced by Bourdet et al. [16] [17] to simplify well test analysis in naturally fractured reservoirs. They studied both pseudo steady state and transient flow in naturally fractured reservoirs; also taking account the effects of wellbore storage and skin. In pseudo steady state flow, pressure derivative curve showed a different

response; a V-shape during the transition time, as presented in the Figure 2.16 an example of Bourdet type curves for fractured reservoirs. In transient flow the derivative curve has a constant value of 0.25 during the transition time.

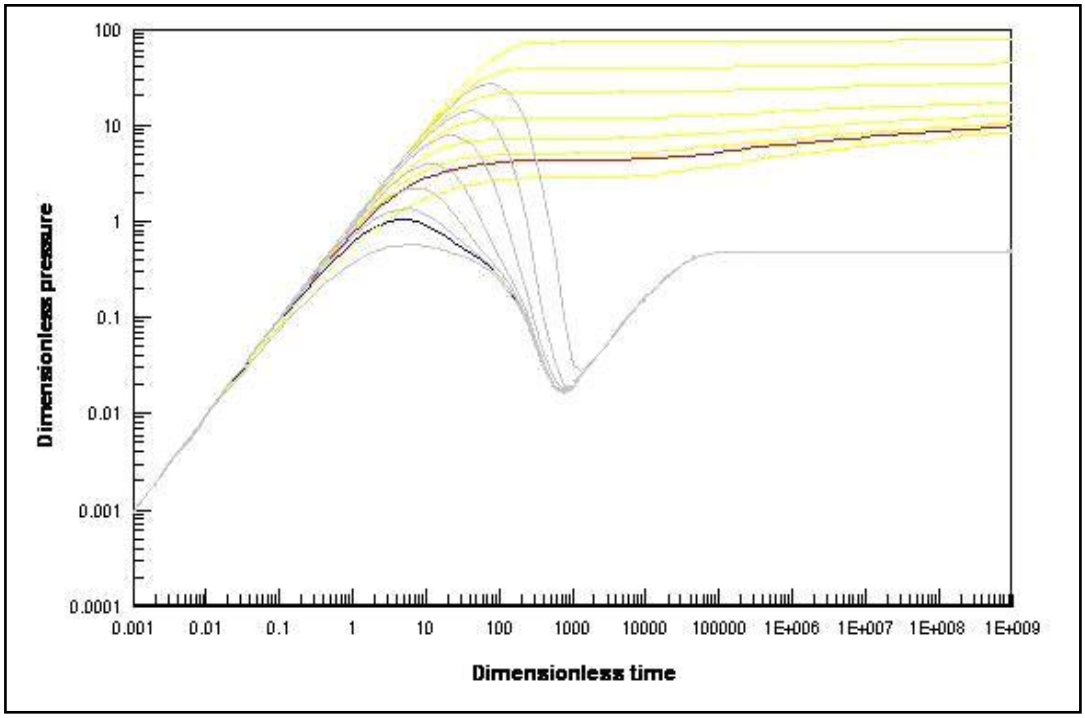

Figure 2- 16-Derivative Curve for Double Porosity Reservoirs, Pseudo Steady State Flow (After Bourdet et al. [17])

Extensive studies were made by several authors for inability of double porosity approach in accounting for more complex reservoirs. Triple porosity system was presented by Abdassah and Ershaghi [18] in 1986. Recently in 2004 Dreier et al. [19] introduced two quadruple porosity models. The pressure response of the model they proposed is shown in the Figure 2.17. Nevertheless, work of Warren and Root constitutes the basis of many of the most commonly used well test analysis techniques for naturally fractured reservoirs. These new methods improve upon the theory of Warren and Root by taking into account different types of matrix-to-fracture flow regimes,

wellbore storage and skin; giving a physical meaning to λ and ω for these kind of reservoirs.

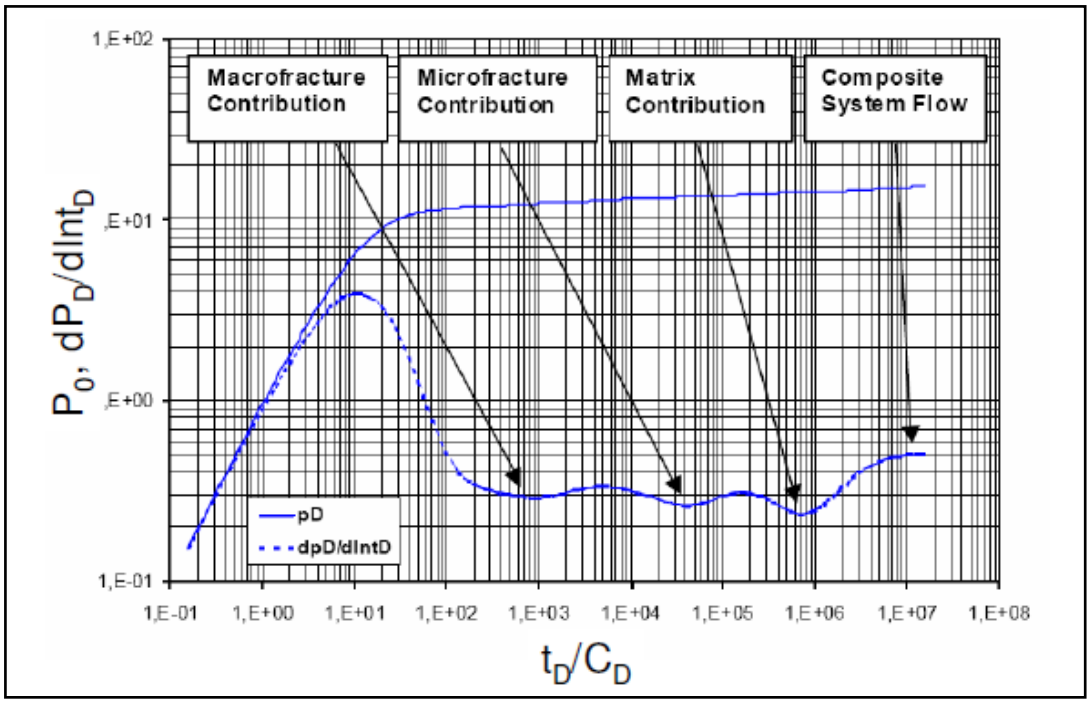

Figure 2- 17-Idealized Pressure Responses in Quadruple Porosity Reservoirs (Dreier et al.) [19]

2.5. CO_2 INJECTION IN CARBONATES

While injecting CO_2 into the carbonates, some changes in rock properties are expected. Because of the dissolution, transportation and later precipitation of rock minerals; rock permeability and effective porosity change. [20] Dissolution of rock minerals might enhance the permeability and effective porosity, whereas precipitation of asphaltene and the deposition of those minerals can result in the opposite effect. [21]

At the CO_2 front where CO_2 is dissolved in water, minerals such as calcite may dissolve readily, results in an increase in permeability and porosity along the flow channel. That process leads to a higher flow rate and increased dissolution, forming what is known as wormholes. For the several enhanced oil recovery applications, CO_2 is known as cause of injectivity decreasing in some cases however it increases permeability near injection wells in carbonate reservoirs. [21]

In a carbonate system the kinetically controlled reaction can be defined as:

$$H_2O + CO_2 + CaCO_3 \leftrightarrow Ca(HCO_3)_2 \quad (2.11)$$

In the calcite chemistry studies, it can be seen that CO_2 is dissolving in water and forms carbonic acid (H_2CO_3) which dissociates to give an acid and then to CO_3. The chemical reactions steps are given as: [21]

$$CO_2 + H_2O \leftrightarrow H_2CO_3 \quad (2.12)$$

$$H_2CO_3 \leftrightarrow H^+ + HCO_3^- \quad (2.13)$$

$$HCO_3^- \leftrightarrow CO_3^{2-} + H^+ \quad (2.14)$$

There are several mechanisms in which a precipitate may reduce permeability including solid deposition on the pore walls because of the attractive forces between particles and the surfaces of the pores, individual particles blocking pore throats, and several particles bridging across a pore throat. [23] Precipitation of the $Ca(HCO_3)_2$ and NaCl is the main reason of the reduction of the permeability in the carbonate formation. Precipitation rate is affected by the pressure drop through the flow paths; consequently it leads to varying rock properties by changing the solubility of the substances. Assuming the flow in the porous media is Darcian, the pressure drop is directly proportional with the axial distance in the direction of flow. From this linear relation and solute transport concept, permeability increase in near well bore region and decrease through the flow direction gradually is expected. [23] Permeability decline caused by only scale formation in the porous bed can reach to 90 % of the initial permeability, depending on solution composition, initial permeability, temperature, and flow rate and solution injection period. However, Omole and Osoba [24] concluded that increase in permeability of dolomite cores by 3 to 5 percent after similar CO_2 treatments while decline in permeability was observed for other experiments. Hence it can be said that the process strongly depends on the distribution of the rock minerals.

CHAPTER 3

STATEMENT OF THE PROBLEM

Well test analysis is a widely used method to determine detailed reservoir information in order to analyze the current behavior and properties of the reservoir. Well test analysis is used not only for short term actions such as well optimization, damage identification and stimulation evaluation but also incorporated into other reservoir management processes such as numerical simulation.

Two crucial parameters can be obtained from well test analysis, effective permeability and average reservoir pressure, and then incorporated into numerical simulation model as input data. Well test has also been used to adjust building simulation models by comparing pressure response which is obtained from simulation model with actual data.

Through the injection of the CO_2, reaction among the formation rock is observed. Consequently these lead to alteration in formation permeability and effective porosity. Change in formation permeability and effective porosity result from dissolution of rock minerals, transportation and later precipitation of them.

In naturally fractured reservoirs, there are two characteristic parameters, storativity ratio (ω) and interporosity flow coefficient (λ), which are related to

fracture porosity and shape factor, respectively. These parameters can be obtained from well test analysis. Fracture porosity and shape factor (expressed in terms of fracture spacing) are required as input data to build dual porosity simulation models.

This research is focused on dual porosity, well test analysis without wellbore storage and skin. The main objective is to determine the effect of carbon dioxide injection to the naturally fractured carbonate reservoirs in terms of investigation radius and reservoir formation properties while estimating the feasibility to integrate the parameters obtained from well test analysis into numerical simulation model. Specifically, it investigates the validity of the use of storativity ratio from well test analysis to estimate the fracture porosity and interporosity flow coefficient to estimate the shape factor or fracture spacing in the presence of carbon dioxide injection

CHAPTER 4

METHOD OF STUDY

4.1 NUMERICAL SIMULATION OF NATURALLY FRACTURED RESERVOIRS

For the field scale injection of CO_2 CMG STARS multi component, non-isothermal process simulator was used. STARS is a three phase multi component thermal additive simulator. Grid systems may be cartesian, cylindrical, or variable depth/variable thickness. Two dimensional and three-dimensional configurations are possible with any of these grid systems. [25]

Modeling of naturally fractured reservoirs is a challenging task. Extensive researches have been conducted in efforts to obtain the best way to represent the complexities involved. The most adequate approach is to idealization of two equivalent continuous media. A representation of a fractured reservoir simulation model is shown in the Figure 4.1. The matrix and fracture systems are designed as two separate grids. A transfer equation that characterizes the flow from matrix to fractures connects to the continuity equations for each system.

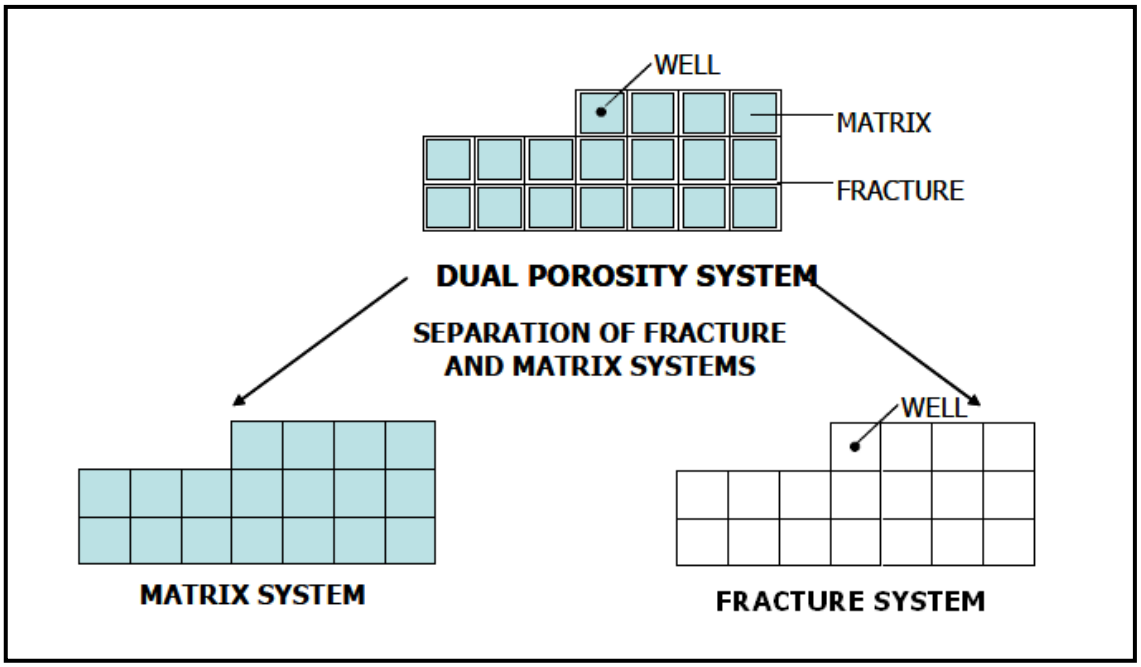

Figure 4- 1-Schematic Representation of Fractured Reservoir Simulation Model [6]

In this study, ten different dual porosity Cartesian, homogeneous and isotropic reservoir cases are developed. In dual porosity model approach, represented in the Figure 4.2, fluid flows through fractures from matrix blocks and there is no flow between or into the matrix blocks.

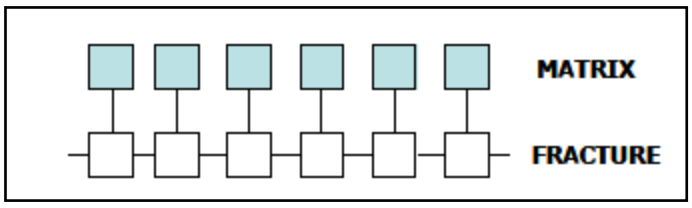

Figure 4- 2-Dual porosity model [6]

In the model same grid dimension, injection and production values are used. The differences of the models are growing out of the varying fracture permeability and fracture spacing values.

Different from the conventional reservoir models, naturally fractured reservoir simulation requires an additional parameter, namely shape factor.

It is a function of fracture spacing. Several researchers expressed the shape factor in different ways, including analytical derivations, numerical derivation and time-dependent functions. Gilman [26] defines the shape factor as a second order, distance-related, geometric parameters used to estimate the mass transfer from matrix to fracture. The general form of the shape factor is expressed as C/L^2, where C is a constant that depends on the number of fracture sets occurring in a reservoir, and L is fracture spacing. Commonly used shape factor constants are listed in the following table.

Table 4- 1 Shape factor constants proposed by several authors

Set of fractures	Warren and Root	Kazemi and Gilman	Coats et al.	Lim and Aziz
1	12	4	8	π^2
2	32	8	16	$2\pi^2$
3	60	12	24	$3\pi^2$

In this study, Gilman [26] and Kazemi expression is used to calculate shape factor, since it is most widely used and easy to apply in well testing and simulation. For three sets of fractures the equation is:

$$\sigma = 4\left[\frac{1}{L_x^2} + \frac{1}{L_y^2} + \frac{1}{L_z^2}\right] \qquad (4.1)$$

Where L_x, L_y, and L_z refer to fracture spacing in x, y, and z directions, respectively. In this study, fracture spacing in all direction is equal to each other. Hence,

$$\sigma = \frac{12}{L_{ma}^2} \qquad (4.2)$$

From the equation it can be understood that shape factor is inversely proportional to fracture spacing. In the Figure 4.3, it demonstrates the relationship between shape factor and fracture spacing by using Kazemi and Gilman approach, assuming that fracture spacing in all directions are equal to each other.

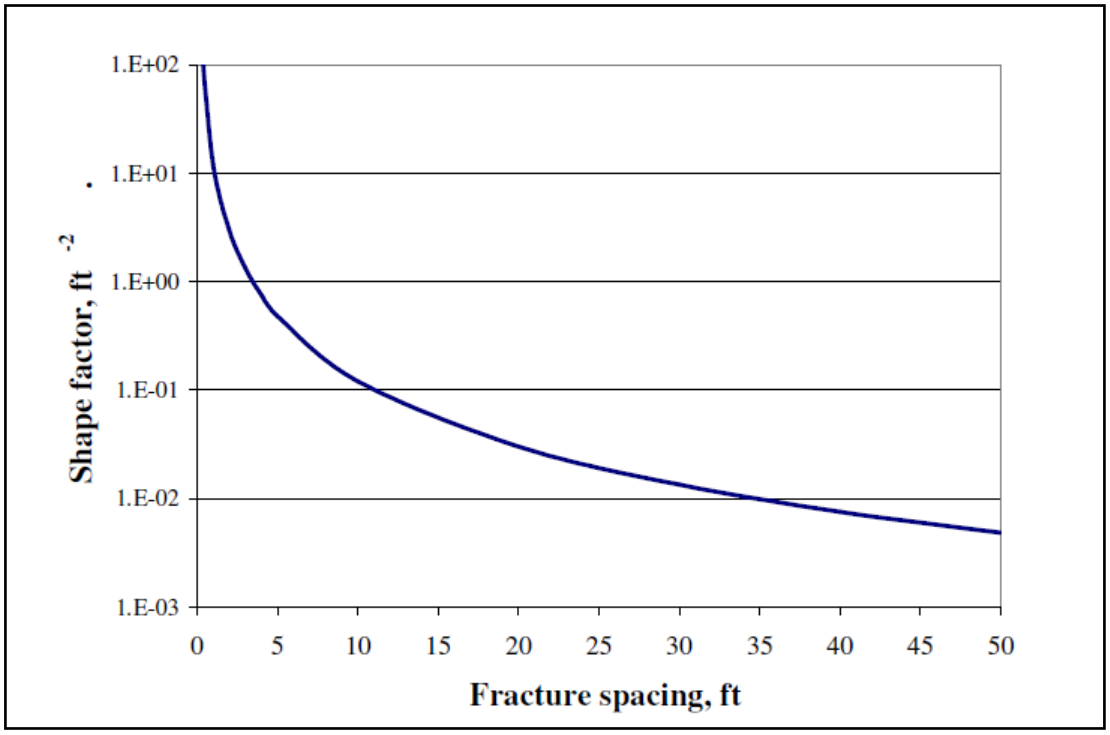

Figure 4- 3-Shape factor as a function of fracture spacing [6]

From Figure 4.3, it can be concluded that as fracture spacing approaches to zero shape factor becomes infinite which means the fractures are very close and the system acts as a continuous media. Also it can be seen that as fracture spacing is increasing, shape factor is decreasing. Based on these

conclusions the range of the fracture spacing was kept on 1 and 50 ft for practical purposes.

Shape factor is one of the most important parameters in naturally fractured reservoir simulation since it is directly proportional to transfer function which links two overlaying porous media.

Another important parameter for naturally fractured reservoir is storativity ratio, ω, which depends on the porosity and the total compressibility values. Storativity ratio is expressed by:

$$\omega = \frac{\emptyset_f c_f}{\emptyset_f c_f + \emptyset_m c_m} \tag{4.3}$$

Where Ø is porosity, c is the total compressibility and subscripts f and m represent fracture and matrix respectively.

Well test analysis could provide a useful indication of fracture porosity by transforming the storativity ratio expression like following:

$$\emptyset_f = \left(\frac{\omega}{1-\omega}\right) \emptyset_m \tag{4.4}$$

Nelson reported range of storativity ratio values by using twenty five naturally fractured reservoirs for practices. Based on that information matrix porosity and fracture porosity distributions are plotted, in the Figure 4.4 and 4.5, respectively. Both distributions shows log normal behavior.

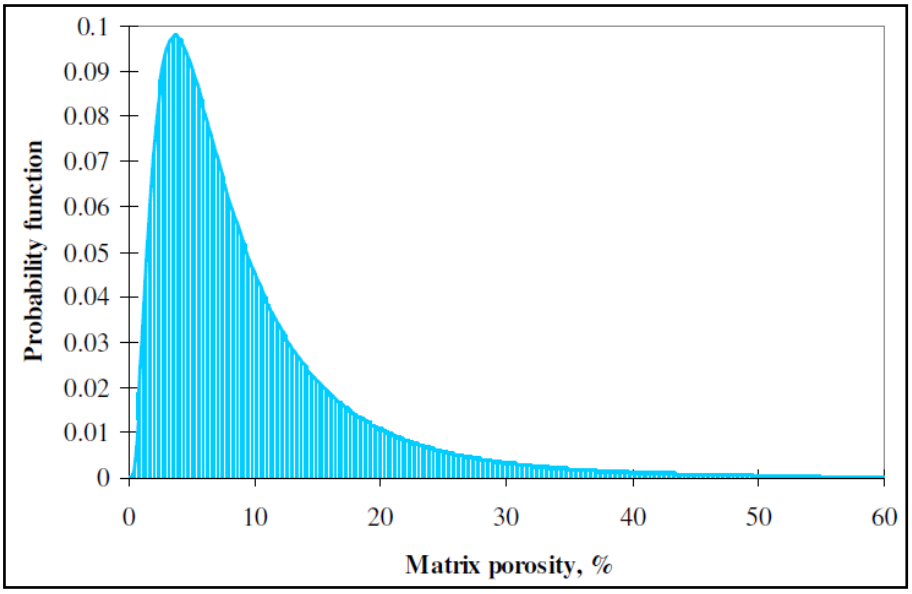

Figure 4- 4-Matrix porosity distribution in naturally fractured reservoirs (6)

The range for matrix porosity is between 1% and 55%; the mean is 9% and the mode is 4%.

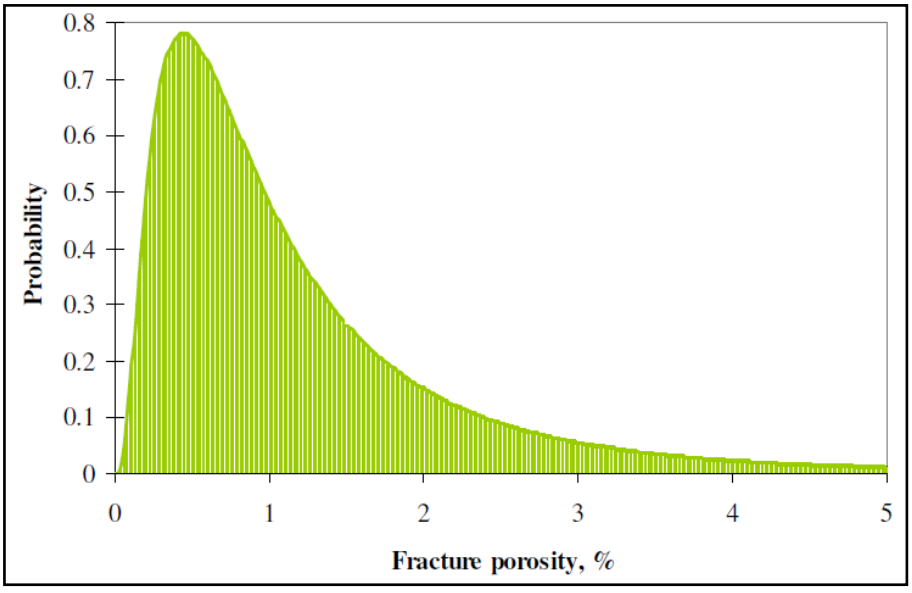

Figure 4- 5-Fracture porosity distribution for naturally fractured reservoirs (6)

Fracture porosity ranges from 0.005% to 5%; the mean is 1% and the mode is 0.4%.

According these two distributions matrix and fracture porosities are taken as 0.15 and 0.01, respectively.

Another important parameter to define naturally fractured reservoir is interporosity flow coefficient (λ) which is given as:

$$\lambda = \frac{\sigma k_m r_w^2}{k_f} \qquad (4.5)$$

For the permeability values Nelson reports was examined and fracture permeability values were taken as 500 md and 1000 md whereas matrix permeability was set as 100 md. According to Van Golf Racht[5], permeability contrast can be taken as high as 1:100. Above this value reservoir is dominated completely by the fracture system, less than 100:1 the system can behave as a single porosity reservoir.

For this study, ten different models were built using STARS, a three dimensional, multiphase, steam and thermal additive simulator from CMG. To perform well test analysis Ecrin from KAPPA was used. [27]

Cartesian, homogenous, dual porosity systems are constructed with a wide range of values for fracture permeability and fracture spacing. An injection well was located at the center of the cartesian system and two producer wells were located at the corner symmetrical from injector. Wells are injected and produced at constant rates several different times starting from 360 days and shut in for build up test for 20 days. Pressure data from production and build up period was extracted to analyze in Ecrin. The values of interporosity flow coefficient, storativity ratio and radius of investigation values obtained from well test are compared with the simulation input data.

Models have grid dimensions of 21 x 21 x 10 cells and reservoir thickness of 100 ft. 10 different cases were designed by changing the fracture permeability and spacing values. All properties are homogeneous and isotropic, including fracture spacing in x, y, and z direction. Table 4.2 summarizes the other common reservoir properties of the models.

Table 4- 2-Main reservoir parameters

RESERVOIR PARAMETERS	VALUES
Grid Cell Dimensions	3804x3804x100 ft
Reservoir Thickness	100 ft
Initial Pressure	1365 psi
Reservoir Temperature	127 °F
Matrix Porosity	0.15
Matrix Compressibility	1×10^{-5} 1/psi
Matrix Permeability	100 md
Fracture Porosity	0.01
Fracture Compressibility	96×10^{-6} 1/psi

The formation is composed of carbonate only and have six components which are water, oil, $CaCO_3$, $Ca(HCO_3)_2$ and NaCl. For every component the molecular weights were entered. Since CO_2 is in gaseous phase, its critical temperature (T_c) and critical pressure (P_c) are entered in order to allow the software to calculate the compressibility factor, z and vaporization enthalpy. Critical values of the water and oil were also entered. Reference temperature and reference pressure were taken as 14.7 psia and 25°C (77°F), respectively. Other properties which were entered for the components can be seen in the Appendix-B-Numerical input file for the first case.

Two reactions are defined in order to express the solution and deposition of calcite. STARS enables user to define chemical kinetics and effects of those reactions on rock properties involving particle transport concept and blockage of pore throats by dissolved particles. Stoichometric equations of principal reactions are summarized in chapter 2.5. The equilibrium of the equation is affected by the concentration of the reactants and the products, pressure and temperature. A rate constant that includes these effects must be defined. Since reactions are treated as source/sink terms for each component and energy, they may be thought of as another way in which to link together the different components of a problem when rate is important. The kinetic model, also known as reaction kinetics, determines the reaction rate of reaction rk. The general expression defined as:

$$rk = r_{rk}.exp\left(\frac{-E_{ak}}{R.T}\right).\prod_{i=}^{nc} C_i \qquad (4.5)$$

The terms in the equation are:

rk: rate of reaction k
r_{rk}: constant part of rk
E_{ak}: temperature dependence of rk
R: gas constant
T: temperature
C_i: concentration of component i in void volume

The term reaction rate, rk, is an important parameter that is used in precipitation calculation. It has effects on permeability and porosity changes. The reaction model's heterogeneous mass transfer (source-sink) terms can be applied to the non-equilibrium capture and release of fines particles by the porous rock. This requires that the reaction rate constants depend upon permeability, to account for the changes in capture efficiency as the droplet

size to pore throat size ratio changes. For the models developed, stoichiometric coefficient of reactors and products were entered. By using molecular weight and stoichiometric coefficients, STARS checks the mass balance, as following:

$$\sum CMM(i)\, sto1(i) = \sum CMM(i)\, sto2(i) \qquad (4.6)$$

After the component properties rock-fluid properties were entered. For the models single rock type, limestone was defined. STARS assigns the wettability as water wet as default and this property was kept default. In order to calculate three phase relative permeability according to Stone's second model, appropriate keyword, *STONE2 was entered. In Stone's second model, the water and gas relative permeabilities are assumed to be functions only of their own saturations and oil permeabilities are calculated by using two phase relative permeabilities, as given in the following equation:

$$k_{ro} = \left(k_{ro(w)} + k_{ro(wi)}k_{rw(o)}\right)\left(k_{ro(g)} + k_{ro(wi)}k_{rg(o)}\right) - k_{ro(wi)}\left(k_{rw(o)} + k_{rg(o)}\right) \qquad (4.7)$$

Where:

$k_{ro(wi)}$= oil relative permeability measured at irreducible water saturation with no gas present

$k_{ro(w)}$= oil relative permeability at S_o= 1- S_w

$k_{ro(g)}$= oil relative permeability at S_o= 1- S_g-S_{wi}

$k_{rw(o)}$= water relative permeability

$k_{rg(o)}$ = gas relative permeability

A vertical injection well is located at the center of the reservoir and set to inject at a constant rate 1 MMSCF/DAY. Two vertical production wells are located at the corner of the reservoir and set to produce at a constant rate 50 bbl/day. CO_2 was injected in supercritical fluid phase which is above critical temperature and pressure values. For CO_2 this point is characterized by a critical pressure of 73.86 bar and a critical temperature of 31.1 °C as seen in Figure 4.8. This phase has lower viscosity (typically around 10^{-4} to 10^{-3} cp), lower density and higher volume expansion than other phases of CO_2.

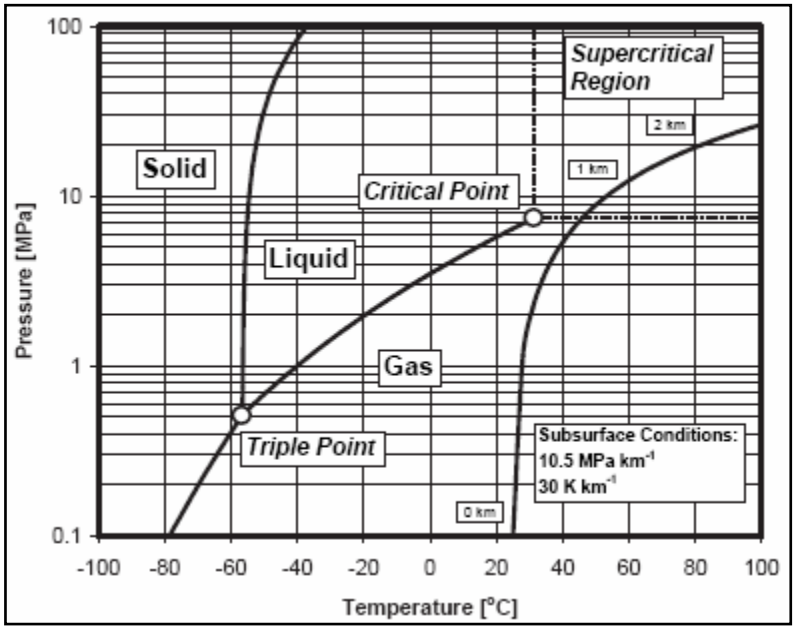

Figure 4- 6-Phase diagram of pure CO_2 [28]

After all the properties entered, ten different simulation models were run by setting the days starting from 360 through the 138000. Different test times have been defined by looking CO_2 spread in the models.

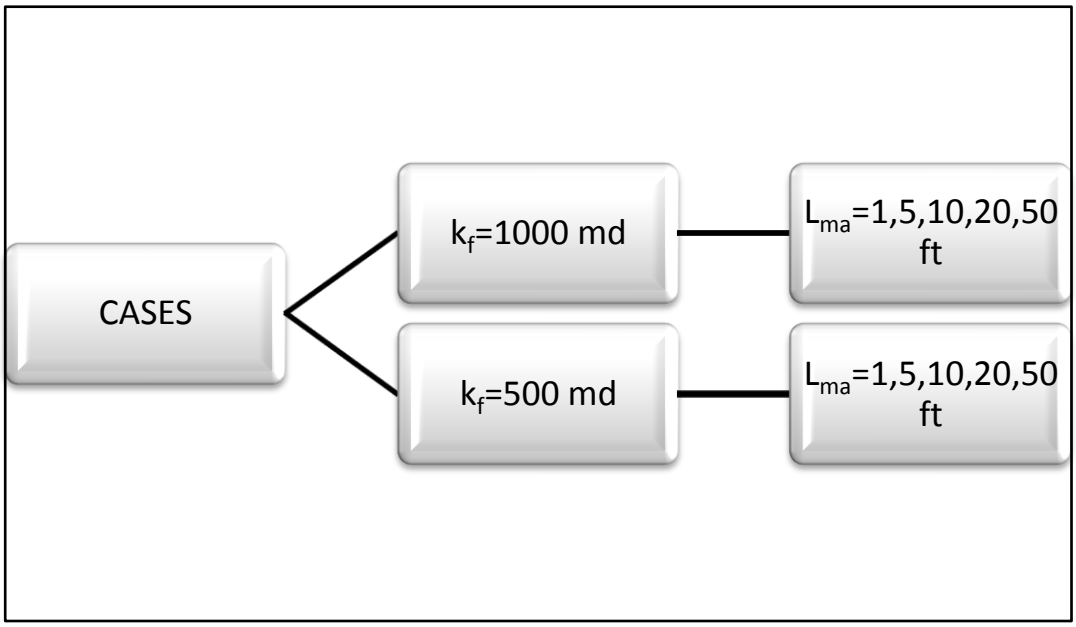

Figure 4- 7 Summary of simulation cases

Simulations were run for different values of fracture permeability, and fracture spacing. Figure 4.9 shows the values used for each of those properties.

In build up test runs, restart option was used in order to save time. A restart file contains information that allows the simulation to continue from another run.

Restarts are done for the following reasons: history matching or sensitivity studies, well specifications that need to be changed, to perform a short simulation run to see if the results are satisfactory, before running bigger, longer jobs, and to save execution time in subsequent runs. For instance, you have completed a simulation run and the preliminary results look good. Now you want to do prediction runs. Because you have created a restart file with the initial run, you may select a time step from the middle of your run

and 'restart' the simulation. The simulator does not need to start at the beginning; it continues execution from the time step you have chosen.

4.2 WELL TEST ANALYSIS

In order to analyze build up tests, Ecrin from KAPPA software is used. Saphir module which is integrated in Ecrin is used for pressure transient analysis. Saphir is a well test interpretation package based on the methodology of the pressure derivative. The basic logic is to guide the user through the complete interpretation process using this methodology, while providing easy access to complementary side facilities.

The different steps of an interpretation using the pressure derivative are accessible mostly from the interpretation page of the control panel. At any point in an interpretation, Saphir checks the advancement of the process allows only applicable options and suggests what should be done next, assuming that all previous steps have been carried out correctly and all the acquired data is valid. The next suggested option is highlighted with a red border. You can override this default step to correct previous actions or access side facilities.

During a well test, a particular flow rate history is applied to a well, and the resulting pressure changes are recorded, either in the same well (typically) or in a nearby well (interference test). From the measured pressure response, and from predictions of how reservoir properties influence that response, an insight can be gained into those reservoir properties. In order to make these predictions, it is necessary to develop mathematical models of the physical behavior taking place in the reservoir.

Pressure data from the buildup period were extracted from STARS runs and the buildup periods were analyzed by the help of Saphir. To perform a pressure transient analysis the rates and the pressure responses from tested wells and, where applicable, nearby wells are required. Additional information that are needed to perform analysis are fluid physical properties; pressure, volume and temperature (PVT).

To create a build up test in Ecrin a reservoir and well properties were entered as follows:

Table 4- 3-Reservoir parameters entered to Ecrin

Well Radius	**Values**
Pay Zone	100 ft
Porosity	0.15
Formation Volume Factor	1.0095
Viscosity	0.5981 cp
Well Radius	0.5 ft
Reservoir Temperature	127 °F

Firstly pressure and flow rate data are loaded and then pressure derivative was extracted. Different production periods were selected to observe the radius of investigation and the effect of CO_2 in the naturally fractured carbonate reservoirs. The buildup tests were made after a certain production time; 360, 720, 1440, 1800, 2880, 3600, 4320, 5400, 7920, 9720, 10,800, and 13,680 days.

In the process of testing a well, we provide an input impulse (usually change in flow rate) and we measure a response (usually change in pressure). During a transient well test, the pressure response is a function of both the

well and the reservoir characteristics and the flowrate history. In interpretation terms, the actual pressure and time are unimportant, with analysis performed in terms of pressure change Δp versus elapsed time Δt, i.e history plot. The interpretation predominantly carried out using semi-log plot, log-log plot and Cartesian plot. The reservoir parameters such as permeability, skin effect, storage coefficient, distance to boundaries, fracture properties, double porosity coefficients, etc. can be gained from interpretation.

At the start of production, pressure in the wellbore drops suddenly. The fluid in the vicinity to the well expands and moves towards lower pressure. This movement is retarded by viscous, inertial and frictional forces. As the fluid moves, it will in turn create a pressure imbalance and this will induce neighboring fluids to move. The process continues until the pressure drop is dissipated. The physical process occurring in the reservoir can be described by the diffusivity equation. In order to use the diffusivity equation it is necessary to determine the boundary conditions. Complex boundary conditions may be solved by applying the "principle of superposition" in space. Variable flow rates can be tackled by applying the "principle of superposition" in time. The radial flow equation does not account for the drop in pressure due to damage or improvement near the wellbore. Instead, the term skin was invented. The early portion of the test is also distorted by wellbore storage effects. Three most common used expressions for the diffusivity equation are as follows:

General form: $\frac{\partial p}{\partial t} = 0.0002637 \frac{k}{\emptyset \mu c_t} \nabla^2 \mathrm{p}$ (4.8)

Radial flow: $\frac{\partial p}{\partial t} = 0.0002637 \frac{k}{\emptyset \mu c_t} \frac{1}{r} \left[\frac{\partial}{\partial r}\left(r \frac{\partial p}{\partial r}\right)\right]$ (4.9)

Linear flow: $\frac{\partial p}{\partial t} = 0.0002637 \frac{k}{\emptyset \mu c_t} \frac{\partial^2 \mathrm{p}}{\partial \mathrm{x}^2}$ (4.10)

In order to simplify the reservoir models by embodying the reservoir parameters and reduce the total number of unknowns dimensionless variables are used often. They have additional advantage of providing model solutions that are independent of any particular unit system. It is an inherent assumption in the definition that permeability, viscosity, compressibility, porosity, formation volume factor and thickness are all constant.

For a line source well, the list of the dimensionless variables is the following:

Dimensionless distance: $r_D = \frac{r}{r_w}$ (4.11)

Dimensionless pressure: $P_D \frac{kh}{141.2Q\mu}(p_i - p)$ (4.12)

Dimensionless time: $t_D = 0.0002637 \frac{kt}{\emptyset \mu c_t r_w^2}$ (4.13)

Where:

k= permeability, md

h= thickness, feet

p_i= initial reservoir pressure, psi

p_{wf}= well flowing pressure, psi

q= production rate, STB/d

B= formation volume factor, resvol/std vol

μ= viscosity, cp

t= time, hours

Ø= porosity, pore volume/bulk volume

C_t= total system compressibility, 1/psi

r_w= wellbore radius, feet

In well test analysis, pressure derivative and pressure plots on log scale interpretation takes place in three different region; early time region, middle time region and late time region as shown in the Figure 4.10. In early time region, wellbore and near wellbore effects are detected. These effects include wellbore storage, skin factor, partial penetration, phase redistribution, and finite- and infinite-conductivity hydraulic fractures. In middle time region, flow regimes are interpreted. Lastly in late time region, boundary effects can be detected. There are a large number of different types of boundaries that may affect the pressure response, including sealing faults, closed reservoirs, and gas/water, oil/water, and gas/oil contacts.

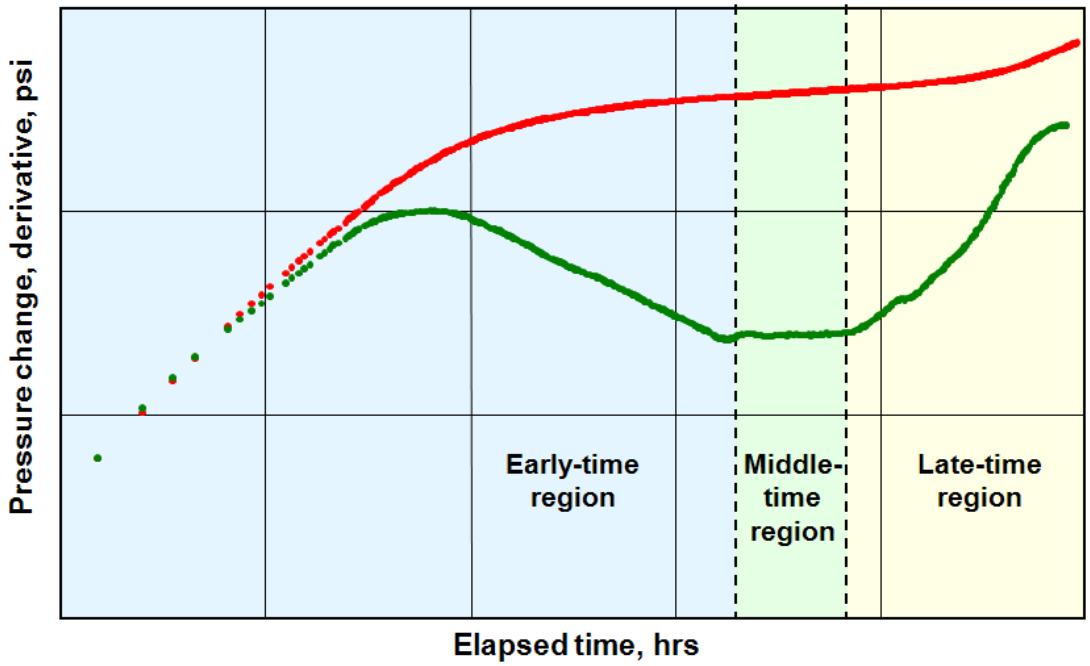

Figure 4- 8-Time regions on the diagnostic plot

Wellbore storage, also called after-flow, after-production, after-injection , and wellbore unloading or loading, has long been recognized as affecting transient pressure behavior. In most of the well test rate is controlled by the wellhead valve or flow line. Although well produce at constant rate at the wellhead, the flow transient within wellbore itself may mean that the flow rate from the reservoir into the wellbore (the sandface flow rate, q_{sf}) may not be constant. This effect is due to the wellbore storage. Wellbore storage can generally caused by the fluid expansion or changing liquid level. The wellbore storage coefficient, C, is the volume of fluid that the wellbore itself will produce due to a unit drop in pressure:

$$C = \frac{V}{\Delta p} \tag{4.14}$$

Where V is the volume produced, Δp is the pressure drop and C has units STB/psi. Dimensionless wellbore storage coefficient, C_D, defined as

$$C_D = \frac{5.615C}{2\pi\emptyset h c_t r_w^2} \tag{4.15}$$

Because of the local heterogeneities, pressure transmission does not take place uniformly through the reservoir. The term skin is brought into the computations to account for the pressure drop, Δp_s, that occurs across a localized zone near the well. Skin is caused by flow converge near the wellbore, visco-inertial flow velocity, and the blocking of pores and fractures that occurs during drilling and production. The skin factor is a dimensionless variable and defined in oil field units as:

$$s = \frac{kh}{141.2qB\mu}\Delta p_s \quad (4.16)$$

The skin value S is dimensionless, and in most cases independent of flowrate, but the corresponding pressure drop Dps is rate-dependent. A positive skin represents near wellbore 'damage', whereas a negative skin historically denotes 'stimulation', and physically means that there is a smaller pressure drop close to the wellbore than would be expected in the ideal case.

For the model created in this study wells are considered as they have no wellbore storage and neutral skin.

One of the classical approaches to well test interpretation has been semi-log plot of p versus log(Δt). Since pressure change is related to logarithm of the time in radial flow, pressure versus logarithm of time will give straight line. For build up tests, MDH plot (Miller-Dyes-Hutchinson) is useful when test is taken sufficiently long. The other important plot is Horner plot which is the graph of p_{ws} versus log((t+Δt)/Δt). From these plots one can calculate permeability-thickness product, kh, and skin factor, S by using the following equations.

$$kh = 162.6\frac{qB\mu}{m} \quad (4.17)$$

$$S = 1.151\left[\frac{\Delta p_{1hr}}{m} - log\left(\frac{k}{\emptyset\mu c_t r_w^2}\right) + 3.23\right] \quad (4.18)$$

By defining dimensionless pressure and dimensionless time, it is possible to create an analytical model of well and reservoir, or theoretical type curve,

which provides a global description of pressure response that is independent of the flowrate or of the actual values of the well and reservoir parameters.
One of the primary uses of dimensionless variables in well test interpretation is log-log type curves. By the definition dimensionless pressure and dimensionless time are linear functions of actual pressure and time, and then the logarithm of actual pressure drop will differ from the logarithm of dimensionless pressure drop by a constant amount.

$$log\Delta p = logp_D - log\frac{kh}{141.2q\mu B} \quad (4.19)$$

$$log\Delta t = logt_D - log\frac{0.000264k}{\emptyset\mu c_t r_w^2} \quad (4.20)$$

Once type curve match is established in log log plot, it will provide some interpretation parameters such as wellbore storage (C), permeability-thickness product (kh), and skin (S). From these reservoir properties one can estimate two important reservoir parameters, the transmissivity or ability to flow, and the storativity or quantity of fluid contained.

By introducing pressure derivative plot with log-log plot, the diagnostic plot was born. The pressure derivative is simply the slope of the semi log plot; the rate of change of pressure with respect to the superposition time function. The basic idea of the pressure derivative plot is to take the slope of the each point at the semi log plot and display it in the log-log plot.

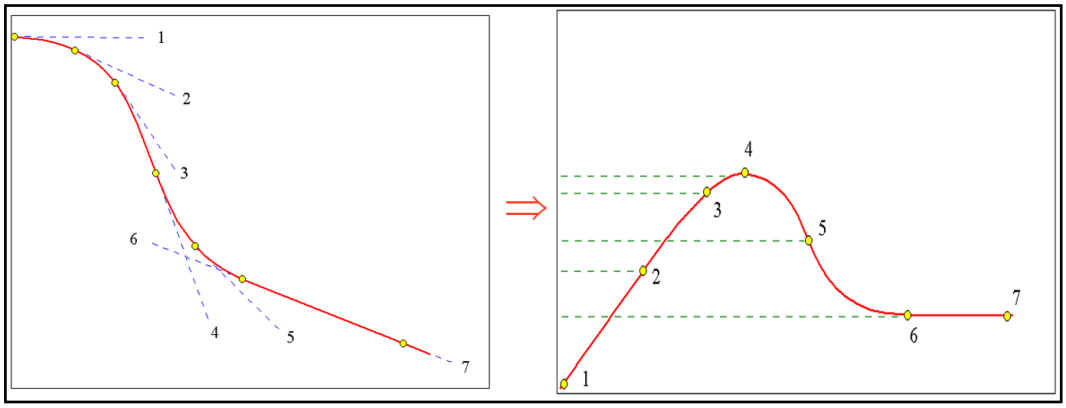

Figure 4- 9-Semi log plot and pressure derivative plot [27]

For buildup transient data the preferred derivative computation is;

$$\frac{d\Delta p}{d\tau} = \frac{p_{(t_{i+1})} - p_{(t_{i-1})}}{\tau_{i+1} - \tau_{i-1}} \qquad (4.21)$$

and

$$\tau_i = ln\frac{t_p + \Delta t_i}{\Delta t_i} \qquad (4.22)$$

Where

T= superposition time

p_i= initial formation pressure

p_{wf}= bottomhole flowing pressure

t_p= duration of production time prior to shut-in

Δt= elapsed time since start of transient test

In pressure derivative analysis, wellbore storage has unit slope since the pressure change is linear with respect to time.

$$\Delta p = C\Delta t \qquad (4.23)$$

$$\Delta p' = \Delta t \frac{dC\Delta t}{d\Delta t} = C\Delta t = \Delta p \qquad (4.24)$$

Hence when the flow at early time corresponds to pure wellbore storage, pressure and pressure derivative curves will merge on a unit slope line on the log log plot.

Skin effect can be seen clearly in pressure derivative curve in log log plot, as seen in the Figure 4.12.

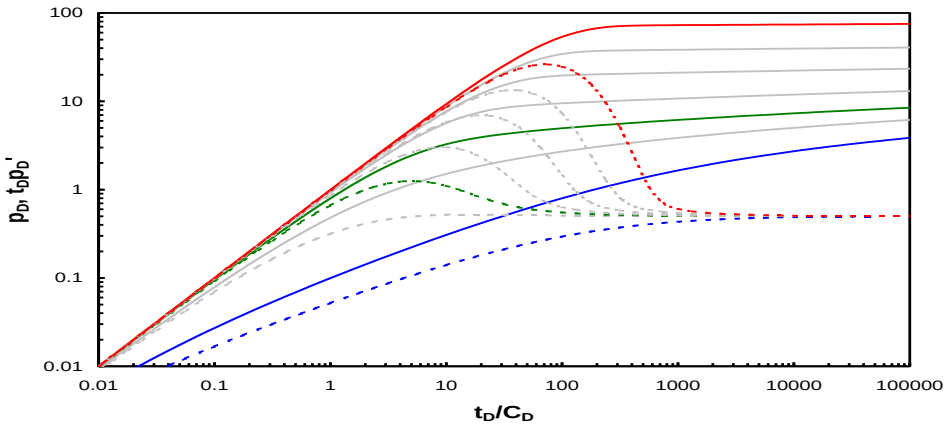

Figure 4- 10- Different skin factor values in log-log plot of pressure derivative [27]

After calculating the skin effect and wellbore storage, the next step is to identify the flow regime. For each flow regime identified from pressure derivative plot a set of reservoir parameters can be computed using that portion of the transient data displayed the characteristic pattern behavior.

Up to now, there are eight flow regime patterns commonly observed in well testing. These are; radial, spherical, linear, bilinear, compression/expansion, steady state, dual porosity/permeability and slope doubling.

In Ecrin there are seven flow regimes that can be selected from the reservoir model option. In this study, since we are using naturally fractured reservoir models, reservoir models were selected as double porosity pseudo-steady state (PSS).

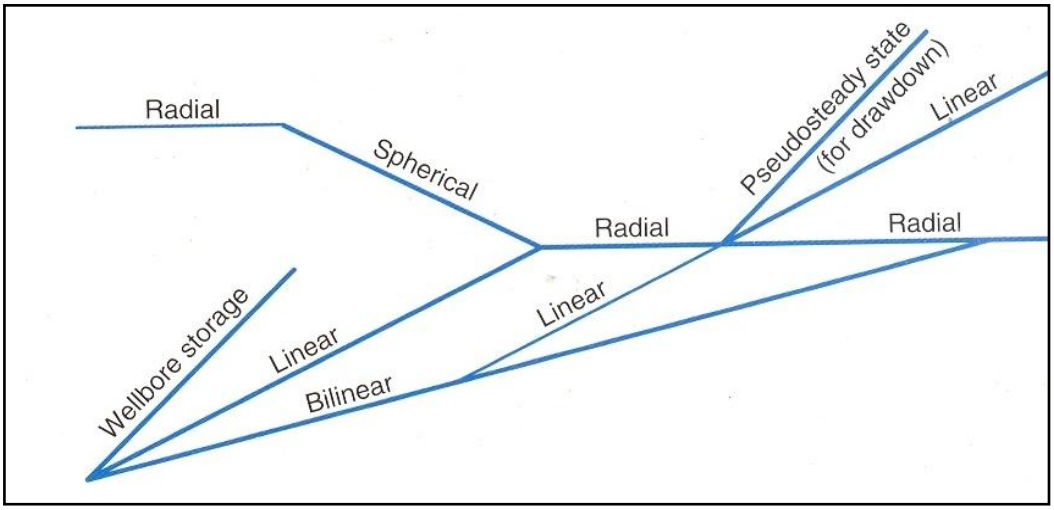

Figure 4- 11-Flow Recognition Log-Log Graphical Aid [27]

In this study the reservoir is naturally fractured, hence the flow regime show the behavior of dual porosity/permeability behavior. The derivative behavior for that case may look like the valley shaped trend. From this flow regime, parameters associated with internal heterogeneity are determined, such as interporosity flow coefficient, storativity or geometric factors.

In dual porosity models, the reservoir made up of matrix blocks with high storativity and low permeability, connecting to the well by fissures of low storativity and high permeability. This model is described with two additional parameters, storativity ratio (ω) and interporosity flow coefficient (λ), of which expressions are as followed respectively:

$$\omega = \frac{(\emptyset C_t)_f}{(\emptyset C_t)_f + (\emptyset C_t)_m} \quad (4.25)$$

$$\lambda = \sigma \frac{k_m}{k_f} r_w^2 \quad (4.26)$$

Storativity ratio is basically the fraction of oil stored in the fracture system. It determines the depth of the dip. Small values of storativity ratio are corresponding to a very high proportion of the hydrocarbon stored in the fracture system, the support during transition is substantial, and the dip is deeper and longer.

Interporosity flow coefficient characterizes the ability of the matrix blocks to flow in the fracture system. It determines the time of the transition controls the speed at which the matrix will react, and therefore the time of transition. For high values of interporosity flow coefficient, the matrix permeability is high comparatively; hence it will start to give up its hydrocarbon almost as soon as the fracture system starts to produce. Contrary low values of interporosity flow coefficient means a very tight matrix and most of the production will be established from fracture system before matrix blocks will appreciably give up their hydrocarbon, and the transition is seen later.

The dual porosity behavior can be seen for the fracture system after the well effect. When the interporosity flow starts, the transition seen as a valley shape in the pressure derivative plot on log-log plot. After transition homogeneous behavior is seen with the storativity of the total system and fracture permeability. The depth of valley is a function of storativity ratio whereas the time transition is the function of interporosity flow coefficient.

By following a systematic approach, self-consistent and correct results can be obtained in well test interpretation. The methodology of interpretation consists of four main parts, data preparation, model recognition, parameter estimation and model verification.

Well tests are conducted as a series of dynamic events according to specified changes in flowrate. Before interpretation data, including well data, manipulation of gauge data and PVT and saturation data must be preprocessed. In addition, the sequence of events should be correlated with well's recent flow rate history and with the flow rate.

In model recognition, log-log pressure derivative plot and some specialized plots such as Horner MDH, are used to identify the flow regime.

Once the reservoir model has been identified, it is necessary to compute the model parameters. At this stage, straight lines are fitting to get the first estimates, than type curve is matched to get a historical point of view and non linear regression which is an efficient technique but requires a narrow range for converge is used.

Lastly for model verification construct variable rate type curves that should closely match the raw pressure and pressure derivative data if the model and parameter estimates are correct. For more complex geometries and multiphase flow numerical analysis can be done.

Reservoirs do not always behave like infinite-acting during well test. The time at which the boundary effect is noticed is dependent on several factors; such as distance to boundary, formation properties and fluid properties. There are

two main types of reservoir boundaries; impermeable and constant pressure. Impermeable boundaries (closed boundary) are present where the reservoir is sealed and no flow occurs. A constant pressure boundary occurs seldom where there is an aquifer support or a large gas cap.

Once CO_2 is injected to a reservoir, some alterations such as; permeability, porosity, and viscosity values occur in a specific part of the original reservoir which is described as a composite reservoir. The composite reservoir consists of an inner swept region and an outer unswept region. Its geometry is quite straightforward. The common analytical composite models are the radial and the linear composite. In most cases this definition is valid within the time limits of a well test and radius of investigation.

Analytical solutions for the pressure behavior of composite reservoirs of various flow geometries have been presented in the following Figure.

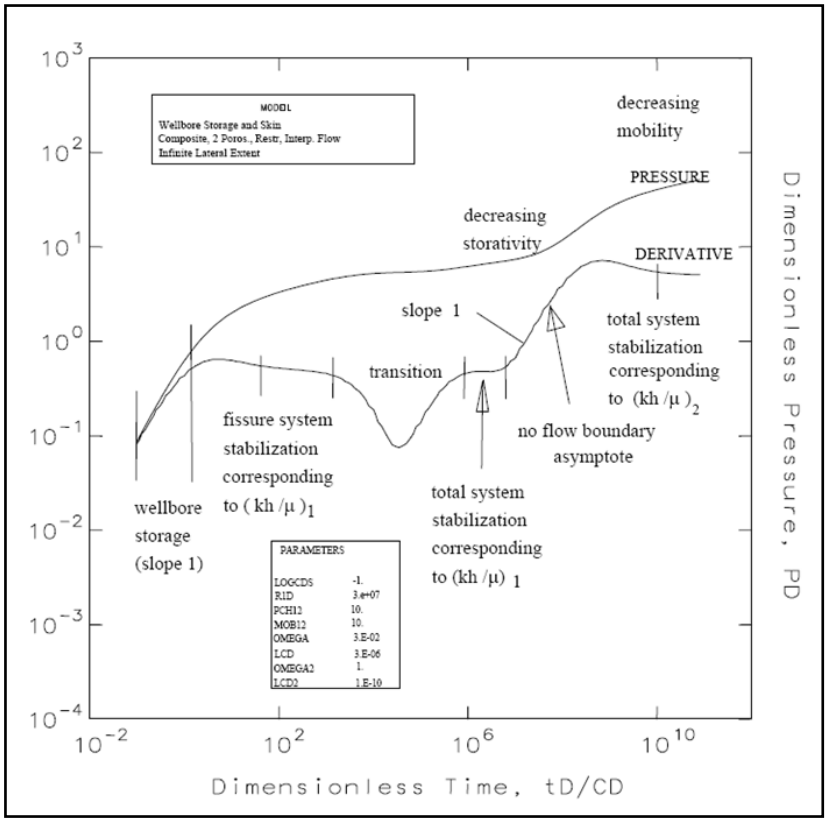

Figure 4- 12 Flow Geometries of a Composite Reservoir [27]

Another result obtained from well test analysis is the radius of investigation. It is an essential concept for designing well tests and for determination of pore volume and the hydrocarbons investigated during test. The most common definition of radius of investigation is linked to the circular area where flow would reach pseudo-steady state at a given time is:

$$r_{inv} = \left(\frac{kt}{948\emptyset\mu C_t}\right)^{1/2} \qquad (4.27)$$

Where time, t, is in hours and radius of investigation is in feet.

In a naturally fractured reservoir radius of investigation is dependent on flow time, the relative storativity of matrix and fractures and the size and shape of the matrix blocks. Several authors define different expression for radius of investigation in naturally fractured reservoirs.

In this study, one radius of investigation calculated for the boundary that is created by the carbon dioxide.

CHAPTER 5

SIMULATION RESULTS, ANALYSIS AND DISCUSSION

After building a numerical model, by changing fracture and spacing, ten different cases (Figure 5.1) were created. For all cases following main reservoir properties summarized in table 5.1 were used.

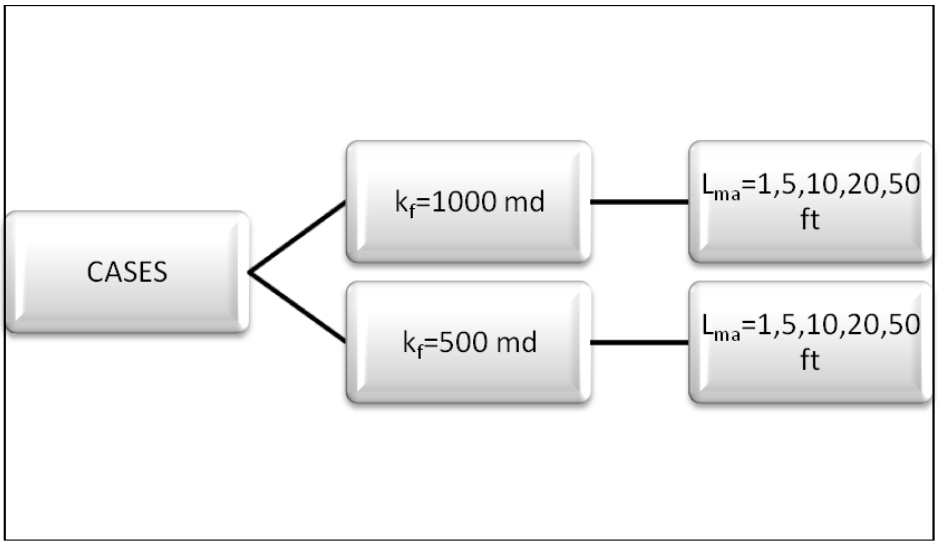

Figure 5- 1 Summary of simulation cases

Table 5- 1 Reservoir parameters

RESERVOIR PARAMETERS	VALUES
Grid Cell Dimensions	3804x3804x100 ft
Reservoir Thickness	100 ft
Initial Pressure	1365 psi
Reservoir Temperature	127 °F
Matrix Porosity	0.15
Matrix Compressibility	1×10^{-5} 1/psi
Matrix Permeability	100 md
Fracture Porosity	0.01
Fracture Compressibility	96×10^{-6} 1/psi

Every case was run for 38 years. In the model, there are three wells, two of which are producers and the other one is injector for carbon dioxide. Producer wells were located at the corner of the reservoir (1, 1, 1 and 1, 20, 1) and the injector was located at the center of the reservoir (1, 11, 1). The vertical injection well was set to inject at a constant rate 1 MMSCF/DAY. Two vertical production wells were set to produce at a constant rate 50 bbl/day.

Build up periods were selected by observing the spread of carbon-dioxide through the grids and layers. After a certain injection time, production wells were shut in for 20 days whereas carbon-dioxide injecting was proceeding.

From the result files pressure data were extracted and load onto KAPPA's Ecrin. Semi-log and log-log analysis have conducted.

For the cases where fracture spacing was equal to 1 ft, well test results were not as expected. For these cases, simulation was run for 38 years and build

up test was conducted after some injection periods, (360, 720, 1440, 1800, 2880, 3600, 4320, 5400, 7920, 9720, 10800, and 13680 days) several times. Fracture permeabilities were taken as 500 md and 1000 md.

In log-log plot, fracture radial flow was not present. Furthermore, transition flow was incomplete or absent. Under these circumstances, well test analysis results could not be reliable. The reason why pressure response did not exhibit any fracture radial flows was related to the fracture spacing value. The reservoir acted as a continuous media because of 1 ft fracture spacing.

Following figure shows the log-log plot response and interpretation results of build up test which was conducted after 720 days of carbon dioxide injection.

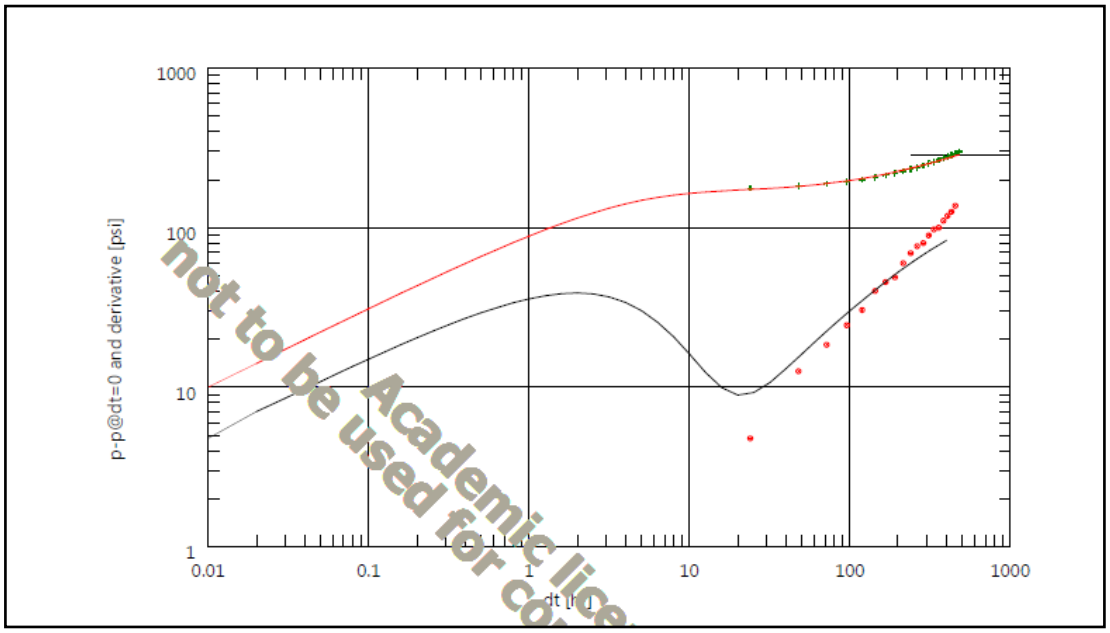

Figure 5- 2-Analysis and results of build up test conducted after 720 days of CO2 injection for the case Lma=1 ft and Kf= 1000 md

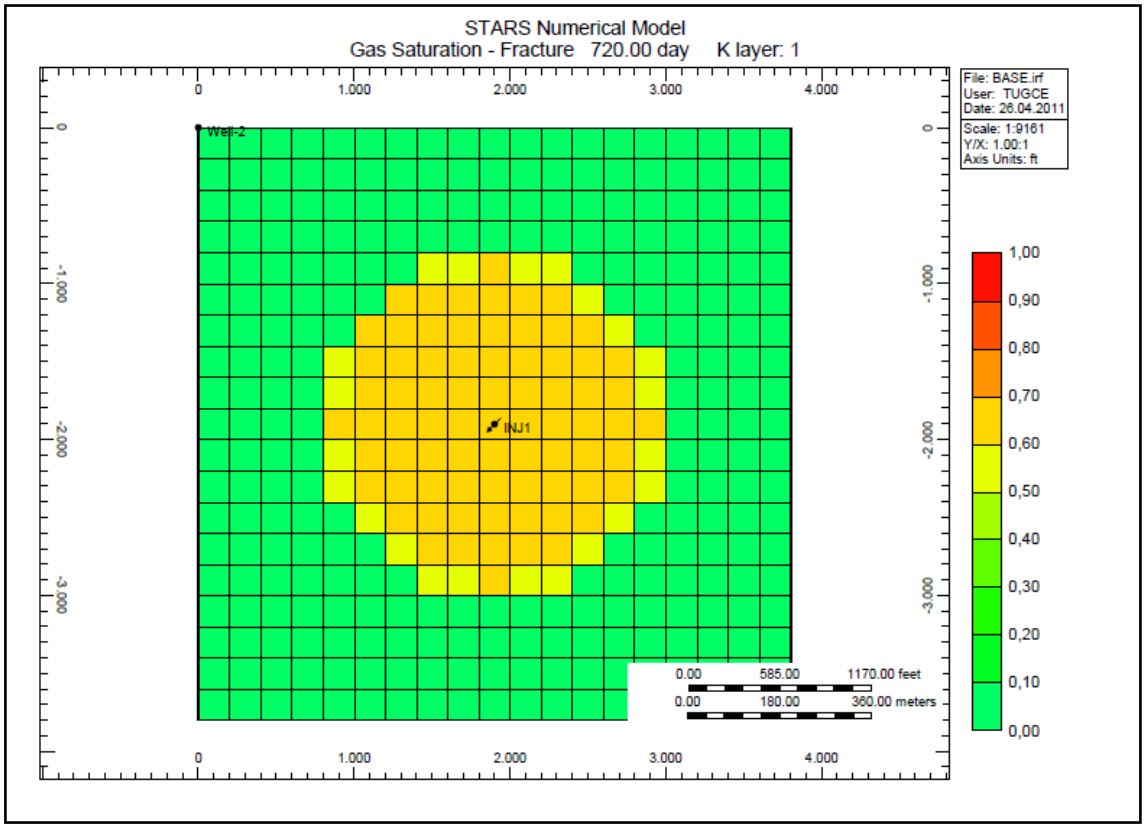

Figure 5- 3-Gas saturation after 720 days of injection for the case Lma=1 ft and Kf= 1000 md

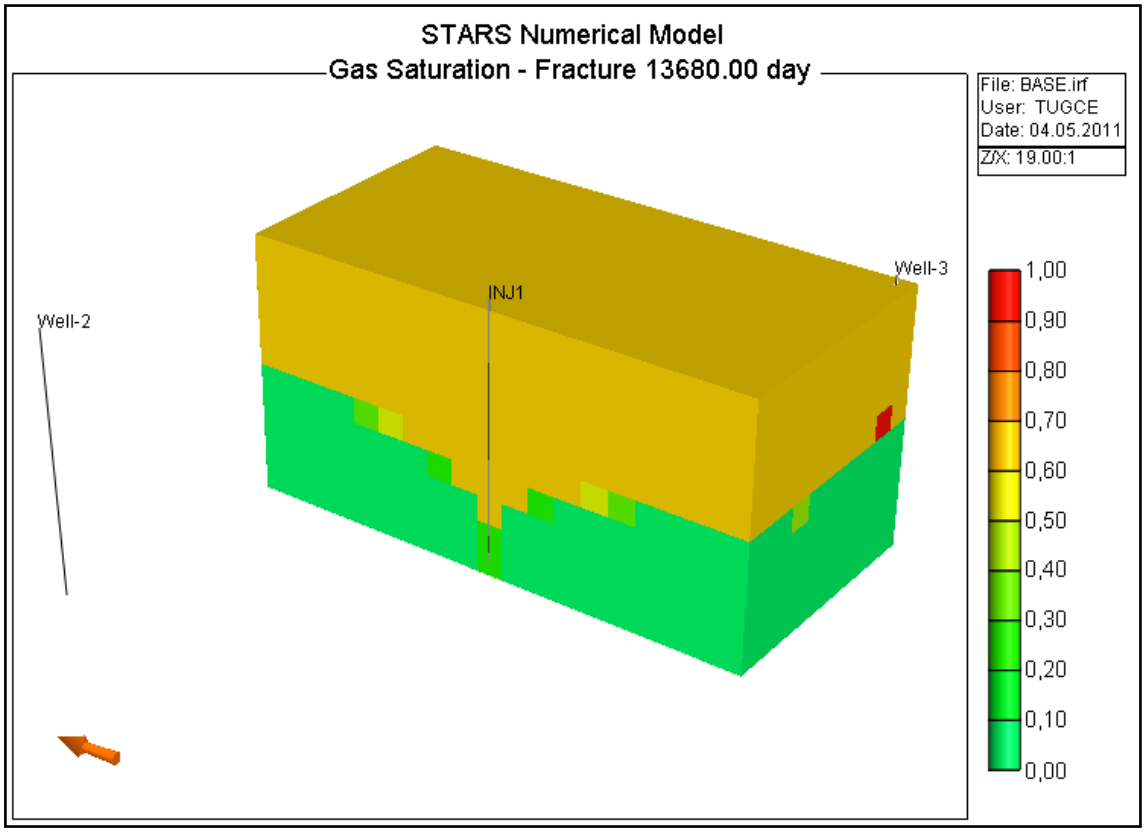

Figure 5- 4-Gas saturation after 38 years of carbon dioxide injection for the case Lma=1 ft and Kf= 1000 md

After performing the analysis for the cases which have fracture spacing value of 1 foot, different values of fracture spacing was set to the models which have fracture permeability of 500 and 1000 md. Log-log and semi-log analysis were carried out for all the cases.

While observing simulation results of carbon-dioxide injection, it can be seen that the carbon-dioxide spread to the layer creating a different zone inside the reservoir which has different rock and fluid properties. It can be concluded that the analysis shows the response of composite reservoir.

To analyze well tests for this case, reservoir has been idealized as composite reservoir. A reservoir undergoing carbon dioxide injection may be described

as a composite reservoir, consisting of an inner carbon dioxide swept region and an outer unswept region.

Boundaries were calculated by observing the spread of carbon dioxide into the grids. Grids which were not filled with carbon-dioxide were counted diagonally till reaching a grid that was filled with carbon-dioxide. Then, the number of grids was multiplied with the diagonal length of a grid which is 282.843 ft.

After calculating the boundary from simulation model, pressure response in log-log plot was examined in order to calculate the carbon-dioxide boundary. In log-log plot, pressure derivative firstly show a double porosity behavior by creating a valley-shape and then it derived horizontally showing the stabilization period. After stabilization period it derived upward, showing the response of the first boundary which was created by the injection of carbon dioxide.

After detecting the first boundary, derivative either derives downward showing the response of double porosity or it derives upward and reaching the external boundary.

As CO_2 was injected to the reservoir, planes at the top of the reservoir were filled with carbon-dioxide. In these cases, unswept region was examined where CO_2 did not spread to the limits of the plane.

When we look at build up test after 13,680 days of carbon-dioxide injection in the ninth case where k_f=500 md and L_{ma}= 20 ft, pressure derivative firstly shows a double porosity behavior then stabilized and derives upward at time

is equal to 2.621 hours, as shown in the Figure 5.17. From this value, boundary was calculated as 555.133 ft.

For the same case, when we look at the carbon-dioxide spread on the numerical model after injecting 13,680 days in the Figure 5.18, we can observe that top five planes were filled with carbon-dioxide. Grid that has gas saturation value of zero is observed at the sixth plane. There are two grids until reaching the carbon-dioxide swept region. By multiplying those with the grid dimension one can calculate the boundary as 565.685 ft.

Boundary analysis for each case and every build up test was performed in the same manner.

From well test analysis interporosity flow coefficient and storativity ratio was calculated and compared with the simulation input for each case. As simulation input these values are calculated for each case by looking at changing porosity and permeability values.

Well tests were analyzed as composite reservoir with circular boundary without wellbore storage and skin. Radius of carbon dioxide unswept region, storativity ratio and interporosity flow coefficients were obtained from the pressure transient analysis. Then, they were compared with the simulation results and tabulated as follows.

5.1 Second Case (k_f=1000md L_{ma}=5 ft)

Table 5- 2-Results and input data for the second case

	Well Test Results		Simulation Inputs	
Injection time, days	**ω**	**λ**	**ω**	**λ**
360	0.360	0.00155	0.355	0.0040
720	0.353	0.00186	0.355	0.0040
4320	0.311	0.00285	0.355	0.0040
7920	0.302	0.00166	0.355	0.0040
9720	0.294	0.00693	0.355	0.0040
10800	0.278	0.00131	0.342	0.0040
13860	0.215	0.00322	0.277	0.0040

Table 5- 3- Boundary calculation for the second case

Injection time,day	Well test,ft	Simulation Result,ft	Comments
360	1903.957	1979.899	(1st plane)
720	1701.749	1697.056	(1st plane)
4320	280.673	282.843	(top layer filled with CO2)(2nd plane)
7920	838.521	848.528	(top 3 layers filled with CO2)(4th plane)
9720	1375.866	1414.214	(top 4 layers filled with CO2)(5th plane)
10800	828.647	848.528	(top 4 layers filled with CO2)(5th plane)
13680	564.479	565.685	(top layer filled with CO2)(2nd plane)

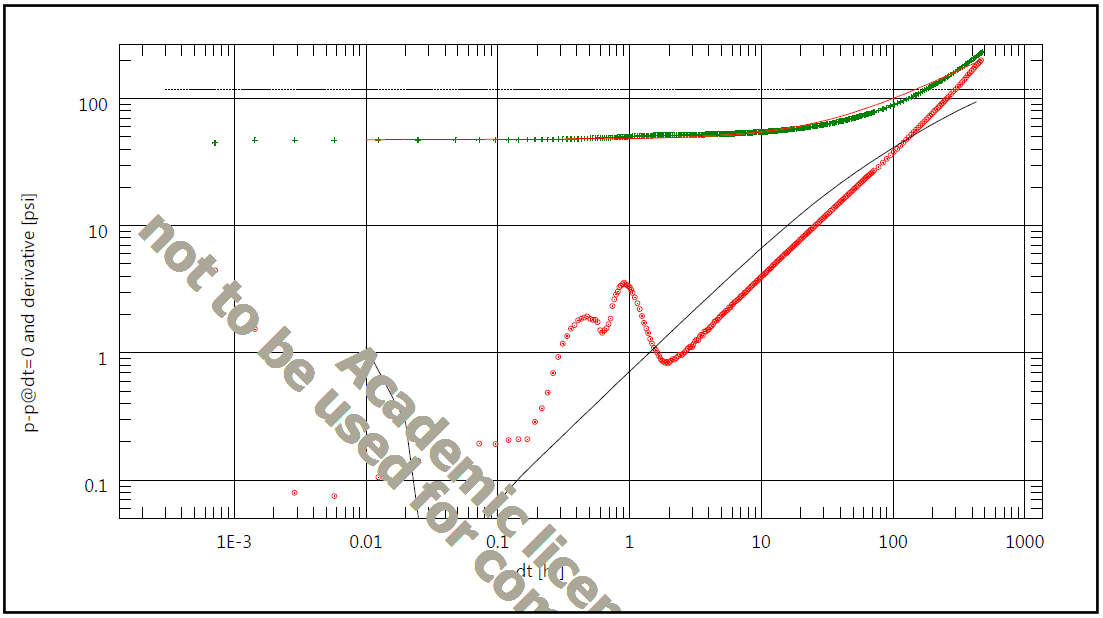

Figure 5- 5-Well test analysis for the second case after 360 days of injection

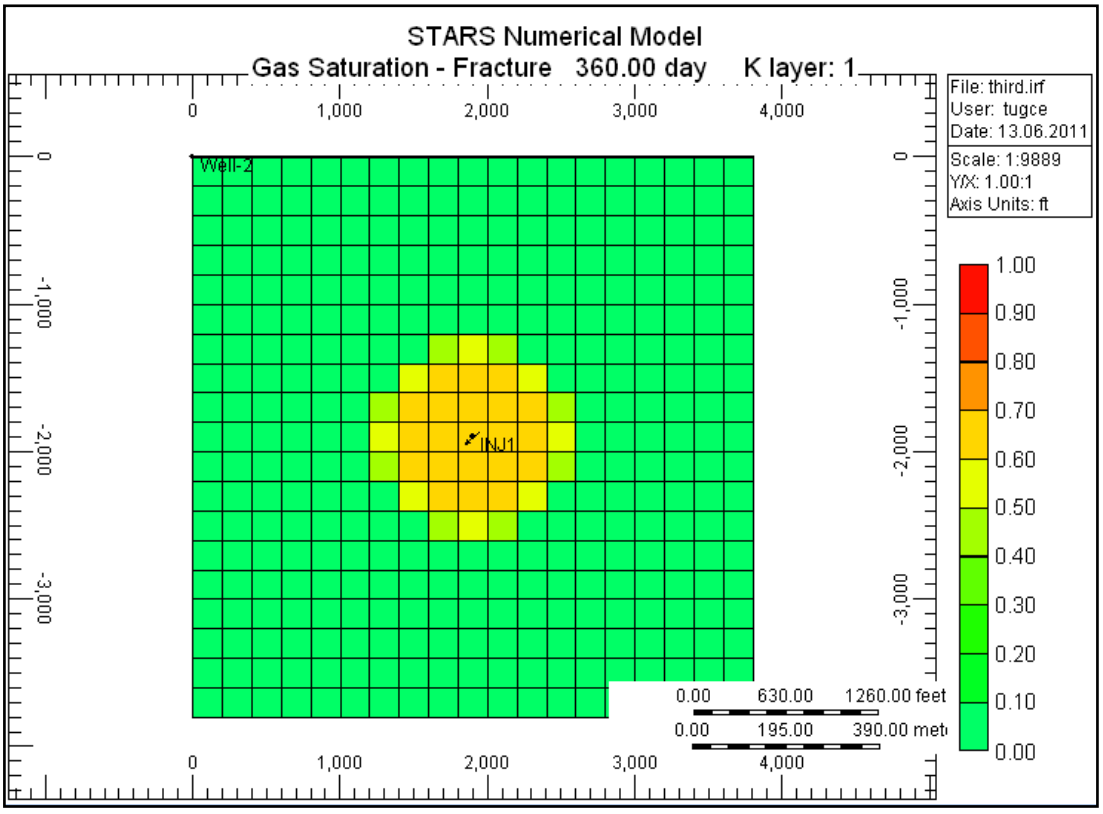

Figure 5- 6-Gas saturation for the second case after 360 days of injection

5.2 Third Case (k_f=1000md L_{ma}=10 ft)

Table 5- 4-Results and input data for the third case

	Well Test Results		Simulation Inputs	
Injection time, days	**ω**	**λ**	**ω**	**λ**
360	0.352	0.0061	0.3637	0.0010
720	0.372	0.00216	0.3637	0.0010
1440	0.363	0.00298	0.3637	0.0010
1800	0.361	0.00443	0.3609	0.0010
5400	0.359	0.00329	0.3571	0.0010
7920	0.341	0.0013	0.3567	0.0010
9720	0.330	0.00115	0.3163	0.0010
13680	0.334	0.00198	0.3082	0.0010

Table 5- 5-Boundary calculation for the third case

Injection time,day	Well test,ft	Simulation Result,ft	Comments
360	1836.019	1979.899	(1st plane)
720	1714.483	1697.056	(1st plane)
1440	1112.698	1131.371	(1st plane)
1800	838.521	848.528	(1st plane)
5400	821.522	848.528	(top 2 layers filled with CO2)(3rd plane)
7920	827.227	848.528	(top 2 layers filled with CO2)(3rd plane)
9720	1644.474	1697.056	(top 4 layers filled with CO2)(5th plane)
13680	1219.093	1272.792	(top 5 layers filled with CO2)(6th plane)

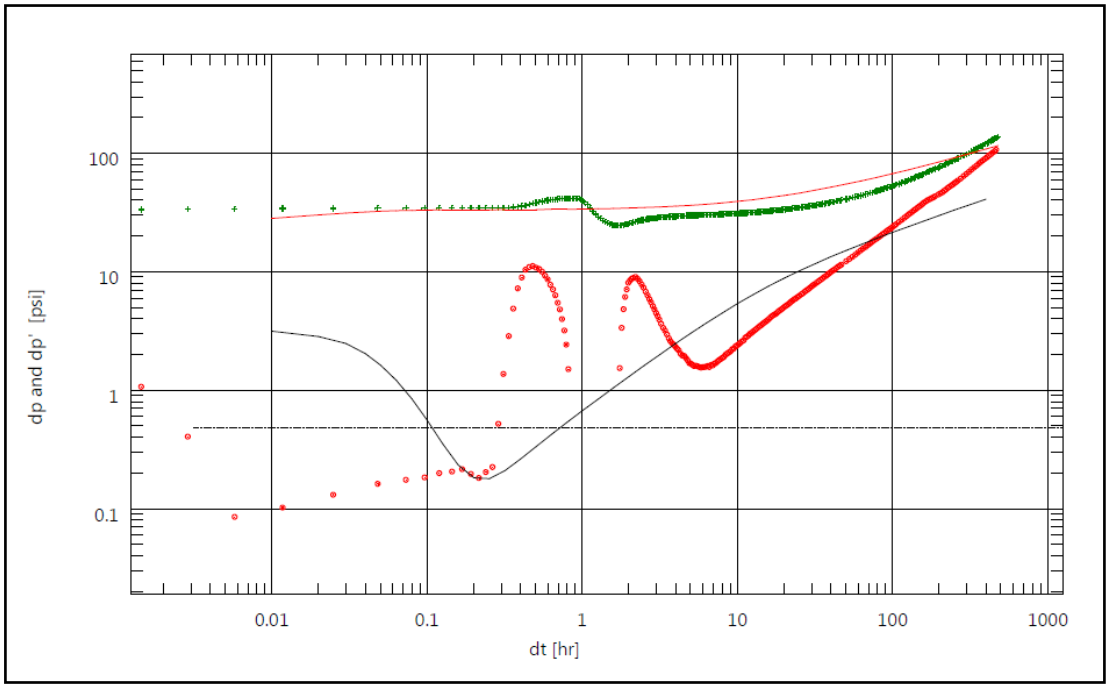

Figure 5- 7-Well test analysis for the third case after 720 days of injection

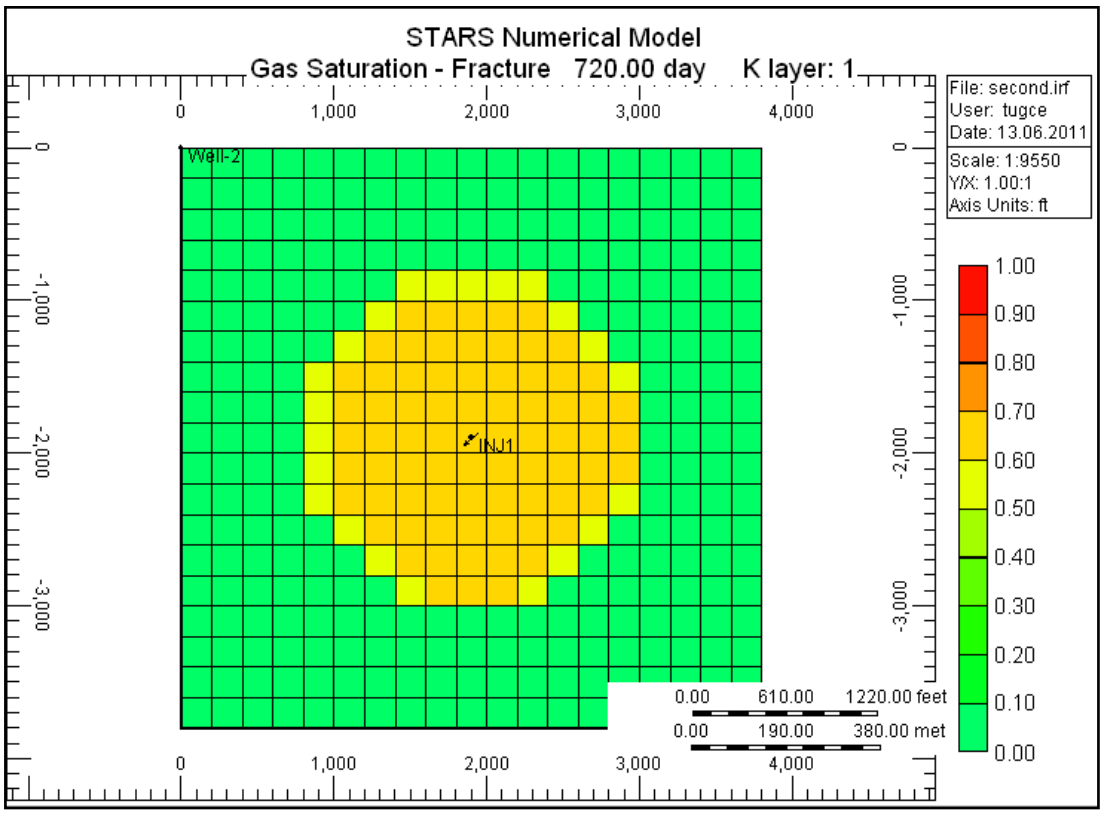

Figure 5- 8-Gas saturation for the third case after 720 days of injection

5.3 Fourth Case (k_f=1000md L_{ma}=20 ft)

Table 5- 6- Results and input data for the fourth case

	Well Test Results		Simulation Inputs	
Injection time, days	**ω**	**λ**	**ω**	**λ**
360	0.3662	0.000263	0.3659	0.00025
720	0.3618	0.00026	0.3659	0.00025
1440	0.3601	0.000457	0.3516	0.00025
1800	0.2753	0.000209	0.2811	0.00025
4320	0.2472	0.000162	0.2671	0.00025
7920	0.2178	0.000122	0.2118	0.00025

Table 5- 7-Boundary calculation for the fourth case

Injection time,day	Well test,ft	Simulation Result,ft	Comments
360	2256.004	2262.742	(1st plane)
720	1691.353	1697.056	(1st plane)
1440	1110.054	1131.371	(1st plane)
1800	844.807	848.528	(1st plane)
4320	821.522	848.528	(top layer filled with CO2)(2nd plane)
7920	513.201	565.685	(top two layers filled with CO2)(3rd plane)

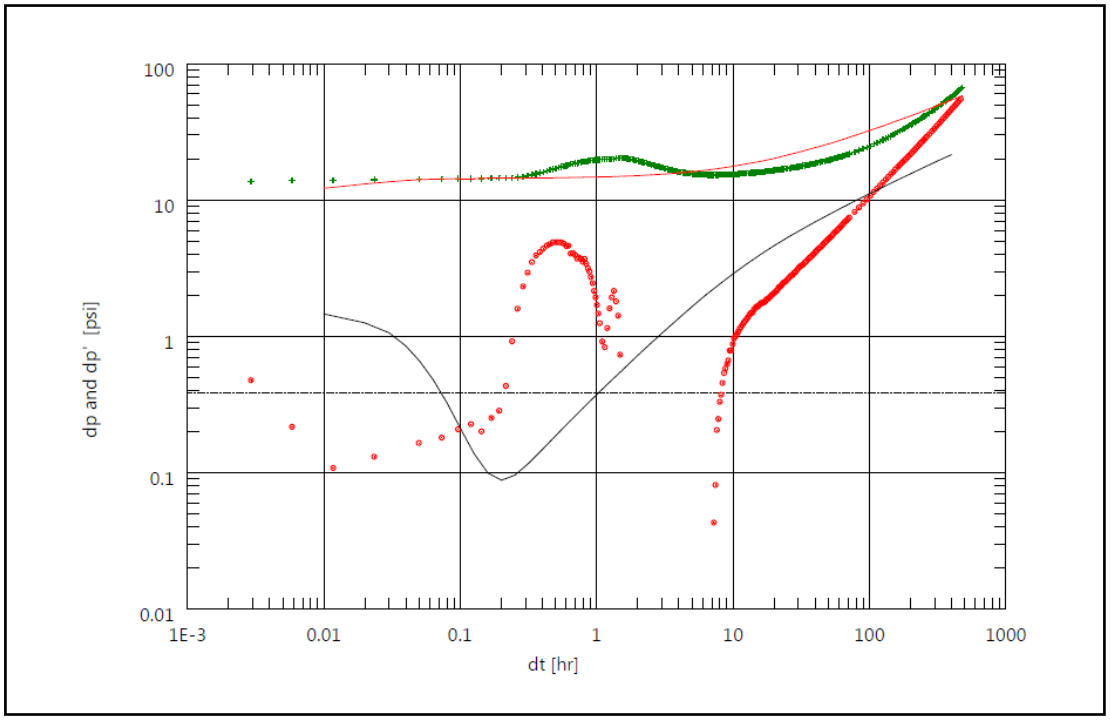

Figure 5- 9Well test analysis for the fourth case after 1800 days of injection

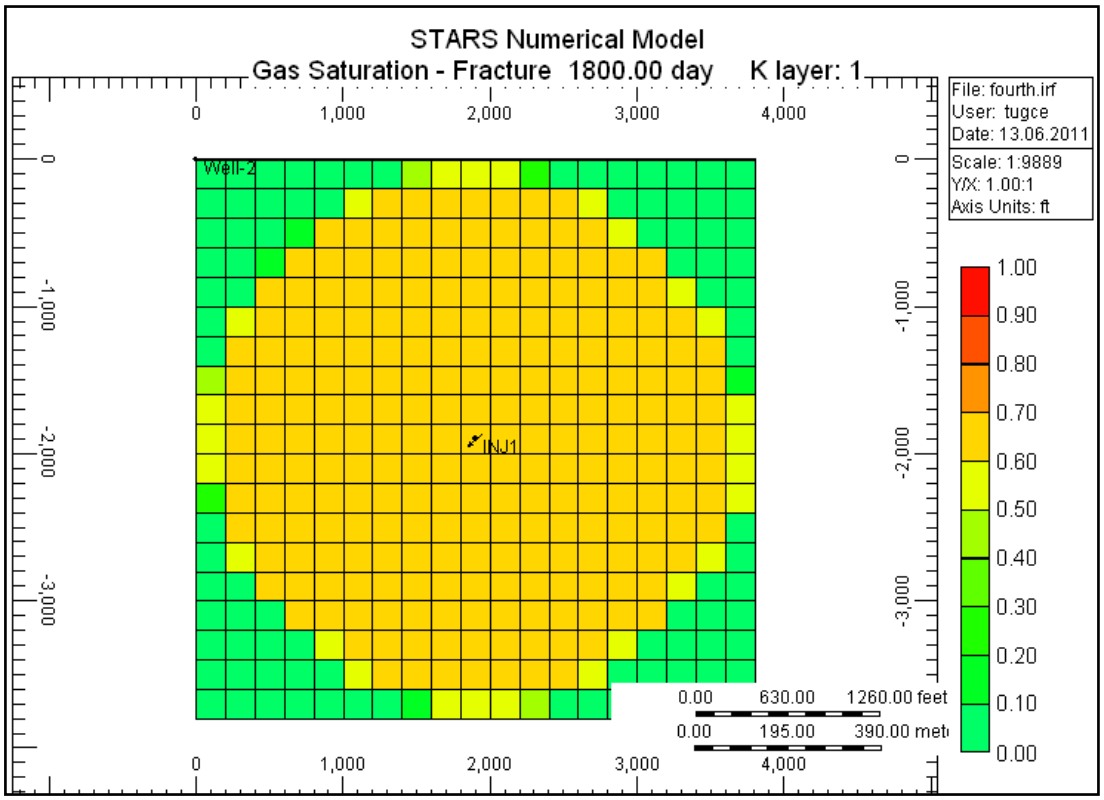

Figure 5- 10-Gas saturation for the fourth case after 1800 days of injection

5.4 Fifth Case (k_f=1000md L_{ma}=50 ft)

Table 5- 8- Results and input data for the fifth case

	Well Test Results		Simulation Inputs	
Injection time, days	**ω**	**λ**	**ω**	**λ**
360	0.392	0.000062	0.3853	0.00004
720	0.358	0.000041	0.3600	0.00004
1440	0.347	0.000033	0.3544	0.00004
1800	0.322	0.000041	0.3021	0.00004
5400	0.314	0.000044	0.3021	0.00004
7920	0.265	0.000057	0.2817	0.00004
9720	0.220	0.000062	0.2176	0.00004
10800	0.169	0.000066	0.1485	0.00004

Table 5- 9- Boundary calculation for the fifth case

Injection time,day	Well test,ft	Simulation Result,ft	Comments
360	1847.542	1979.899	(1st plane)
720	1690.310	1697.056	(1st plane)
1440	1100.479	1131.370	(1st plane)
1800	875.562	848.528	(1st plane)
5400	281.008	282.842	(1st plane)
7920	842.717	848.528	(top layer filled with CO2)(2nd plane)
9720	828.647	848.528	(top layer filled with CO2)(2nd plane)
10800	898.363	848.528	(top layer filled with CO2)(2nd plane)

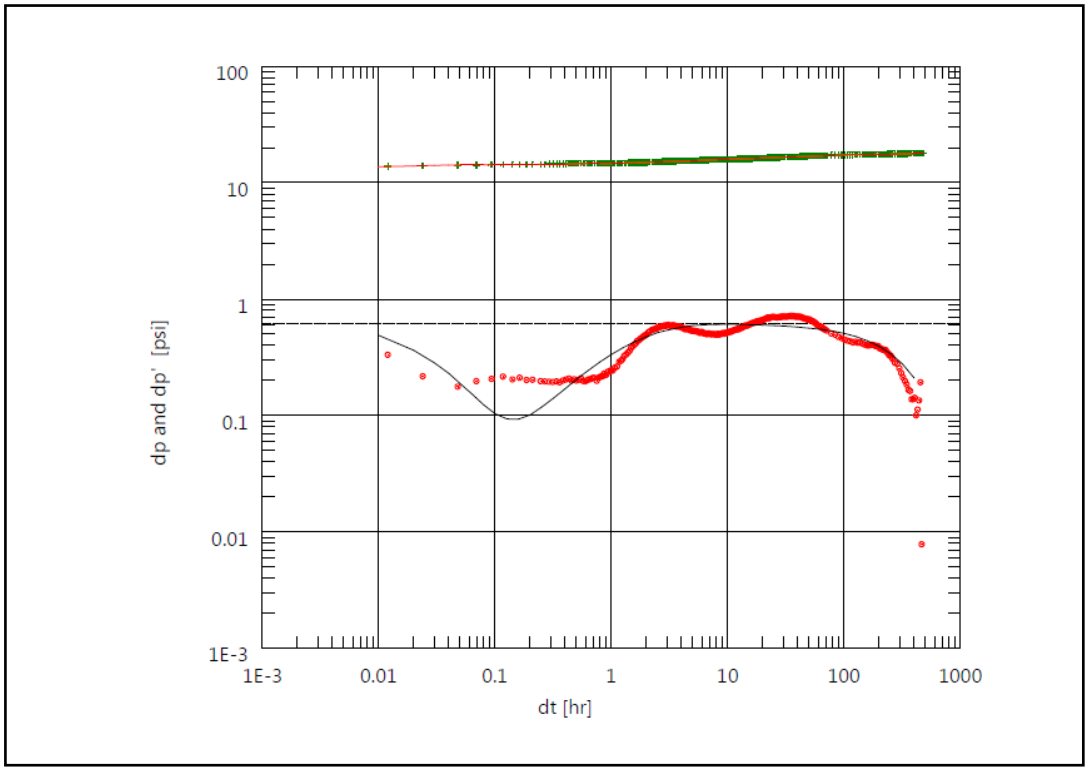

Figure 5- 11- Well test analysis for the fifth case after 5400 days of injection

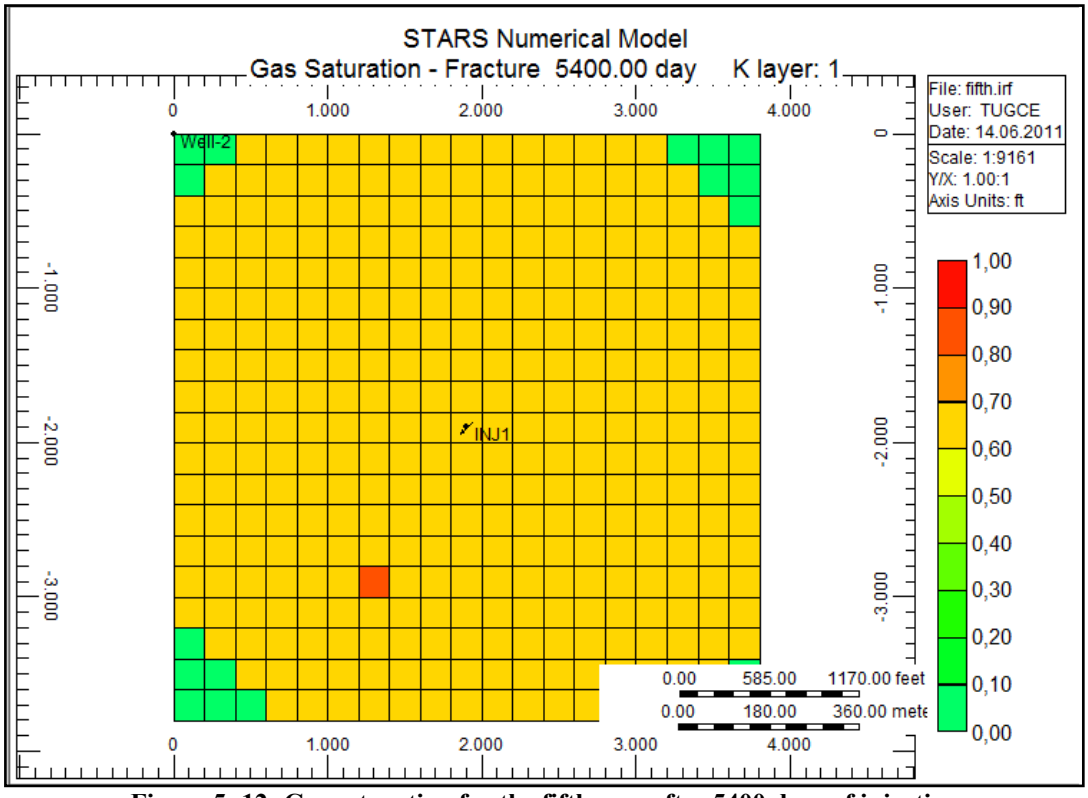

Figure 5- 12- Gas saturation for the fifth case after 5400 days of injection

5.5 Seventh Case (k_f=500md L_{ma}=5 ft)

Table 5- 10- Results and input data for the seventh case

	Well Test Results		Simulation Inputs	
Injection time, days	**ω**	**λ**	**ω**	**λ**
360	0.393	0.00612	0.3851	0.00800
720	0.384	0.00787	0.3826	0.00800
1440	0.378	0.00761	0.3826	0.00795
1800	0.369	0.00863	0.3794	0.00795
4320	0.345	0.00944	0.3525	0.00795
5400	0.321	0.00568	0.3296	0.00795
7920	0.286	0.00624	0.2981	0.00795
9720	0.248	0.00829	0.2579	0.00795
10800	0.191	0.00740	0.1816	0.00795

Table 5- 11- Boundary calculation for the seventh case

Injection time,day	Well test,ft	Simulation Result,ft	Comments
360	1964.741	1979.899	(1st plane)
720	1666.845	1697.056	(1st plane)
1440	1363.850	1414.214	(1st plane)
1800	1115.337	1131.371	(1st plane)
4320	239.685	282.843	(1st plane)
5400	153.348	141.421	(top layer filled with CO2)(2nd plane)
7920	1111.641	1131.371	(top 3 layers filled with CO2)(4th plane)
9720	543.251	565.685	(top 3 layers filled with CO2)(4th plane)
10800	840.622	848.528	(top 4 layers filled with CO2)(5th plane)

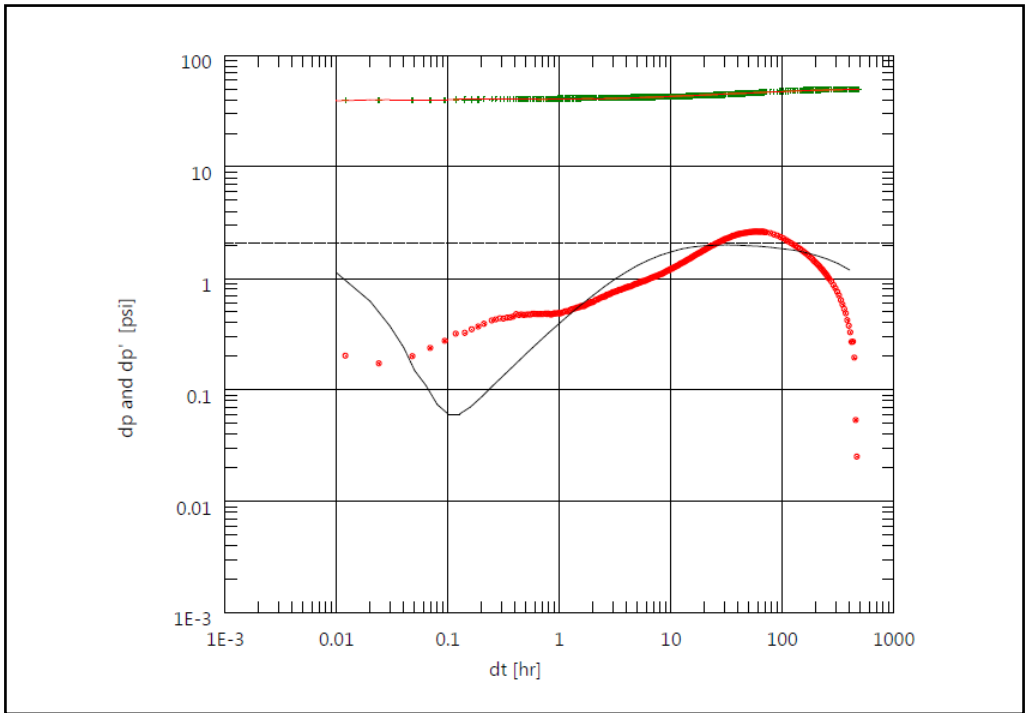

Figure 5- 13- Well test analysis for the seventh case after 7920 days of injection

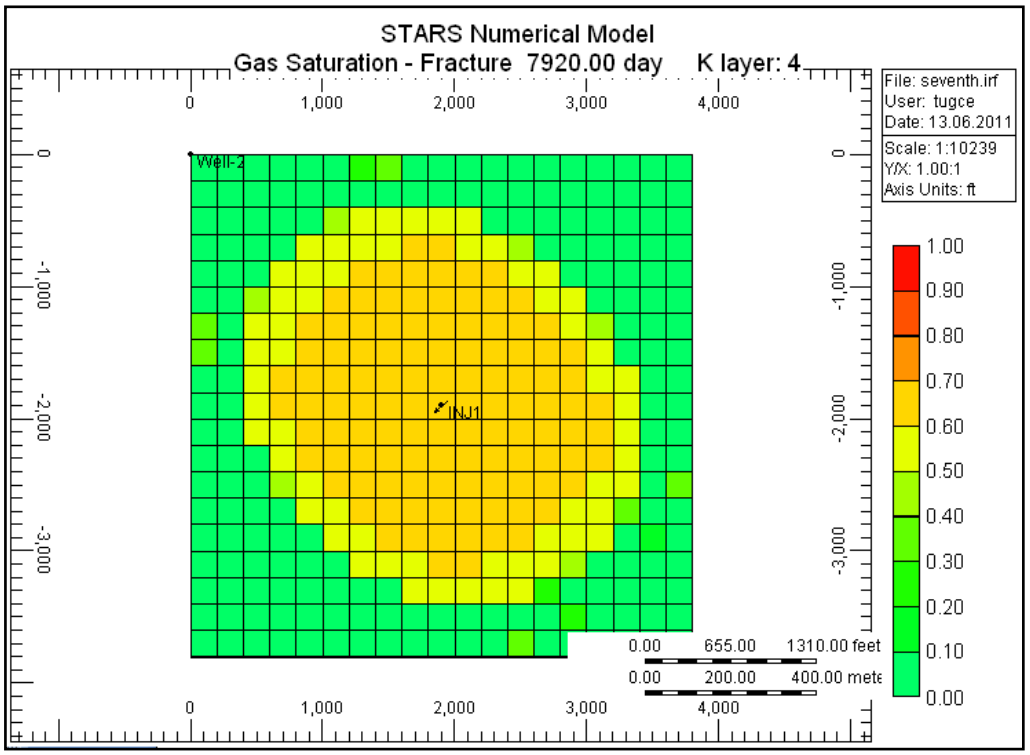

Figure 5- 14-Gas saturation for the seventh case after 7920 days of injection

5.6 Eighth Case (k_f=500md L_{ma}=10 ft)

Table 5- 12- Results and input data for the eighth case

	Well Test Results		Simulation Inputs	
Injection time, days	**ω**	**λ**	**ω**	**λ**
360	0.399	0.00388	0.3759	0.00200
720	0.378	0.00412	0.3646	0.00200
1440	0.359	0.00362	0.3481	0.00199
1800	0.345	0.00386	0.3465	0.00199
2880	0.336	0.00301	0.3311	0.00199
3600	0.332	0.00487	0.3255	0.00199
4320	0.305	0.00315	0.3189	0.00199
7920	0.274	0.00541	0.2989	0.00199
9720	0.212	0.00618	0.2491	0.00199
10800	0.203	0.00407	0.2243	0.00199
13680	0.091	0.00211	0.1135	0.00199

Table 5- 13- Boundary calculation for the eighth case

Injection time,day	Well test,ft	Simulation Result,ft	Comments
360	2217.749	2262.742	(1st plane)
720	1666.845	1697.056	(1st plane)
1440	1385.803	1414.214	(1st plane)
1800	1117.601	1131.371	(1st plane)
2880	544.332	565.685	(1st plane)
3600	514.939	565.685	(1st plane)
4320	247.266	282.842	(1st plane)
7920	1350.856	1414.214	(top 4 layers filled with CO2)(5th plane)
9720	556.613	565.685	(top 4 layers filled with CO2)(5th plane)
10800	1355.548	1414.214	(top 5 layers filled with CO2)(6th plane)
13680	1371.501	1414.214	(top 6 layers filled with CO2)(7th plane)

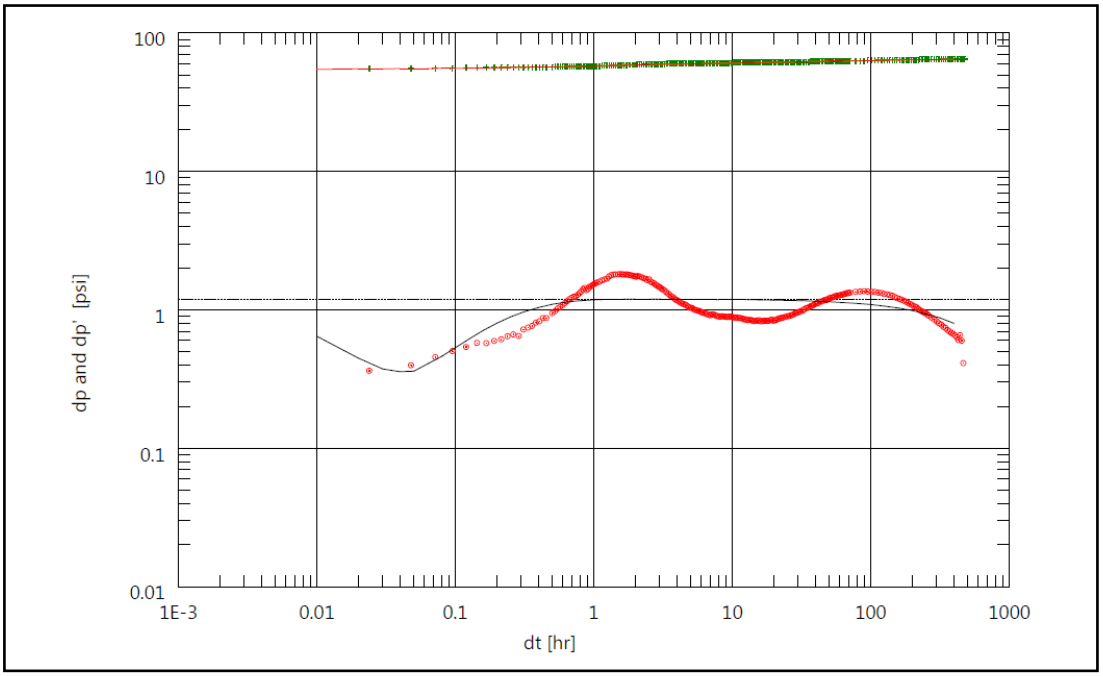

Figure 5- 15- Well test analysis for the eighth case after 10800 days of injection

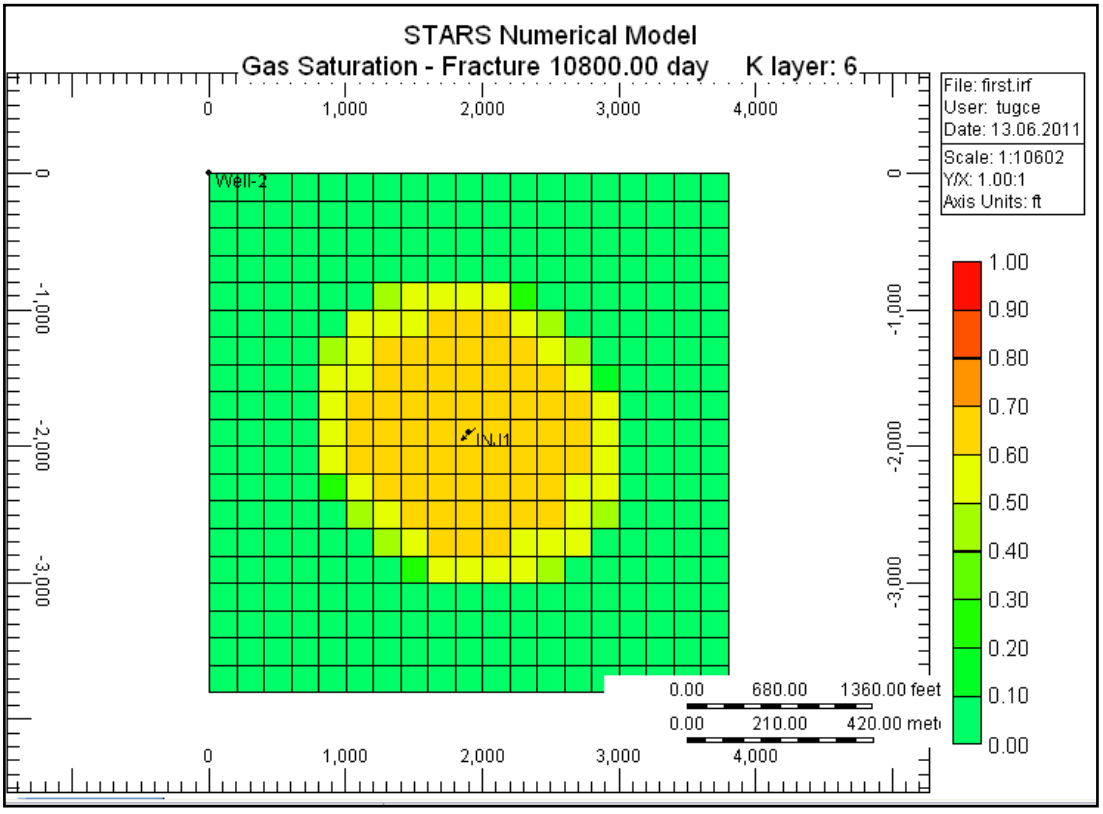

Figure 5- 16-Gas saturation for the eighth case after 10800 days of injection

5.7 Ninth Case (k_f=500md L_{ma}=20 ft)

Table 5- 14- Results and input data for the ninth case

	Well Test Results		Simulation Inputs	
Injection time, days	**ω**	**λ**	**ω**	**λ**
360	0.404	0.000688	0.3881	0.0005
720	0.370	0.000443	0.3694	0.0005
1440	0.346	0.000661	0.3598	0.0005
1800	0.322	0.000781	0.3389	0.0005
2880	0.295	0.000479	0.3098	0.0005
5400	0.248	0.000630	0.2522	0.0005
9720	0.237	0.000505	0.2255	0.0005
13680	0.214	0.000669	0.2117	0.0005

Table 5- 15- Boundary calculation for the ninth case

Injection time,day	Well test,ft	Simulation Result,ft	Comments
360	2249.334373	2262.7417	(1st plane)
720	1638.386106	1697.056275	(1st plane)
1440	1372.443758	1414.213562	(1st plane)
1800	1126.977867	1131.37085	(1st plane)
2880	803.330195	848.5281374	(1st plane)
5400	841.3206452	848.5281374	(top 2 layers filled with CO2)(3rd plane)
9720	1127.395112	1131.37085	(top 4 layers filled with CO2)(5th plane)
13680	555.1327012	565.6854249	(top 5 layers filled with CO2)(6th plane)

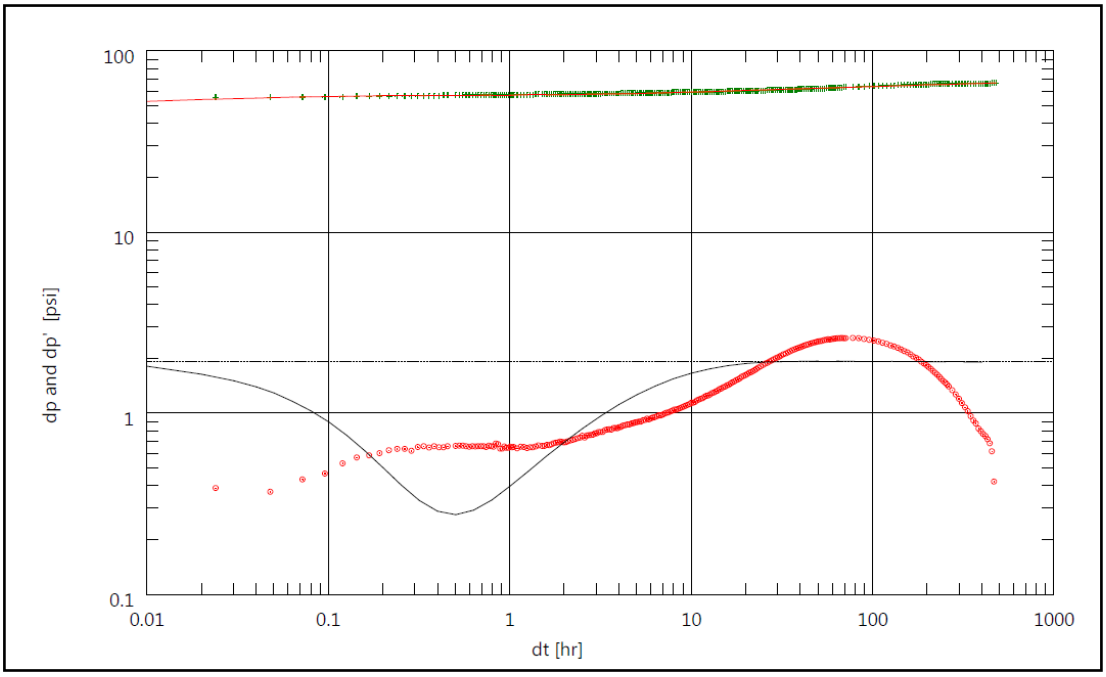

Figure 5- 17-Well test analysis for the ninth case after 13680 days of injection

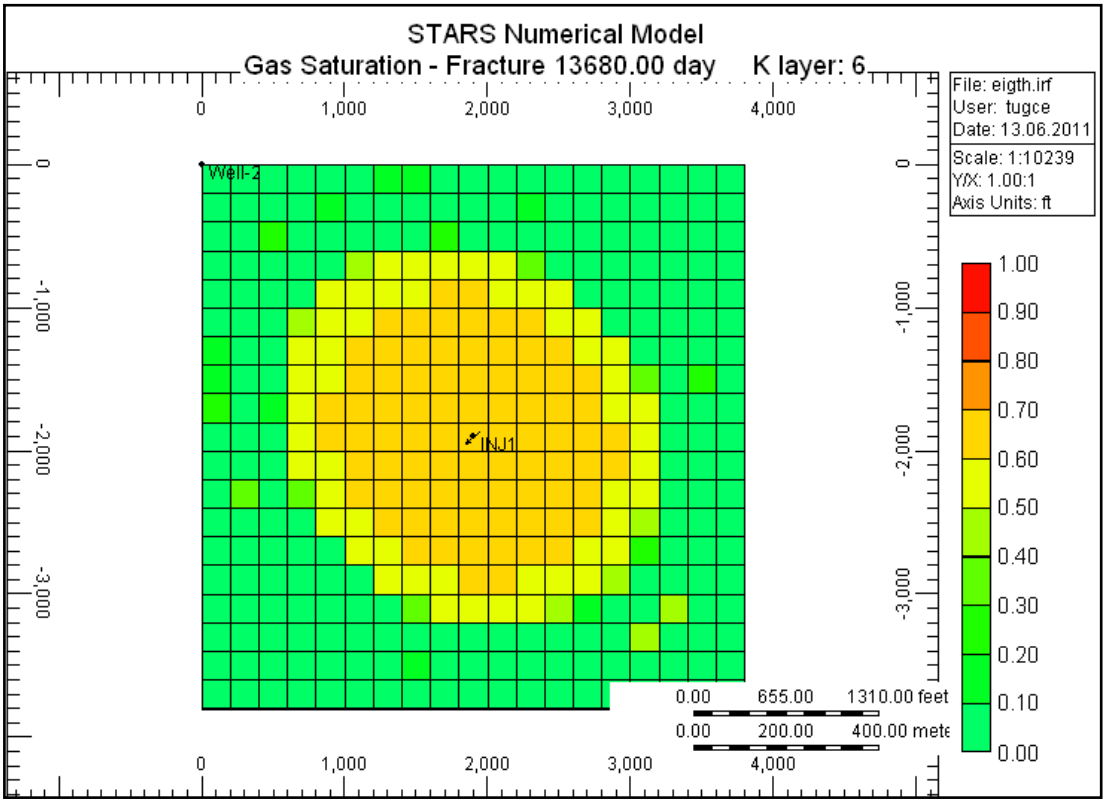

Figure 5- 18-Gas saturation for the ninth case after 13680 days of injection

5.8 Tenth Case (k_f=500md L_{ma}=50 ft)

Table 5- 16-Results and input data for the tenth case

	Well Test Results		Simulation Inputs	
Injection time, days	**ω**	**λ**	**ω**	**λ**
360	0.396	0.000235	0.3899	0.0001
720	0.371	0.000093	0.3863	0.0001
1440	0.330	0.000129	0.3660	0.0001
1800	0.323	0.000106	0.3581	0.0001
5400	0.299	0.000229	0.3321	0.0001
9720	0.168	0.000164	0.1480	0.0001
10800	0.124	0.000194	0.1135	0.0001

Table 5- 17-Boundary calculations for tenth case

Injection time,day	Well test,ft	Simulation Result,ft	Comments
360	2244.101	2262.742	(1st plane)
720	1928.470	1979.899	(1st plane)
1440	1386.931	1414.214	(1st plane)
1800	1102.508	1131.371	(1st plane)
5400	263.0713	282.843	(top layer filled with CO2)(2nd plane)
9720	557.563	565.685	(top 3 layers filled with CO2)(4th plane)
10800	1393.275	1414.214	(top 4 layers filled with CO2)(5th plane)

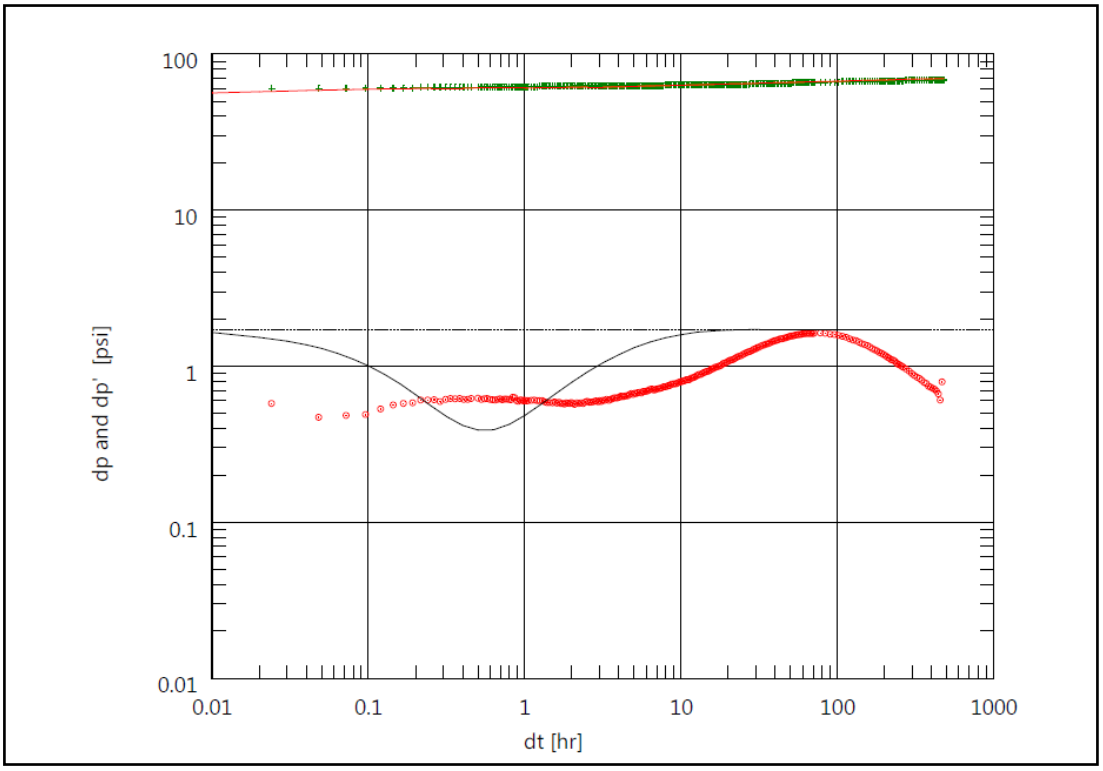

Figure 5- 19- Well test analysis for the tenth case after 10800days of injection

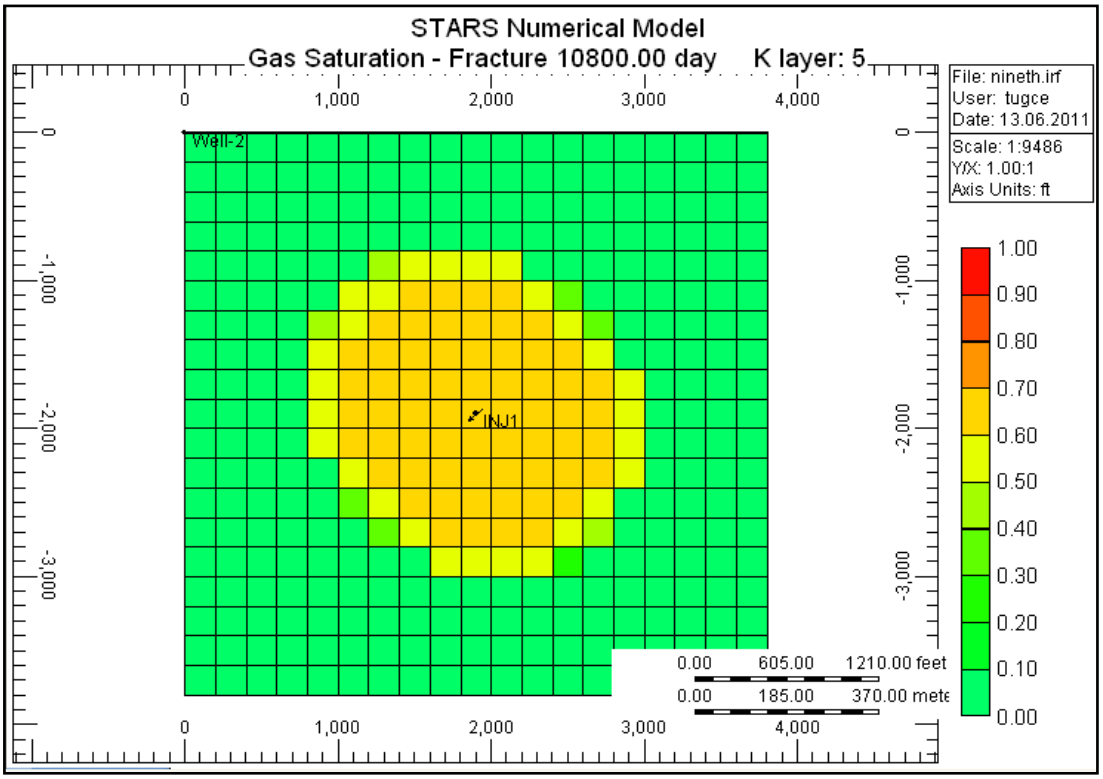

Figure 5- 20-Gas saturation for the tenth case after 10800 days of injection

In all cases, interporosity flow coefficient and storativity ratio estimated from well test analysis were slightly different.

As carbon dioxide is injected to the reservoir, fracture porosity decreases as shown in the Figure 5.22. Therefore reduction in the storativity ratio is observed in different test time.

Permeability of reservoir slightly changes during the injection of carbon-dioxide. The change is mainly observed around the injector. Value of permeability change near the production well is very small, which can be neglected. (Figure 5.23)

In the cases which fracture spacing has value of 20 feet and 50 feet; the system radial flow cannot be reached. One of the reasons of the absence of the system radial flow can be insufficient shut in period. Although shut-in periods were increased up to 30 days for the first, system radial flow still not reached.

In log-log plot pressure response stabilized at average reservoir pressure and pressure derivative was decreasing and approaching through the zero. In semi log plot, pressure plot draw a horizontal line and stabilized at average reservoir pressure. These responses show the behavior of the circular boundary.

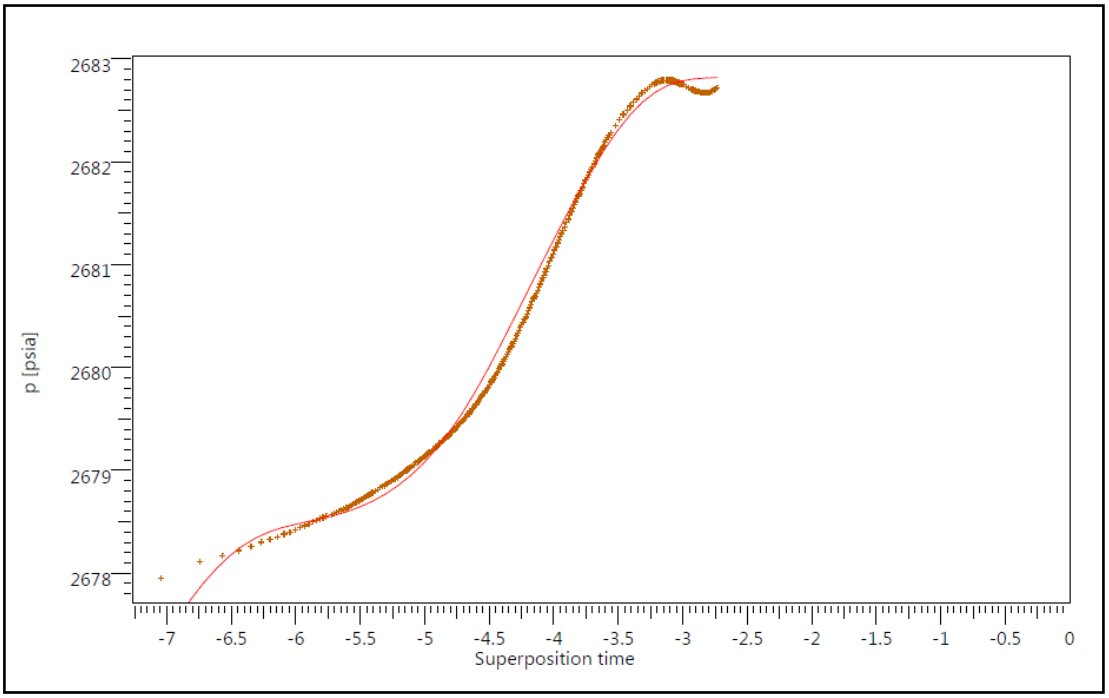

Figure 5- 21-Semi log analysis example for the fifth case with circular boundary

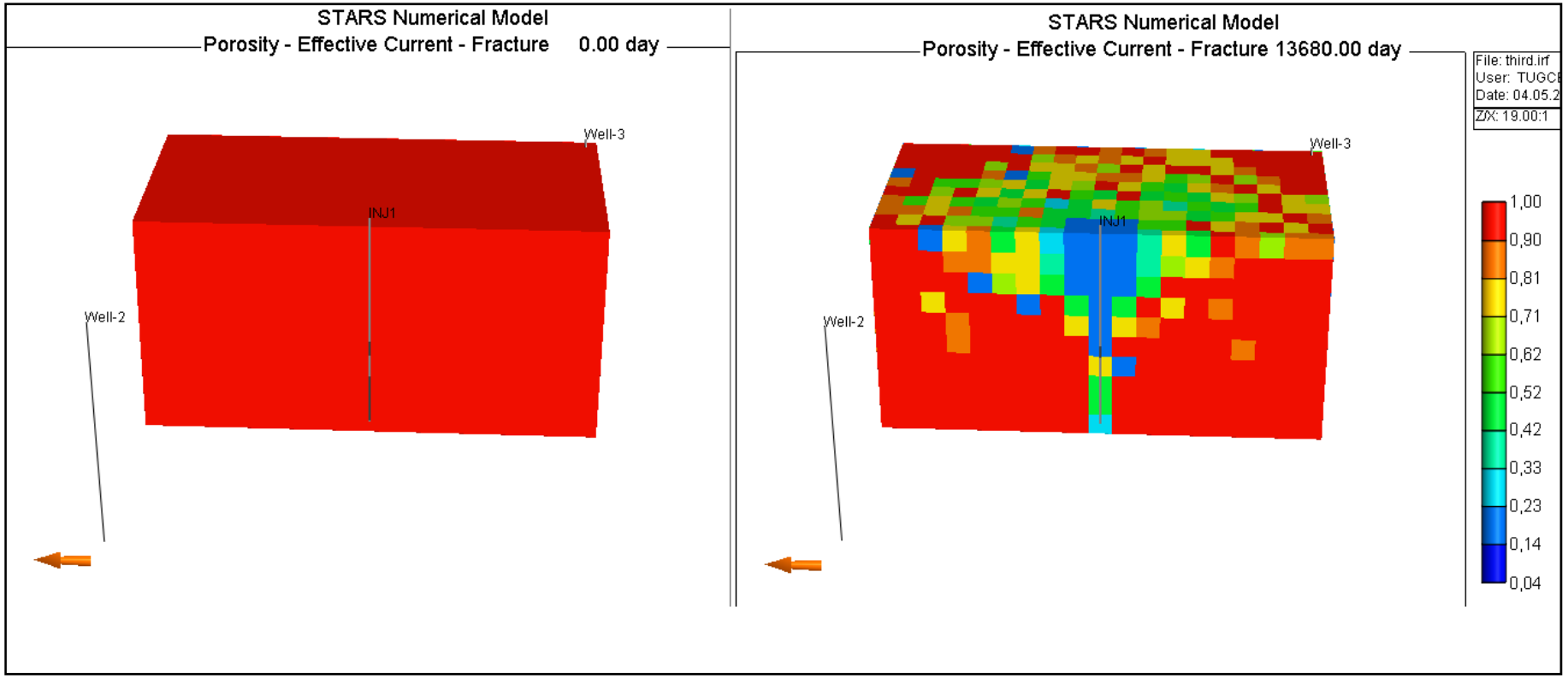

Figure 5- 22-Porosity alteration after 38 years of CO2 injection

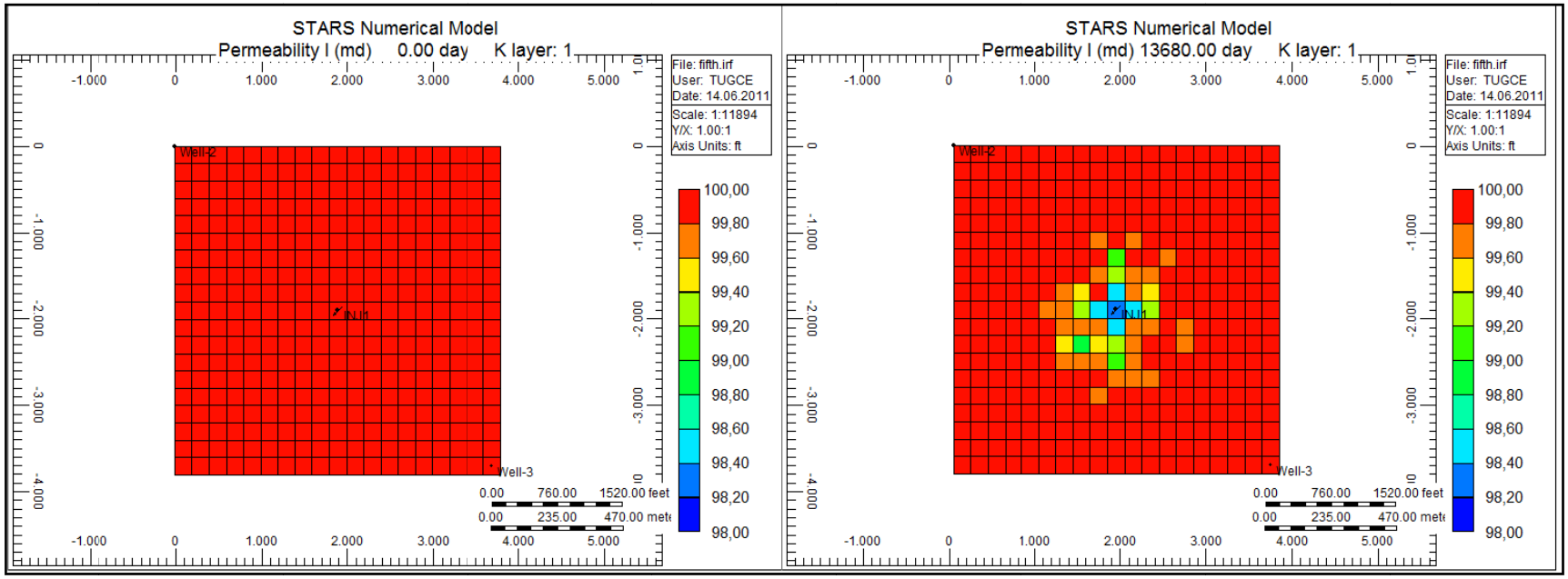

Figure 5- 23-Permeability alteration after 38 years of CO2 injection

CHAPTER 6

CONCLUSION

Various models are constructed to perform well test analysis in naturally fractured reservoirs in the presence of carbon dioxide. Results estimated from well tests analysis compared with the calculated input data. Based upon work performed for this thesis the following conclusions were drawn.

1. Chemical reactions occurred at the reservoir resulted in the permeability and porosity reduction cause change in the storativity ratio and interporosity flow coefficient.

2. The existence of carbon dioxide in naturally fractured reservoirs can cause uncertainty in well test analysis result.

3. Storativity ratio obtained from the analysis is decreasing as carbon dioxide injected to the system in all cases with different fracture spacing.

4. In order to obtain reliable results from the well test analysis, well test pressure response should exhibit a complete flow regimes; fracture radial flow, transition flow, and system radial flow.

5. In reservoir which fracture spacing has the value of 1 ft, the estimation cannot be done, since presence of any fracture radial flow is missing. The reservoir acts as a continuous media.

6. In reservoir with fracture spacing bigger than 20 ft, fracture radial flow period is longer than the smaller values. In these values, transitional flow and system radial flow could not be existed.

7. In higher fracture permeability case, the transition and system radial flows could be distorted because of the boundary effect.

8. CO_2 injection creates separate zones and alters some parameters in the reservoir. The analytical solutions which model these cases are composite models. Well test analyses of that are performed in terms of these models.

9. Calculated swept boundaries, interporosity flow coefficient and storativity ratio values from well test analysis comply with the simulation results.

REFERENCES

1. Warren J.E. and Root P.J.: "The Behavior of NFR" 245, SPEJ, September, 1963.

2. Abduss Satter and Jim Baldwin, Rich Jespersen.: "Computer Assisted Reservoir Management," Tulsa, Oklahoma : PennWell Corperation, 2000.

3. Robert C. Earlougher, Jr.: "Advances in Well Test Analysis," New York : Society of Petroleum Engineers AIME, 1977.

4. Lee, John.: "Well Testing," New York : Society of Petroleum Engineers of AIME, 1982. 0895203170.

5. T.D., Van Golf-Racht.: "Fundamentals of Fractured Reservoir Engineering," New York : Elsevier Scientific Publishing Company, 1982.

6. Nelson, R.A.: "Geologic Analysis of Naturally Fractured Reservoirs," Woburn,MA : Gulf Professional Publishing, 2001.

7. Aguilera, Roberto.: "Naturally Fractured Reservoirs," Tulsa, Oklahoma : PennWell Publishing Company, 1980.

8. Pollard, P.: "Evaluation of Acid Treatments from Pressure Buildup Analysis," Trans. AIME, 1959. 216, 38.

9. Pirson, R.S. and Pirson, S. J.: "An Extension of the Pollard Analysis Method of Well Pressure Build-up and Drawdown Tests," Dallas,Texas : SPE Annual Fall Meeting, 1961.

10. Kazemi, H.: "Pressure Transient Analysis of NFR with Uniform Fracture," SPEJ, 1969. 451.

11. Mavor, M.J and Cinco-ley, H.: "Transient Pressure Behavior of NFR," Ventura, California : SPE California Regional Meeting, 1979. SPE 7977.

12. De Swaan O. A.: "Analytic Solutions for Determining NFR Properties by Well Testing," SPEJ, 1976, 117.

13. Najuireta, H. L.: "A Theory for the Pressure Transient Analysis in NFR," New Orleans : SPE Annual TEchnical Conference, 1976. SPE 6017.

14. Moench, A. F.: "Double-Porosity Models for a Fissured Groundwater Reservoir with Fracture Skin," Water Resources Research, 1984. 831.

15. Cinco-Ley, H., Samaniego, V. F. and Dominguez, A. N.: "Unsteady-State Flow Behavior for a Well Near a Natural Fracture," New Orleans : SPE Annual Technical Conference and Exhibition, 1976. SPE6019.

16. Bourdet, D., Ayoub J., Whittle T., Pirard Y., and Kniazeff V.: "Interpreting Well Tests in Fractured Reservoirs," World Oil. 1983, 77.

17. Bourdet, D., Whittle T., Douglas A., and Pirard Y.: "New Type Curves Aid Analysis of Fissured Zone Well Tests," World Oil. 1984, 111.

18. Abdassah, D. and Ershaghi, I.: "Triple-porosity Systems for Representing Naturally Fractured Reservoirs, 113, SPE Formation Evaluation, 1986.

19. Dreier, J., Ozkan, E. and Kazemi, H.: "New Analytical Pressure-Transient Models To Detect And Characterize Reservoirs With Multiple Fracture Systems," Puebla, Mexico : International Petroleum Conference, 2004.

20. Izgec, O., Demiral, B. and Bertin, H. Irvine, and Akın S.: "CO_2 Injection in Carbonates," California : SPE937733, 2005. SPE Western Regional Meeting.

21. Abdulrazag, Y. Z., Shedid, A. S. and Reyadh, A. A.: "An Experimental Investigation of Interactions Between Supercritical CO_2, Aspheltenic Crude Oil, and Reservoir Brine in Carbonate Cores," Houston, Texas : SPE International Symposium on Oilfield Chemistry, 2007. SPE104750.

22. Izgec, O., Demiral, B. and Bertin, and Akın S.: "Experimental and Numerical Modeling of Direct Injection of CO_2 Into Carbonate Formations.

San Antonio : SPE Annual Technical Conference and Exhibition, 2006. SPE100809.

23. Pruess, K. and Xu, T.: "Numerical Modeling of Aquifer Disposal of CO_2," San Antonio, Texas : SPE/EPA/DOE Exploration and Production Enviromental Conferance, 2001. SPE83695.

24. Omole O., Osoba J.S.: "Carbondioxide – dolomite rock interaction during CO_2 flooding process," 34th Annual Technical Meeting of the Petroleum Society of CIM, Canada, 1983.

25. Computer Modeling Group (CMG): CMG STARS User's Guide, Computer Modeling Group LTD., Calgary, Alberta, Canada, 2003

26. Gilman, J.R.: "Practical Aspects of Simulation of Fractured Reservoirs," International Forum on Reservoir Simulation, Germany, June 23-27 2003.

27. KAPPA: Ecrin User Guide, KAPPA Engineering, Paris, France, 2010.

28. Piri, M., Prévost, J.H., and Fuller, R.: "Carbon Dioxide in Saline Aquifers: Evaporation, Precipitation and Compressibility Effects", Conference Proceedings, Fourth Annual Conference on Carbon Capture and Sequestration DOE/NETL, May 2-5, 2005.

APPENDIX A

CRICUAL SIMULATION PARAMETERS

Chemical Reactions

Chemical reactions have traditionally been used almost exclusively in combustion processes. However, reactions may be used in any thermal or isothermal simulation if desired. Since reactions are treated as source/sink terms for each component and energy, they may be thought of as another way in which to link together the different components of a problem when rate is important. In particular, inter-phase mass transfer rates can be modeled, involving either well defined components or "dispersed phase" components such as emulsion droplets. The general heterogeneous mass transfer reaction no. k is represented symbolically as:

$$\sum_{i=1}^{nc} s_{ki} . A_i . \rightarrow \sum_{i=1}^{nc} s'_{ki} . A_i + H_{rk}$$

In this equation:

S_{ki}: reactant stoichiometric coefficient of reaction k

S'_{ki}: product stoichiometric coefficient of reaction k

H_{rk}: Reaction enthalpy

This equation proceeds at the rate of rk moles per day per reservoir volume. As expressed above, this relationship has one degree of freedom, which is a proportionality factor. The quantities ski, s'ki and Hrk can be multiplied by an

arbitrary factor a, but rk must be divided by a so that the source/sink terms remain

$$(s'_{ki} - s_{ki}).rk, H_{rk}.rk$$

Usually the factor a is chosen such that ski = 1 for the main reacting component.

The kinetic model, also known as reaction kinetics, determines the speed of reaction rk. The general expression is

$$rk = r_{rk}.\exp(\frac{-E_{ak}}{R.T}).\prod_{i=1}^{nc} C_i$$

The activation energy Eak determines the temperature dependence of rk. While the enthalpies of reaction can be characterized between well defined limits (and can even be calculated from first principles), the observed activation energies can vary dramatically. This is because certain components in the rock surface can act as catalysts. The concentration factor for reacting component i is

$$Ci = \varphi f.\rho j.sj.xjij = w, o, g$$

where j is the phase in which component i is reacting, and xji represents water, oil

or gas mole fractions.

Here:

j*f* : fluid porosity

r*j* : *density*

sj: saturation

xji: water, oil, or gas mole fraction

For the solid component

$Ci = \mathrm{j}v.ci$

$\mathrm{j}v$: void porosity (ratio of void volume to gross volume)

ci : the concentration of component i in void volume

The partial pressure form Ci = yi pg is available also. The factor rrk is the constant part of rk. Its unit can be quite complex, and must account for the units of the various Ci, which are moles per pore volume or pressure, raised to the power of rik and then multiplied together.

The kinetic model can represent a reacting component in only one phase at a time. If a component reacts in more than one phase, it must be modeled in two separate reactions.

Because the component conservation equations have mole units and the reactions are treated as source/sink terms, moles of each component and energy will be conserved. However, the reaction stoichiometry should be mass conserving as well in order for the reaction to make sense physically. This is important especially when the molecular weight of a pseudo-oil component is not well-defined or is arbitrary.

Mass-conserving stoichiometry satisfies:

$$\sum_{i=1}^{nc} s_{ki}.M_i = \sum_{i=1}^{nc} s'_{ki}.M_i$$

Even though a molecular weight is not required by the STARS model for the solid component, a reasonable value should be chosen for the above calculation.

If mass is not conserved in a reaction, the effect probably will not show up in the simulation until the final results are analyzed or compared with a laboratory report.

On the other hand, conservation of volume during reaction is not required in general. However, there is one condition under which large volume changes caused by reactions should be avoided. It is when Sg = 0 and there are reactions between liquids, or between liquids and solids.

Consider a liquid-saturated reservoir (Sg = 0) in which a heavy oil cracks into a into a solid fuel. Even though this reaction is meant to happen at higher temperatures, the model will calculate a nonzero reaction rate at the initial reservoir temperature. Therefore, some oil will be replaced by the solid from the start of the simulation. A significant discrepancy between the volumes consumed and produced, in conjunction with a low overall reservoir compressibility, will result in large uncontrollable pressure changes. This situation can be remedied by situation can be remedied by ensuring that volumes are more nearly conserved.

APPENDIX B

NUMERICAL MODEL INPUT FILE FOR THE FIRST CASE

```
RESULTS SIMULATOR STARS 200600

RANGECHECK ON
**  ==============  INPUT/OUTPUT CONTROL
======================
**CHECKONLY              **checking of entire data
**complete & write current time step and stop simulation run
INTERRUPT RESTART-STOP
**DIM *MDICLU 106000      **Max. number of solver fill connections
TITLE1 'STARS Numerical Model'
TITLE2 'CO2 INJECTION INTO FRACTURED RESERVOIR'
*MAXERROR    20      **maximum error number
*PRNTORIEN  1 1      **standart order as grid array input


*INUNIT     *FIELD
DIM MDLU 450512
*OUTUNIT    *FIELD
WPRN GRID TIME
OUTPRN GRID ALL
OUTSRF GRID ALL
*WRST *TIME



**  ==============  GRID AND RESERVOIR DEFINITION
=================

*GRID  *CART 21 21 10 **Cartesian grid
*KDIR  *DOWN          **First layer at the top of the reservoir

**Blocks Dimensions
*DI   *IVAR 2 19*200 2   **47504 ft
```

```
*DJ   *JVAR 2 19*200 2   **47504 ft
*DK   *KVAR  10*10      **1004 ft

*DTOP 441*3000  **Top of the grids (ft)
DUALPOR
SHAPE GK
**$ Property: NULL Blocks  Max: 1  Min: 1
**$  0 = null block, 1 = active block
NULL MATRIX CON           1
**$ Property: NULL Blocks  Max: 1  Min: 1
**$  0 = null block, 1 = active block
NULL FRACTURE CON           1
difrac con 1
djfrac con 1
dkfrac con 1
por fracture con 0.01
**$ Property: Porosity  Max: 0.15  Min: 0.15
POR MATRIX CON        0.15
**$ Property: Permeability I (md)   Max: 1000  Min: 1000
PERMI FRACTURE CON         1000
**$ Property: Permeability I (md)   Max: 100  Min: 100
PERMI MATRIX CON          100
permj fracture  con 1000
PERMJ MATRIX EQUALSI
permk fracture  con 1000
PERMK MATRIX EQUALSI
**$ Property: Pinchout Array  Max: 1  Min: 1
**$  0 = pinched block, 1 = active block
PINCHOUTARRAY CON           1
END-GRID
rocktype 1                    **  Fracture is an extended region of high
                            **  permeability with assumed fracture
thtype fracture con 1             **  width of 0.2 m, i.e., (part of the
cpor 96e-6
rockcp 34          **  (matrix rock is included).
thconr 254
thconw 8.32016616
thcono 1.8
thcong 2.7733887
hlossprop overbur 35 24
        underbur 35 24
**  Matrix properties
ROCKTYPE 2 COPY 1
CPOR 1e-5
```

```
HLOSSPROP OVERBUR 35 24
      UNDERBUR 35 24

thtype matrix con 2

rockcp 34
thconr 254
thconw 8.32
thcono 1.49
thcong 2.78

*permck 2.5

**  ==============  OTHER RESERVOIR PROPERTIES
**********************

*END-GRID

*ROCKTYPE 1
*THTYPE MATRIX *con 1
*THTYPE FRACTURE CON 1
*CPOR  1E-06         **9.77789E-07 **formation compresibility 1/Psi
*CTPOR 0.0000021     **rock thermal expansion 1/F (3.8E-06 1/K)
*ROCKCP 34           **volumetric heat capacity Btu/cuft-F

*THCONR 41.48065061           **Reservoir thermal rock conductivity (Btu/ft-day-
F)
*THCONW 8.32016616        **Water thermal conductivity
*THCONG 2.7733887         **Gas thermal conductivity

*HLOSSPROP *OVERBUR 35 24      **Volumetric heat capacity (Btu/cuft-F)
Thermal conductivity (Btu/ft-day-F)
        *UNDERBUR 35 24     **Default values


**  ==============  FLUID DEFINITIONS  ======================

**component types  w+g+s  w+g  w  w
**             -----  ---  --  --
*MODEL              6    3   2   1
**solids : CaCO3 + Ca(HCO3)2 + NaCl

*COMPNAME 'WATER'   'OIL'  'CO2'  'CaCO3'  'Ca(HCO3)'  'NaCl'
**        -------   ---    ------  -----    ------      ------
```

```
*KV1      0         0 **1.7202E+6           **Gas-Liquid K value correlation coeffs
*KV2      0         0         **1 to numx(w)
*KV3      0         0
*KV4      1         0 **-6869.59
*KV5      0         0 **-376.64

**COMPNAME 'WATER' 'OIL'  'CO2'  'CaCO3'  'Ca(HCO3)'  'NaCl'
**        ------- ---   ------ -----    ------      ------
*CMM      18.016   180    44.010 100.0911 162.1171    58.4428  **Molecular weight
(lb/lbmol) [1 to ncomp]
*TCRIT    705.47  1216.94 87.89                        **Critical Temperature (F) [1
to numy]
*PCRIT    3198    2645.49     1070.38                    **Critical Pressure (psi)  [1
to numy]

*PRSR 14.7       **Reference pressure (psi) for density
*TEMR 77         **Reference temperature (F)[25 C] for T-dependent and thermal
properties
*PSURF 14.7      **Pressure @surface conditions (psi)
*TSURF 68        **Temperature @surface conditions (F)[20 C]



**COMPNAME 'WATER'  'OIL'       'CO2'
**        ------- ----        ------
*CPG1     7.701      -1.89       4.728            **1st coeff of gas heat capacity
correlation (Btu/lbmol-F)
*CPG2     2.553E-4   0.1275      9.744E-3          ** 1 to numy
*CPG3     7.781E-7   -3.898E-5   4.130E-6
*CPG4    -0.1473E-9  4.631E-9    0.7025E-9
*HVR      1657            991            **1st coeff of vaporization enthalpy correlation
(Btu/lbmol-F)

**EV Default value is used
**Default liquid heat capacities are used

*SOLID_DEN  'CaCO3'    169.2422011  0   0 **Density (lb/cuft)  Compressibility
(1/psi)  Thermal expansisivity (1/F) @reference temperature & pressure
*SOLID_DEN  'Ca(HCO3)'  132.015784   0   0
*SOLID_DEN  'NaCl'      136          0   0
*SOLID_DEN  'CO2'       118.551      0   0

**COMPNAME 'WATER'     'OIL'
**        -------
```

```
*MASSDEN  63.61409183  54.6     **lb/cuft [1 to numx]

*GASD-ZCOEF *IMPLICIT


**COMPNAME 'WATER'   'OIL'
**         -------
*AVISC   0.0047352  0.0115577    **coeff of viscosity calculation (cp) [1 to numx]
*BVISC   2728.2     2315.2       **(F)

*XNACL    0.10         **brine concentration (mass fraction of salt)

**Reaction CO2+H2O+CaCO3-->Ca(HCO3)2

**COMPNAME 'WATER' 'OIL' 'CO2' 'CaCO3' 'Ca(HCO3)' 'NaCl'
**         -------  ---  ------ -----    ------   ------
*STOREAC     1      0      1     1        0         0
*STOPROD     0      0      0     0        1         0
*RPHASE      1      0     3     4        4         4
*RORDER      1      0     1     0        1         1

*FREQFAC 5  **3500        **reaction frequency factor (1/min)
*EACT    0           **activation energy (Btu/lbmol)
*RENTH   0           **reaction enthalpy (Btu/lbmol)

**PERMSCALE        **Permeability        Scaling factor      Rate
                   **EFFPT                 FREQT              Constant
                   **(md)                                    (1/min)
                    **90                  2.000               **
                    **120                  1.000               **
                    **200                  0.675               **
                    **400                  0.200               **
                    **800                  0.100               **
                    **2000                 0.075               **

**Reaction Ca(HCO3)2-->CO2+H2O+CaCO3

**COMPNAME 'WATER' 'OIL' 'CO2' 'CaCO3' 'Ca(HCO3)' 'NaCl'
**         -------  ----  ------ -----    ------   ------
*STOREAC      0      0      0      0      1         0
*STOPROD      1      0      1      1      0         0
*RPHASE       1      0      3      4      4         4      **1->liquid 4->solid
*RORDER       1      0      1      1      1         1        **reaction & concentration
dependence
```

```
*FREQFAC 0  **550        **reaction frequency factor (1/min)
*EACT    0         **activation energy (Btu/lbmol)
*RENTH   0          **reaction enthalpy (Btu/lbmol)
*O2CONC

**PERMSCALE       **Permeability        Scaling factor      Rate
                  **EFFPT                FREQT               Constant
                  **(md)                                     (1/min)
                    **90                2.000               **
                    **120               1.000               **
                    **200               0.675               **
                    **400               0.200               **
                    **800               0.100               **
                    **1000              0.075               **



**  ==============  ROCK-FLUID PROPERTIES
======================

*ROCKFLUID
*RPT 1 *STONE2 *WATWET     **default
*KRTYPE MATRIX *CON 1            **default
*KRTYPE FRACTURE *CON 1

*SWT   **  Water-oil relative permeabilities

**       Sw      Krw       Krow
**      -----    ------   ------
          0.300000 0.000000 0.490000
          0.350000 0.000001 0.422500
          0.400000 0.000016 0.360000
          0.450000 0.000116 0.302500
          0.500000 0.000481 0.250000
          0.550000 0.001463 0.202500
          0.600000 0.003671 0.160000
          0.650000 0.008101 0.122500
          0.700000 0.016341 0.090000
          0.750000 0.030934 0.062500
          0.800000 0.056086 0.040000
          0.850000 0.099257 0.022500
          0.900000 0.175474 0.010000
```

```
          0.950000 0.324355 0.002500
          1.000000 1.000000 0.000000


*SLT   **  Liquid-gas relative permeabilities

**      Sl       Krg          Krog          Pcog(psi)
**     -----    ------        ------        ------
          0.30 0.02618252723 0.00000000 **300.4194910
          0.35 0.01590044522 0.00000054 **290.3470123
          0.40 0.00939117745 0.00001593 **270.8099503
          0.45 0.00534448235 0.00011634 **260.6195202
          0.50 0.00289843166 0.00048123 **250.6648570
          0.55 0.00147693480 0.00146270 **240.8765181
          0.60 0.00069373574 0.00367093 **240.2085954
          0.65 0.00029223596 0.00810145 **230.6292027
          0.70 0.00010585125 0.01634141 **230.1150163
          0.75 0.00003073591 0.03093357 **220.6478342
          0.80 0.00000627673 0.05608634 **220.2120140
          0.85 0.00000067232 0.09925704 **210.7917975
          0.90 0.00000001483 0.17547384 **210.3665181
          0.95 0.00000000000 0.32435518 **200.8943675
        1.00 0.00000000000 0.49000000 **200



**DIFFI_GAS 'CO2' *CON  1.21E-03  **sqft/day
**DIFFJ_GAS 'CO2' *EQUALSI
**DIFFK_GAS 'CO2' *EQUALSI


**ADSCOMP 'CO2' 'GAS'       **adsorpted component
**ADSLANG 5.41 0 2.1        **Langmuir isotherm coefficients
**ADSROCK 1
**adsoption rock type
**ADMAXT 2.56E-6           **maximum adsoption capacity
**ADRT 0                  **completely reversible adsoption
**ADSPHBLK 'ALL'           **resistance factor is calculated for all phase
**PORFT 1                 **all pore volume is accessible
**RRFT 2.5                **no residual resistance effect


** ==============  INITIAL CONDITIONS  ======================
```

```
*INITIAL
*VERTICAL *DEPTH_AVE          **perform depth-averaged capillary-gravity
vertical equilibrium calculation
*REFDEPTH  3050               **reference depth within the reservoir (ft)
*REFPRES   1348               **pressure @reference depth (psi)
**TRANZONE                    **transition zone for water-gas system by using water
oil capillary pressure curve

**DWOC 2000
**DGOC 2000

**Pressure gradient (psi/ft)=0.442075025
**Geothermal gradient (F/100 ft)=2.2

**PRES  *con 1348.                **initial reservoir pressure (psi)
*TEMP MATRIX  *con 127.            **initial reservoir temperature (F)
*TEMP FRACTURE *CON 127.

**Override vertical equilibrium saturations
**SW *CON 1          **initial water saturation
**SO *CON 0          **initial oil saturation
**SG *CON 0          **initial gas saturation

*CONC_SLD  'CaCO3' MATRIX       *CON   0.0      **0.311855699  **initial
concentration (lbmol/cuft)  [0.1 g/cucm]
*CONC_SLD  'Ca(HCO3)'MATRIX     *CON   0.0
*CONC_SLD  'NaCl'  MATRIX       *CON   0.0      **0.534094533
**CONC_SLD 'CO2' MATRIX         *CON   0.0
*CONC_SLD  'CaCO3'  FRACTURE    *CON   0.0      **0.311855699  **initial
concentration (lbmol/cuft)  [0.1 g/cucm]
*CONC_SLD   'Ca(HCO3)' FRACTURE   *CON   0.0
*CONC_SLD  'NaCl'   FRACTURE     *CON   0.0      **0.534094533
**CONC_SLD  'CO2'  FRACTURE      *CON   0.0

**  ==============  NUMERICAL CONTROL  ======================


*NUMERICAL     ** All these can be defaulted.
MAXSTEPS 9000
TFORM SXY
**TFORM *SXY   **standart use of primary variables
**CONVERGE *TOTRES *TIGHT
**NEWTONCYC 30   **maximum number of newton iteration in a timestep
**UNRELAX 1
```

```
**UPSTREAM *KLEVEL
**PRECC 1
**NORTH 30
**SDEGREE *GAUSS
**use pivot stabilization
PIVOT ON
** max iteration number for Jacobian matrix solution
ITERMAX 50
AIM STAB
**AIM *STAB *BACK 5   **backward switching 5
**MINPRES 100        **min simulation pressure  psi
**MAXPRES 5000        **max simulation pressure  psi
**MINTEMP 60         **min simulation temperature F
**MAXTEMP 300         **max simulation temperature F
**PVTOSCMAX 5         **max number of phase switches
**MAXLAYPRE 3         **default value
**NCUT 20            **number of timestep size cut



**  ============== WELL & RECURRENT DATA
======================

*RUN
*TIME0
** Timestep size (days)
DTWELL 1
**
** ** WELL SPECIFICATION W1-------
** *WELL 1 'W1' *VERT 11 11   **Well location (i,j)
**$
WELL  'INJ1'
**COMPNAME 'WATER' 'CO2' 'CaCO3' 'Ca(HCO3)' 'NaCl'
**         ------- ------ -----    ------   ------
           **supercritic condition (F)
           **supercritic condition (psia)
                        **scf/day
                      **psia
                  **CONT
INJECTOR MOBWEIGHT IMPLICIT 'INJ1'
INCOMP  GAS  0.  0.  1.
TINJW  127.
PINJW  1620.
```

```
OPERATE  MAX  STG  1e+006  CONT
OPERATE  MAX  BHP  2700.  CONT
MONITOR  MIN  STG  500.  SHUTIN
**           rad      geofac     wfrac      skin
**           (rw-ft)   (Appendix A)
** i   j   k     ff   status
**$        rad  geofac  wfrac  skin
GEOMETRY  K  0.375  0.249  1.  0.
PERF  GEO  'INJ1'
**$ UBA      ff  Status  Connection
   11 11 6   1.  OPEN    FLOW-FROM  'SURFACE'  REFLAYER
   11 11 7   1.  OPEN    FLOW-FROM  1
   11 11 8   1.  OPEN    FLOW-FROM  2
   11 11 9   1.  OPEN    FLOW-FROM  3
   11 11 10  1.  OPEN    FLOW-FROM  4
   11 11 5   1.  OPEN    FLOW-FROM  5
   11 11 4   1.  OPEN    FLOW-FROM  6
   11 11 3   1.  OPEN    FLOW-FROM  7
   11 11 2   1.  OPEN    FLOW-FROM  8
   11 11 1   1.  OPEN    FLOW-FROM  9
**$
WELL  'Well-2'
PRODUCER 'Well-2'
OPERATE  MAX  STO  50.  CONT
**$        rad  geofac  wfrac  skin
GEOMETRY  K  0.28  0.249  1.  0.
PERF  GEO  'Well-2'
**$ UBA     ff  Status  Connection
   1 1 1   1.  OPEN    FLOW-TO  'SURFACE'  REFLAYER
   1 1 2   1.  OPEN    FLOW-TO  1
   1 1 3   1.  OPEN    FLOW-TO  2
   1 1 4   1.  OPEN    FLOW-TO  3
   1 1 5   1.  OPEN    FLOW-TO  4
   1 1 6   1.  OPEN    FLOW-TO  5
   1 1 7   1.  OPEN    FLOW-TO  6
   1 1 8   1.  OPEN    FLOW-TO  7
   1 1 9   1.  OPEN    FLOW-TO  8
   1 1 10  1.  OPEN    FLOW-TO  9
**$
WELL  'Well-3'
PRODUCER 'Well-3'
OPERATE  MAX  STO  50.  CONT
**$        rad  geofac  wfrac  skin
GEOMETRY  K  0.28  0.249  1.  0.
```

```
PERF  GEO  'Well-3'
**$ UBA      ff  Status  Connection
   20 20 1   1.  OPEN    FLOW-TO  'SURFACE'  REFLAYER
   20 20 2   1.  OPEN    FLOW-TO  1
   20 20 3   1.  OPEN    FLOW-TO  2
   20 20 4   1.  OPEN    FLOW-TO  3
   20 20 5   1.  OPEN    FLOW-TO  4
   20 20 6   1.  OPEN    FLOW-TO  5
   20 20 7   1.  OPEN    FLOW-TO  6
   20 20 8   1.  OPEN    FLOW-TO  7
   20 20 9   1.  OPEN    FLOW-TO  8
   20 20 10  1.  OPEN    FLOW-TO  9
```

*TIME 360
*TIME 720
*TIME 1080
*TIME 1440
*TIME 1800
*TIME 2160
*TIME 2520
*TIME 2880
*TIME 3240
*TIME 3600
*TIME 3960
*TIME 4320
*TIME 4680
*TIME 5040
*TIME 5400
*TIME 5760
*TIME 6120
*TIME 6480
*TIME 6840
*TIME 7200
*TIME 7560
*TIME 7920
*TIME 8280
*TIME 8640
*TIME 9000
*TIME 9360
*TIME 9720
*TIME 10080
*TIME 10440
*TIME 10800
*TIME 11160
*TIME 11520
*TIME 11880
*TIME 12240
*TIME 12600
*TIME 12960
*TIME 13320
*TIME 13680
*TIME 14040
*TIME 14400
*TIME 14760
*TIME 15120
*TIME 15480
*TIME 15840
*TIME 16200
*TIME 16560
*TIME 16920
*TIME 17280
*TIME 17640
*TIME 18000
*TIME 18360
*TIME 18720
*TIME 19080
*TIME 19440
*TIME 19800
*TIME 20160
*TIME 20520
*TIME 20880
*TIME 21240
*TIME 21600
*TIME 21960
*TIME 22320
*TIME 22680
*TIME 23040
*TIME 23400
*TIME 23760
*TIME 24120
*TIME 24480
*TIME 24840
*TIME 25200
*TIME 25560
*TIME 25920
*TIME 26280
*TIME 26640
*TIME 27000
*TIME 27360
*TIME 27720
*TIME 28080
*TIME 28440
*TIME 28800
*TIME 29160
*TIME 29520
*TIME 29880
*TIME 30240
*TIME 30600
*TIME 30960
*TIME 31320
*TIME 31680
*TIME 32040
*TIME 32400
*TIME 32760
*TIME 33120
*TIME 33480
*TIME 33840
*TIME 34200
*TIME 34560
TIME 34698
TIME 34729
TIME 34758
TIME 34789
TIME 34819
TIME 34850
TIME 34880
TIME 34911
*TIME 34920
TIME 34942
TIME 34972
TIME 35003
TIME 35033
TIME 35064
TIME 35095
TIME 35123
TIME 35154
TIME 35184
TIME 35215
TIME 35245
TIME 35276
*TIME 35280
TIME 35307
TIME 35337
TIME 35368
TIME 35398
TIME 35429
TIME 35460
TIME 35488
TIME 35519
TIME 35549
TIME 35580
TIME 35610
*TIME 35640
TIME 35641
TIME 35672
TIME 35702
TIME 35733
TIME 35763
TIME 35794
TIME 35825
TIME 35853
TIME 35884
TIME 35914
TIME 35945
TIME 35975
*TIME 36000
TIME 36006
TIME 36037
TIME 36067
TIME 36098
TIME 36128
TIME 36159
TIME 36190
TIME 36219
TIME 36250
TIME 36280
TIME 36311
TIME 36341
*TIME 36360
TIME 36372
TIME 36403
TIME 36433
TIME 36464
TIME 36494
TIME 36525
TIME 36556
TIME 36584
TIME 36615
TIME 36645
TIME 36676
TIME 36706
*TIME 36720
TIME 36737
TIME 36768
TIME 36798
TIME 36829
TIME 36859
TIME 36890
TIME 36921

TIME 36949
TIME 36980
TIME 37010
TIME 37041
TIME 37071
*TIME 37080
TIME 37102
TIME 37133
TIME 37163
TIME 37194
TIME 37224
TIME 37255
TIME 37286
TIME 37314
TIME 37345
TIME 37375
TIME 37406
TIME 37436
*TIME 37440
TIME 37467
TIME 37498
TIME 37528
TIME 37559
TIME 37589
TIME 37620
TIME 37651
TIME 37680
TIME 37711
TIME 37741
TIME 37772
*TIME 37800
TIME 37802
TIME 37833
TIME 37864
TIME 37894
TIME 37925
TIME 37955
TIME 37986
TIME 38017
TIME 38045
TIME 38076
TIME 38106
TIME 38137
*TIME 38160
TIME 38167
TIME 38198
TIME 38229
TIME 38259
TIME 38290
TIME 38320
TIME 38351
TIME 38382
TIME 38410
TIME 38441
TIME 38471
TIME 38502
*TIME 38520
TIME 38532
TIME 38563
TIME 38594
TIME 38624
TIME 38655
TIME 38685
TIME 38716
TIME 38747
TIME 38775
TIME 38806
TIME 38836
TIME 38867
*TIME 38880
TIME 38897
TIME 38928
TIME 38959
TIME 38989
TIME 39020
TIME 39050
TIME 39081
TIME 39112
TIME 39141
TIME 39172
TIME 39202
TIME 39233
*TIME 39240
TIME 39263
TIME 39294
TIME 39325
TIME 39355
TIME 39386
TIME 39416
TIME 39447
TIME 39478
TIME 39506
TIME 39537
TIME 39567
TIME 39598
*TIME 39600
TIME 39628
TIME 39659
TIME 39690
TIME 39720
TIME 39751
TIME 39781
TIME 39812
TIME 39843
TIME 39871
TIME 39902
TIME 39932
*TIME 39960
TIME 39963
TIME 39993
TIME 40024
TIME 40055
TIME 40085
TIME 40116
TIME 40146
TIME 40177
TIME 40208
TIME 40236
TIME 40267
TIME 40297
*TIME 40320
TIME 40328
TIME 40358
TIME 40389
TIME 40420
TIME 40450
TIME 40481
TIME 40511
TIME 40542
TIME 40573
TIME 40602
TIME 40633
TIME 40663
*TIME 40680
TIME 40694
TIME 40724
TIME 40755
TIME 40786
TIME 40816
TIME 40847
TIME 40877
TIME 40908
TIME 40939
TIME 40967
TIME 40998
TIME 41028
*TIME 41040
TIME 41059
TIME 41089
TIME 41120
TIME 41151
TIME 41181
TIME 41212
TIME 41242
TIME 41273
TIME 41304
TIME 41332
TIME 41363
TIME 41393
*TIME 41400
TIME 41424
TIME 41454
TIME 41485
TIME 41516
TIME 41546
TIME 41577
TIME 41607
TIME 41638
TIME 41669
TIME 41697
TIME 41728
TIME 41758
*TIME 41760
TIME 41789
TIME 41819
TIME 41850

TIME 41881
TIME 41911
TIME 41942
TIME 41972
TIME 42003
TIME 42034
TIME 42063
TIME 42094
*TIME 42120
TIME 42124
TIME 42155
TIME 42185
TIME 42216
TIME 42247
TIME 42277
TIME 42308
TIME 42338
TIME 42369
TIME 42400
TIME 42428
TIME 42459
*TIME 42480
TIME 42489
TIME 42520
TIME 42550
TIME 42581
TIME 42612
TIME 42642
TIME 42673
TIME 42703
TIME 42734
TIME 42765
TIME 42793
TIME 42824
*TIME 42840
TIME 42854
TIME 42885
TIME 42915
TIME 42946
TIME 42977
TIME 43007
TIME 43038
TIME 43068
TIME 43099
TIME 43130
TIME 43158
TIME 43189
*TIME 43200
TIME 43219
TIME 43250
TIME 43280
TIME 43311
TIME 43342
TIME 43372
TIME 43403
TIME 43433
TIME 43464
TIME 43495
TIME 43524
TIME 43555
*TIME 43560
TIME 43585
TIME 43616
TIME 43646
TIME 43677
TIME 43708
TIME 43738
TIME 43769
TIME 43799
TIME 43830
TIME 43861
TIME 43889
*TIME 43920
TIME 43950
TIME 43981
TIME 44011
TIME 44042
TIME 44073
TIME 44103
TIME 44134
TIME 44164
TIME 44195
TIME 44226
TIME 44254
*TIME 44280
TIME 44285
TIME 44315
TIME 44346
TIME 44376
TIME 44407
TIME 44438
TIME 44468
TIME 44499
TIME 44529
TIME 44560
TIME 44591
TIME 44619
*TIME 44640
TIME 44650
TIME 44680
TIME 44711
TIME 44741
TIME 44772
TIME 44803
TIME 44833
TIME 44864
TIME 44894
TIME 44925
TIME 44956
TIME 44985
*TIME 45000
TIME 45016
TIME 45046
TIME 45077
TIME 45107
TIME 45138
TIME 45169
TIME 45199
TIME 45230
TIME 45260
TIME 45291
TIME 45322
TIME 45350
*TIME 45360
TIME 45381
TIME 45411
TIME 45442
TIME 45472
TIME 45503
TIME 45534
TIME 45564
TIME 45595
TIME 45625
TIME 45656
TIME 45687
TIME 45715
*TIME 45720
TIME 45746
TIME 45776
TIME 45807
TIME 45837
TIME 45868
TIME 45899
TIME 45929
TIME 45960
TIME 45990
TIME 46021
TIME 46052
*TIME 46080
TIME 46111
TIME 46141
TIME 46172
TIME 46202
TIME 46233
TIME 46264
TIME 46294
TIME 46325
TIME 46355
TIME 46386
TIME 46417
*TIME 46440
TIME 46446
TIME 46477
TIME 46507
TIME 46538
TIME 46568
TIME 46599
TIME 46630
TIME 46660
TIME 46691
TIME 46721
TIME 46752
TIME 46783
*TIME 46800
TIME 46811
TIME 46842

TIME 46872
TIME 46903
TIME 46933
TIME 46964
TIME 46995
TIME 47025
TIME 47056
TIME 47086
TIME 47117
TIME 47148
*TIME 47160
TIME 47176
TIME 47207
TIME 47237
TIME 47268
TIME 47298
TIME 47329
TIME 47360
TIME 47390
TIME 47421
TIME 47451
TIME 47482
TIME 47513
*TIME 47520
TIME 47541
TIME 47572
TIME 47602
TIME 47633
TIME 47663
TIME 47694
TIME 47725
TIME 47755
TIME 47786
TIME 47816
TIME 47847
TIME 47878
*TIME 47880
TIME 47907
TIME 47938
TIME 47968
TIME 47999
TIME 48029
TIME 48060
TIME 48091
TIME 48121
TIME 48152
TIME 48182
TIME 48213
*TIME 48240
TIME 48244
TIME 48272
TIME 48303
TIME 48333
TIME 48364
TIME 48394
TIME 48425
TIME 48456
TIME 48486
TIME 48517
TIME 48547
TIME 48578
*TIME 48600
TIME 48609
TIME 48637
TIME 48668
TIME 48698
TIME 48729
TIME 48759
TIME 48790
TIME 48821
TIME 48851
TIME 48882
TIME 48912
TIME 48943
*TIME 48960
TIME 48974
TIME 49002
TIME 49033
TIME 49063
TIME 49094
TIME 49124
TIME 49155
TIME 49186
TIME 49216
TIME 49247
TIME 49277
TIME 49308
*TIME 49320
TIME 49339
TIME 49368
TIME 49399
*TIME 49680
*TIME 50040
*TIME 50400
*TIME 50760
*TIME 51120
*TIME 51480
*TIME 51840
*TIME 52200
*TIME 52560
*TIME 52920
*TIME 53280
*TIME 53640
*TIME 54000
*TIME 54360
*TIME 54720
*TIME 55080
*TIME 55440
*TIME 55800
*TIME 56160
*TIME 56520
*TIME 56880
*TIME 57240
*TIME 57600
*TIME 57960
*TIME 58320
*TIME 58680
*TIME 59040
*TIME 59400
*TIME 59760
*TIME 60120
*TIME 60480
*TIME 60840
*TIME 61200
*TIME 61560
*TIME 61920
*TIME 62280
*TIME 62640
*TIME 63000
*TIME 63360
*TIME 63720
*TIME 64080
*TIME 64440
*TIME 64800
*TIME 65160
*TIME 65520
*TIME 65880
*TIME 66240
*TIME 66600
*TIME 66960
*TIME 67320
*TIME 67680
*TIME 68040
*TIME 68400
*TIME 68760
*TIME 69120
*TIME 69480
*TIME 69840
*TIME 70200
*TIME 70560
*TIME 70920
*TIME 71280
*TIME 71640
*TIME 72000
*TIME 72360
*TIME 72720
*TIME 73080
*TIME 73440
*TIME 73800
*TIME 74160
*TIME 74520
*TIME 74880
*TIME 75240
*TIME 75600
*TIME 75960
*TIME 76320
*TIME 76680
*TIME 77040
*TIME 77400
*TIME 77760
*TIME 78120
*TIME 78480
*TIME 78840
*TIME 79200
*TIME 79560
*TIME 79920

*TIME 80280
*TIME 80640
*TIME 81000
*TIME 81360
*TIME 81720
*TIME 82080
*TIME 82440
*TIME 82800
*TIME 83160
*TIME 83520
*TIME 83880
*TIME 84240
*TIME 84600
*TIME 84960
*TIME 85320
*TIME 85680
*TIME 86040
*TIME 86400
*TIME 86760
*TIME 87120
*TIME 87480
*TIME 87840
*TIME 88200
*TIME 88560
*TIME 88920
*TIME 89280
*TIME 89640
*TIME 90000
*TIME 90360
*TIME 90720
*TIME 91080
*TIME 91440
*TIME 91800
*TIME 92160
*TIME 92520
*TIME 92880
*TIME 93240
*TIME 93600
*TIME 93960
*TIME 94320
*TIME 94680
*TIME 95040
*TIME 95400
*TIME 95760
*TIME 96120
*TIME 96480
*TIME 96840
*TIME 97200
*TIME 97560
*TIME 97920
*TIME 98280
*TIME 98640
*TIME 99000
*TIME 99360
*TIME 99720
*TIME 100080
*TIME 100440
*TIME 100800
*TIME 101160
*TIME 101520
*TIME 101880
*TIME 102240
*TIME 102600
*TIME 102960
*TIME 103320
*TIME 103680
*TIME 104040
*TIME 104400
*TIME 104760
*TIME 105120
*TIME 105480
*TIME 105840
*TIME 106200
*TIME 106560
*TIME 106920
*TIME 107280
*TIME 107640
*TIME 108000
*TIME 108360
*TIME 108720
*TIME 109080
*TIME 109440
*TIME 109800
*TIME 110160
*TIME 110520
*TIME 110880
*TIME 111240
*TIME 111600
*TIME 111960
*TIME 112320
*TIME 112680
*TIME 113040
*TIME 113400
*TIME 113760
*TIME 114120
*TIME 114480
*TIME 114840
*TIME 115200
*TIME 115560
*TIME 115920
*TIME 116280
*TIME 116640
*TIME 117000
*TIME 117360
*TIME 117720
*TIME 118080
*TIME 118440
*TIME 118800
*TIME 119160
*TIME 119520
*TIME 119880
*TIME 120240
*TIME 120600
*TIME 120960
*TIME 121320
*TIME 121680
*TIME 122040
*TIME 122400
*TIME 122760
*TIME 123120
*TIME 123480
*TIME 123840
*TIME 124200
*TIME 124560
*TIME 124920
*TIME 125280
*TIME 125640
*TIME 126000
*TIME 126360
*TIME 126720
*TIME 127080
*TIME 127440
*TIME 127800
*TIME 128160
*TIME 128520
*TIME 128880
*TIME 129240
*TIME 129600
*TIME 129960
*TIME 130320
*TIME 130680
*TIME 131040
*TIME 131400
*TIME 131760
*TIME 132120
*TIME 132480
*TIME 132840
*TIME 133200
*TIME 133560
*TIME 133920
*TIME 134280
*TIME 134640
*TIME 135000
*TIME 135360
*TIME 135720
*TIME 136080
*TIME 136440
*TIME 136800
*TIME 137160
*TIME 137520
*TIME 137880
*TIME 138240
*TIME 138600
*TIME 138960
*TIME 139320
*TIME 139680
*TIME 140040
*TIME 140400
*TIME 140760
*TIME 141120
*TIME 141480
*TIME 141840
*TIME 142200
*TIME 142560
*TIME 142920
*TIME 143280

```
*STOP  **Run ends here

RESULTS SPEC 'Permeability K' MATRIX
RESULTS SPEC SPECNOTCALCVAL -99999
RESULTS SPEC REGION 'All Layers (Whole Grid)'
RESULTS SPEC REGIONTYPE 'REGION_WHOLEGRID'
RESULTS SPEC LAYERNUMB 0
RESULTS SPEC PORTYPE 1
RESULTS SPEC EQUALSI 0 1
RESULTS SPEC STOP


RESULTS SPEC 'Permeability J' MATRIX
RESULTS SPEC SPECNOTCALCVAL -99999
RESULTS SPEC REGION 'All Layers (Whole Grid)'
RESULTS SPEC REGIONTYPE 'REGION_WHOLEGRID'
RESULTS SPEC LAYERNUMB 0
RESULTS SPEC PORTYPE 1
RESULTS SPEC EQUALSI 0 1
RESULTS SPEC STOP


RESULTS SPEC 'Porosity' MATRIX
RESULTS SPEC SPECNOTCALCVAL -99999
RESULTS SPEC REGION 'All Layers (Whole Grid)'
RESULTS SPEC REGIONTYPE 'REGION_WHOLEGRID'
RESULTS SPEC LAYERNUMB 0
RESULTS SPEC PORTYPE 1
RESULTS SPEC CON 0.15
RESULTS SPEC STOP
```

APPENDIX C

NUMERICAL MODEL INPUT FILE FOR THE SEVENTH CASE AFTER 10800 DAYS OF INJECTION TO PERFORM A BUILD UP ANALYSIS

```
RESULTS SIMULATOR STARS 200600

FILENAMES INDEX-IN 'fifth.irf'
RANGECHECK ON
**  ==============  INPUT/OUTPUT CONTROL
======================
**CHECKONLY              **checking of entire data
**complete & write current time step and stop simulation run
INTERRUPT RESTART-STOP
**DIM *MDICLU 106000      **Max. number of solver fill connections
*MAXERROR    20      **maximum error number
*PRNTORIEN  1 1      **standart order as grid array input


*INUNIT     *FIELD
DIM MDLU 450512
*OUTUNIT    *FIELD
WPRN GRID TIME
OUTPRN GRID ALL
OUTSRF GRID ALL
*RESTART
*RESTIME 10800




**  ==============  GRID AND RESERVOIR DEFINITION
================
```

```
*GRID  *CART 21 21 10 **Cartesian grid
*KDIR  *DOWN          **First layer at the top of the reservoir

**Blocks Dimensions
*DI   *IVAR 2 19*200 2   **47504 ft
*DJ   *JVAR 2 19*200 2   **47504 ft
*DK   *KVAR  10*10      **1004 ft

*DTOP 441*3000  **Top of the grids (ft)
DUALPOR
SHAPE GK
**$ Property: NULL Blocks  Max: 1  Min: 1
**$  0 = null block, 1 = active block
NULL MATRIX CON           1
**$ Property: NULL Blocks  Max: 1  Min: 1
**$  0 = null block, 1 = active block
NULL FRACTURE CON           1
difrac con 50
djfrac con 50
dkfrac con 50
por fracture con 0.01
**$ Property: Porosity  Max: 0.15  Min: 0.15
POR MATRIX CON        0.15
**$ Property: Permeability I (md)   Max: 1000  Min: 1000
PERMI FRACTURE CON         1000
**$ Property: Permeability I (md)   Max: 100  Min: 100
PERMI MATRIX CON          100
permj fracture  con 1000
PERMJ MATRIX EQUALSI
permk fracture  con 1000
PERMK MATRIX EQUALSI
**$ Property: Pinchout Array  Max: 1  Min: 1
**$  0 = pinched block, 1 = active block
PINCHOUTARRAY CON           1
END-GRID
rocktype 1                    **  Fracture is an extended region of high
                            **  permeability with assumed fracture
thtype fracture con 1             **  width of 0.2 m, i.e., (part of the
cpor 96e-6
rockcp 34           **  (matrix rock is included).
thconr 254
thconw 8.32016616
thcono 1.8
thcong 2.7733887
```

```
hlossprop overbur 35 24
        underbur 35 24
**  Matrix properties
ROCKTYPE 2 COPY 1
CPOR 1e-5
HLOSSPROP OVERBUR 35 24
       UNDERBUR 35 24

thtype matrix con 2

rockcp 34
thconr 254
thconw 8.32
thcono 1.49
thcong 2.78

*permck 2.5

**  ==============  OTHER RESERVOIR PROPERTIES
=======================

*END-GRID

*ROCKTYPE 1
*THTYPE MATRIX *con 1
*THTYPE FRACTURE CON 1
*CPOR  1E-06         **9.77789E-07 **formation compresibility 1/Psi
*CTPOR 0.0000021     **rock thermal expansion 1/F (3.8E-06 1/K)
*ROCKCP 34           **volumetric heat capacity Btu/cuft-F

*THCONR 41.48065061          **Reservoir thermal rock conductivity (Btu/ft-day-
F)
*THCONW 8.32016616       **Water thermal conductivity
*THCONG 2.7733887        **Gas thermal conductivity

*HLOSSPROP *OVERBUR 35 24      **Volumetric heat capacity (Btu/cuft-F)
Thermal conductivity (Btu/ft-day-F)
        *UNDERBUR 35 24     **Default values


**  ==============  FLUID DEFINITIONS  =====================

**component types  w+g+s  w+g  w  w
**             -----  ---  --  --
```

```
*MODEL              6   3   2   1
**solids : CaCO3 + Ca(HCO3)2 + NaCl

*COMPNAME 'WATER'   'OIL'  'CO2'  'CaCO3'  'Ca(HCO3)'  'NaCl'
**        -------   ---    ------  -----    ------      ------
*KV1       0         0 **1.7202E+6           **Gas-Liquid K value correlation coeffs
*KV2       0         0         **1 to numx(w)
*KV3       0         0
*KV4       1         0 **-6869.59
*KV5       0         0 **-376.64

**COMPNAME 'WATER' 'OIL'  'CO2'  'CaCO3'  'Ca(HCO3)'  'NaCl'
**        -------  ---   ------  -----    ------      ------
*CMM       18.016   180    44.010 100.0911 162.1171    58.4428  **Molecular weight
(lb/lbmol) [1 to ncomp]
*TCRIT     705.47  1216.94 87.89                        **Critical Temperature (F) [1
to numy]
*PCRIT     3198    2645.49     1070.38                    **Critical Pressure (psi)  [1
to numy]

*PRSR 14.7       **Reference pressure (psi) for density
*TEMR 77         **Reference temperature (F)[25 C] for T-dependent and thermal
properties
*PSURF 14.7      **Pressure @surface conditions (psi)
*TSURF 68        **Temperature @surface conditions (F)[20 C]



**COMPNAME 'WATER'  'OIL'       'CO2'
**        -------  ----        ------
*CPG1     7.701      -1.89       4.728            **1st coeff of gas heat capacity
correlation (Btu/lbmol-F)
*CPG2     2.553E-4   0.1275      9.744E-3          ** 1 to numy
*CPG3     7.781E-7   -3.898E-5   4.130E-6
*CPG4    -0.1473E-9  4.631E-9    0.7025E-9
*HVR      1657            991            **1st coeff of vaporization enthalpy correlation
(Btu/lbmol-F)

**EV Default value is used
**Default liquid heat capacities are used

*SOLID_DEN  'CaCO3'    169.2422011  0   0 **Density (lb/cuft)  Compressibility
(1/psi)  Thermal expansisivity (1/F) @reference temperature & pressure
*SOLID_DEN  'Ca(HCO3)'  132.015784   0   0
```

```
*SOLID_DEN  'NaCl'      136         0   0
*SOLID_DEN  'CO2'       118.551     0   0

**COMPNAME 'WATER'     'OIL'
**         -------
*MASSDEN  63.61409183  54.6     **lb/cuft [1 to numx]

*GASD-ZCOEF *IMPLICIT


**COMPNAME 'WATER'   'OIL'
**         -------
*AVISC   0.0047352  0.0115577    **coeff of viscosity calculation (cp) [1 to numx]
*BVISC   2728.2     2315.2       **(F)

*XNACL    0.10         **brine concentration (mass fraction of salt)

**Reaction CO2+H2O+CaCO3-->Ca(HCO3)2

**COMPNAME 'WATER' 'OIL' 'CO2' 'CaCO3' 'Ca(HCO3)' 'NaCl'
**         -------  ---  ------ -----    ------   ------
*STOREAC     1      0      1     1        0         0
*STOPROD     0      0      0     0        1         0
*RPHASE      1      0     3     4        4         4
*RORDER      1      0     1     0        1         1

*FREQFAC 5  **3500        **reaction frequency factor (1/min)
*EACT    0           **activation energy (Btu/lbmol)
*RENTH   0           **reaction enthalpy (Btu/lbmol)

**PERMSCALE        **Permeability        Scaling factor      Rate
                 **EFFPT                FREQT               Constant
                 **(md)                                     (1/min)
                  **90                  2.000               **
                  **120                 1.000               **
                  **200                 0.675               **
                  **400                 0.200               **
                  **800                 0.100               **
                  **2000                0.075               **

**Reaction Ca(HCO3)2-->CO2+H2O+CaCO3

**COMPNAME 'WATER' 'OIL' 'CO2' 'CaCO3' 'Ca(HCO3)' 'NaCl'
**         -------  ----  ------ -----    ------   ------
```

```
*STOREAC     0     0     0     0     1        0
*STOPROD     1     0     1     1     0        0
*RPHASE      1     0     3     4     4        4     **1->liquid 4->solid
*RORDER      1     0     1     1     1        1       **reaction & concentration
dependence

*FREQFAC 0  **550        **reaction frequency factor (1/min)
*EACT    0          **activation energy (Btu/lbmol)
*RENTH   0          **reaction enthalpy (Btu/lbmol)
*O2CONC

**PERMSCALE       **Permeability        Scaling factor      Rate
              **EFFPT              FREQT             Constant
              **(md)                                 (1/min)
                **90               2.000             **
                **120              1.000             **
                **200              0.675             **
                **400              0.200             **
                **800              0.100             **
                **1000             0.075              **



**  ==============  ROCK-FLUID PROPERTIES
======================

*ROCKFLUID
*RPT 1 *STONE2 *WATWET     **default
*KRTYPE MATRIX *CON 1            **default
*KRTYPE FRACTURE *CON 1

*SWT   **  Water-oil relative permeabilities

**       Sw      Krw       Krow
**      -----    ------   ------
          0.300000 0.000000 0.490000
          0.350000 0.000001 0.422500
          0.400000 0.000016 0.360000
          0.450000 0.000116 0.302500
          0.500000 0.000481 0.250000
          0.550000 0.001463 0.202500
          0.600000 0.003671 0.160000
          0.650000 0.008101 0.122500
```

```
          0.700000 0.016341 0.090000
          0.750000 0.030934 0.062500
          0.800000 0.056086 0.040000
          0.850000 0.099257 0.022500
          0.900000 0.175474 0.010000
          0.950000 0.324355 0.002500
          1.000000 1.000000 0.000000


*SLT   **  Liquid-gas relative permeabilities

**      Sl       Krg          Krog          Pcog(psi)
**    -----    ------        ------        ------
          0.30 0.02618252723 0.00000000 **300.4194910
          0.35 0.01590044522 0.00000054 **290.3470123
          0.40 0.00939117745 0.00001593 **270.8099503
          0.45 0.00534448235 0.00011634 **260.6195202
          0.50 0.00289843166 0.00048123 **250.6648570
          0.55 0.00147693480 0.00146270 **240.8765181
          0.60 0.00069373574 0.00367093 **240.2085954
          0.65 0.00029223596 0.00810145 **230.6292027
          0.70 0.00010585125 0.01634141 **230.1150163
          0.75 0.00003073591 0.03093357 **220.6478342
          0.80 0.00000627673 0.05608634 **220.2120140
          0.85 0.00000067232 0.09925704 **210.7917975
          0.90 0.00000001483 0.17547384 **210.3665181
          0.95 0.00000000000 0.32435518 **200.8943675
        1.00 0.00000000000 0.49000000 **200



**DIFFI_GAS 'CO2' *CON  1.21E-03  **sqft/day
**DIFFJ_GAS 'CO2' *EQUALSI
**DIFFK_GAS 'CO2' *EQUALSI


**ADSCOMP 'CO2' 'GAS'       **adsorpted component
**ADSLANG 5.41 0 2.1        **Langmuir isotherm coefficients
**ADSROCK 1
**adsoption rock type
**ADMAXT 2.56E-6            **maximum adsoption capacity
**ADRT 0                   **completely reversible adsoption
**ADSPHBLK 'ALL'            **resistance factor is calculated for all phase
**PORFT 1                  **all pore volume is accessible
```

```
**RRFT 2.5                **no residual resistance effect


** ============== INITIAL CONDITIONS ======================
*INITIAL
*VERTICAL *DEPTH_AVE          **perform depth-averaged capillary-gravity
vertical equilibrium calculation
*REFDEPTH  3050              **reference depth within the reservoir (ft)
*REFPRES   1348              **pressure @reference depth (psi)
**TRANZONE                   **transition zone for water-gas system by using water
oil capillary pressure curve

**DWOC 2000
**DGOC 2000

**Pressure gradient (psi/ft)=0.442075025
**Geothermal gradient (F/100 ft)=2.2

**PRES  *con 1348.                **initial reservoir pressure (psi)
*TEMP MATRIX  *con 127.            **initial reservoir temperature (F)
*TEMP FRACTURE *CON 127.

**Override vertical equilibrium saturations
**SW *CON 1          **initial water saturation
**SO *CON 0          **initial oil saturation
**SG *CON 0          **initial gas saturation

*CONC_SLD  'CaCO3' MATRIX       *CON   0.0      **0.311855699  **initial
concentration (lbmol/cuft)  [0.1 g/cucm]
*CONC_SLD  'Ca(HCO3)'MATRIX     *CON   0.0
*CONC_SLD  'NaCl'  MATRIX       *CON   0.0      **0.534094533
**CONC_SLD 'CO2' MATRIX        *CON   0.0
*CONC_SLD  'CaCO3'  FRACTURE    *CON   0.0      **0.311855699  **initial
concentration (lbmol/cuft)  [0.1 g/cucm]
*CONC_SLD   'Ca(HCO3)' FRACTURE   *CON   0.0
*CONC_SLD  'NaCl'   FRACTURE     *CON   0.0      **0.534094533
**CONC_SLD  'CO2'  FRACTURE      *CON   0.0

** ============== NUMERICAL CONTROL ======================


*NUMERICAL     ** All these can be defaulted.
MAXSTEPS 1000000
```

```
TFORM SXY
**TFORM *SXY   **standart use of primary variables
**CONVERGE *TOTRES *TIGHT
**NEWTONCYC 30   **maximum number of newton iteration in a timestep
**UNRELAX 1
**UPSTREAM *KLEVEL
**PRECC 1
**NORTH 30
**SDEGREE *GAUSS
**use pivot stabilization
PIVOT ON
** max iteration number for Jacobian matrix solution
ITERMAX 50
AIM STAB
**AIM *STAB *BACK 5   **backward switching 5
**MINPRES 100        **min simulation pressure  psi
**MAXPRES 5000        **max simulation pressure  psi
**MINTEMP 60          **min simulation temperature F
**MAXTEMP 300         **max simulation temperature F
**PVTOSCMAX 5         **max number of phase switches
**MAXLAYPRE 3         **default value
**NCUT 20            **number of timestep size cut



**  ============== WELL & RECURRENT DATA
======================

*RUN
*TIME0
** Timestep size (days)
DTWELL 1
**
** ** WELL SPECIFICATION W1-------
** *WELL 1 'W1' *VERT 11 11   **Well location (i,j)
**$
WELL  'INJ1'
**COMPNAME 'WATER' 'CO2' 'CaCO3' 'Ca(HCO3)' 'NaCl'
**         ------- ------ -----    ------   ------
           **supercritic condition (F)
           **supercritic condition (psia)
                          **scf/day
                        **psia
```

```
                **CONT
INJECTOR MOBWEIGHT IMPLICIT 'INJ1'
INCOMP  GAS  0.  0.  1.
TINJW  127.
PINJW  1620.
OPERATE  MAX  STG  1e+006  CONT
OPERATE  MAX  BHP  2700.  CONT
MONITOR  MIN  STG  500.  SHUTIN
**          rad      geofac     wfrac      skin
**          (rw-ft)   (Appendix A)
** i   j   k     ff   status
**$         rad  geofac  wfrac  skin
GEOMETRY  K  0.375  0.249  1.  0.
PERF  GEO  'INJ1'
**$ UBA       ff  Status  Connection
   11 11 6   1.  OPEN    FLOW-FROM  'SURFACE'  REFLAYER
   11 11 7   1.  OPEN    FLOW-FROM  1
   11 11 8   1.  OPEN    FLOW-FROM  2
   11 11 9   1.  OPEN    FLOW-FROM  3
   11 11 10  1.  OPEN    FLOW-FROM  4
   11 11 5   1.  OPEN    FLOW-FROM  5
   11 11 4   1.  OPEN    FLOW-FROM  6
   11 11 3   1.  OPEN    FLOW-FROM  7
   11 11 2   1.  OPEN    FLOW-FROM  8
   11 11 1   1.  OPEN    FLOW-FROM  9
**$
WELL  'Well-2'
PRODUCER 'Well-2'
OPERATE  MAX  STO  50.  CONT
**$         rad  geofac  wfrac  skin
GEOMETRY  K  0.28  0.249  1.  0.
PERF  GEO  'Well-2'
**$ UBA     ff  Status  Connection
   1 1 1   1.  OPEN    FLOW-TO  'SURFACE'  REFLAYER
   1 1 2   1.  OPEN    FLOW-TO  1
   1 1 3   1.  OPEN    FLOW-TO  2
   1 1 4   1.  OPEN    FLOW-TO  3
   1 1 5   1.  OPEN    FLOW-TO  4
   1 1 6   1.  OPEN    FLOW-TO  5
   1 1 7   1.  OPEN    FLOW-TO  6
   1 1 8   1.  OPEN    FLOW-TO  7
   1 1 9   1.  OPEN    FLOW-TO  8
   1 1 10  1.  OPEN    FLOW-TO  9
**$
```

```
WELL  'Well-3'
PRODUCER 'Well-3'
OPERATE  MAX  STO  50.  CONT
**$         rad  geofac  wfrac  skin
GEOMETRY  K  0.28  0.249  1.  0.
PERF  GEO  'Well-3'
**$ UBA       ff  Status  Connection
   20 20 1   1.  OPEN    FLOW-TO  'SURFACE'  REFLAYER
   20 20 2   1.  OPEN    FLOW-TO  1
   20 20 3   1.  OPEN    FLOW-TO  2
   20 20 4   1.  OPEN    FLOW-TO  3
   20 20 5   1.  OPEN    FLOW-TO  4
   20 20 6   1.  OPEN    FLOW-TO  5
   20 20 7   1.  OPEN    FLOW-TO  6
   20 20 8   1.  OPEN    FLOW-TO  7
   20 20 9   1.  OPEN    FLOW-TO  8
   20 20 10  1.  OPEN    FLOW-TO  9
time     10800
SHUTIN 'Well-2'
SHUTIN 'Well-3'
```

time	10800.000002	time	10800.03602	time	10800.08002
time	10800.000004	time	10800.03702	time	10800.08102
time	10800.000008	time	10800.03802	time	10800.08202
time	10800.000016	time	10800.03902	time	10800.08302
time	10800.000032	time	10800.04002	time	10800.08402
time	10800.000064	time	10800.04102	time	10800.08502
time	10800.000128	time	10800.04202	time	10800.08602
time	10800.000256	time	10800.04302	time	10800.08702
time	10800.000512	time	10800.04402	time	10800.08802
time	10800.001024	time	10800.04502	time	10800.08902
time	10800.00202	time	10800.04602	time	10800.09002
time	10800.00302	time	10800.04702	time	10800.09102
time	10800.00402	time	10800.04802	time	10800.09202
time	10800.00502	time	10800.04902	time	10800.09302
time	10800.00602	time	10800.05002	time	10800.09402
time	10800.00702	time	10800.05102	time	10800.09502
time	10800.00802	time	10800.05202	time	10800.09602
time	10800.00902	time	10800.05302	time	10800.09702
time	10800.01002	time	10800.05402	time	10800.09802
time	10800.01102	time	10800.05502	time	10800.09902
time	10800.01202	time	10800.05602	time	10800.10002
time	10800.01302	time	10800.05702	time	10800.10102
time	10800.01402	time	10800.05802	time	10800.10202
time	10800.01502	time	10800.05902	time	10800.10302
time	10800.01602	time	10800.06002	time	10800.10402
time	10800.01702	time	10800.06102	time	10800.10502
time	10800.01802	time	10800.06202	time	10800.10602
time	10800.01902	time	10800.06302	time	10800.10702
time	10800.02002	time	10800.06402	time	10800.10802
time	10800.02102	time	10800.06502	time	10800.10902
time	10800.02202	time	10800.06602	time	10800.11002
time	10800.02302	time	10800.06702	time	10800.11102
time	10800.02402	time	10800.06802	time	10800.11202
time	10800.02502	time	10800.06902	time	10800.11302
time	10800.02602	time	10800.07002	time	10800.11402
time	10800.02702	time	10800.07102	time	10800.11502
time	10800.02802	time	10800.07202	time	10800.11602
time	10800.02902	time	10800.07302	time	10800.11702
time	10800.03002	time	10800.07402	time	10800.11802
time	10800.03102	time	10800.07502	time	10800.11902
time	10800.03202	time	10800.07602	time	10800.12002
time	10800.03302	time	10800.07702	time	10800.12102
time	10800.03402	time	10800.07802	time	10800.12202
time	10800.03502	time	10800.07902	time	10800.12302

time	10800.12402	time	10800.16802	time	10800.21202
time	10800.12502	time	10800.16902	time	10800.21302
time	10800.12602	time	10800.17002	time	10800.21402
time	10800.12702	time	10800.17102	time	10800.21502
time	10800.12802	time	10800.17202	time	10800.21602
time	10800.12902	time	10800.17302	time	10800.21702
time	10800.13002	time	10800.17402	time	10800.21802
time	10800.13102	time	10800.17502	time	10800.21902
time	10800.13202	time	10800.17602	time	10800.22002
time	10800.13302	time	10800.17702	time	10800.22102
time	10800.13402	time	10800.17802	time	10800.22202
time	10800.13502	time	10800.17902	time	10800.22302
time	10800.13602	time	10800.18002	time	10800.22402
time	10800.13702	time	10800.18102	time	10800.22502
time	10800.13802	time	10800.18202	time	10800.22602
time	10800.13902	time	10800.18302	time	10800.22702
time	10800.14002	time	10800.18402	time	10800.22802
time	10800.14102	time	10800.18502	time	10800.22902
time	10800.14202	time	10800.18602	time	10800.23002
time	10800.14302	time	10800.18702	time	10800.23102
time	10800.14402	time	10800.18802	time	10800.23202
time	10800.14502	time	10800.18902	time	10800.23302
time	10800.14602	time	10800.19002	time	10800.23402
time	10800.14702	time	10800.19102	time	10800.23502
time	10800.14802	time	10800.19202	time	10800.23602
time	10800.14902	time	10800.19302	time	10800.23702
time	10800.15002	time	10800.19402	time	10800.23802
time	10800.15102	time	10800.19502	time	10800.23902
time	10800.15202	time	10800.19602	time	10800.24002
time	10800.15302	time	10800.19702	time	10800.24102
time	10800.15402	time	10800.19802	time	10800.24202
time	10800.15502	time	10800.19902	time	10800.24302
time	10800.15602	time	10800.20002	time	10800.24402
time	10800.15702	time	10800.20102	time	10800.24502
time	10800.15802	time	10800.20202	time	10800.24602
time	10800.15902	time	10800.20302	time	10800.24702
time	10800.16002	time	10800.20402	time	10800.24802
time	10800.16102	time	10800.20502	time	10800.24902
time	10800.16202	time	10800.20602	time	10800.25002
time	10800.16302	time	10800.20702	time	10800.25102
time	10800.16402	time	10800.20802	time	10800.25202
time	10800.16502	time	10800.20902	time	10800.25302
time	10800.16602	time	10800.21002	time	10800.25402
time	10800.16702	time	10800.21102	time	10800.25502

time	10800.25602	time	10800.30002	time	10800.34402
time	10800.25702	time	10800.30102	time	10800.34502
time	10800.25802	time	10800.30202	time	10800.34602
time	10800.25902	time	10800.30302	time	10800.34702
time	10800.26002	time	10800.30402	time	10800.34802
time	10800.26102	time	10800.30502	time	10800.34902
time	10800.26202	time	10800.30602	time	10800.35002
time	10800.26302	time	10800.30702	time	10800.35102
time	10800.26402	time	10800.30802	time	10800.35202
time	10800.26502	time	10800.30902	time	10800.35302
time	10800.26602	time	10800.31002	time	10800.35402
time	10800.26702	time	10800.31102	time	10800.35502
time	10800.26802	time	10800.31202	time	10800.35602
time	10800.26902	time	10800.31302	time	10800.35702
time	10800.27002	time	10800.31402	time	10800.35802
time	10800.27102	time	10800.31502	time	10800.35902
time	10800.27202	time	10800.31602	time	10800.36002
time	10800.27302	time	10800.31702	time	10800.36102
time	10800.27402	time	10800.31802	time	10800.36202
time	10800.27502	time	10800.31902	time	10800.36302
time	10800.27602	time	10800.32002	time	10800.36402
time	10800.27702	time	10800.32102	time	10800.36502
time	10800.27802	time	10800.32202	time	10800.36602
time	10800.27902	time	10800.32302	time	10800.36702
time	10800.28002	time	10800.32402	time	10800.36802
time	10800.28102	time	10800.32502	time	10800.36902
time	10800.28202	time	10800.32602	time	10800.37002
time	10800.28302	time	10800.32702	time	10800.37102
time	10800.28402	time	10800.32802	time	10800.37202
time	10800.28502	time	10800.32902	time	10800.37302
time	10800.28602	time	10800.33002	time	10800.37402
time	10800.28702	time	10800.33102	time	10800.37502
time	10800.28802	time	10800.33202	time	10800.37602
time	10800.28902	time	10800.33302	time	10800.37702
time	10800.29002	time	10800.33402	time	10800.37802
time	10800.29102	time	10800.33502	time	10800.37902
time	10800.29202	time	10800.33602	time	10800.38002
time	10800.29302	time	10800.33702	time	10800.38102
time	10800.29402	time	10800.33802	time	10800.38202
time	10800.29502	time	10800.33902	time	10800.38302
time	10800.29602	time	10800.34002	time	10800.38402
time	10800.29702	time	10800.34102	time	10800.38502
time	10800.29802	time	10800.34202	time	10800.38602
time	10800.29902	time	10800.34302	time	10800.38702

time 10800.38802
time 10800.38902
time 10800.39002
time 10800.39102
time 10800.39202
time 10800.39302
time 10800.39402
time 10800.39502
time 10800.39602
time 10800.39702
time 10800.39802
time 10800.39902
time 10800.40002
time 10800.40102
time 10800.40202
time 10800.40302
time 10800.40402
time 10800.40502
time 10800.40602
time 10800.40702
time 10800.40802
time 10800.40902
time 10800.41002
time 10800.41102
time 10800.41202
time 10800.41302
time 10800.41402
time 10800.41502
time 10800.41602
time 10800.41702
time 10800.41802
time 10800.41902
time 10800.42002
time 10800.42102
time 10800.42202
time 10800.42302
time 10800.42402
time 10800.42502
time 10800.42602
time 10800.42702
time 10800.42802
time 10800.42902
time 10800.43002
time 10800.43102
time 10800.43202
time 10800.43302
time 10800.43402
time 10800.43502
time 10800.43602
time 10800.43702
time 10800.43802
time 10800.43902
time 10800.44002
time 10800.44102
time 10800.44202
time 10800.44302
time 10800.44402
time 10800.44502
time 10800.44602
time 10800.44702
time 10800.44802
time 10800.44902
time 10800.45002
time 10800.45102
time 10800.45202
time 10800.45302
time 10800.45402
time 10800.45502
time 10800.45602
time 10800.45702
time 10800.45802
time 10800.45902
time 10800.46002
time 10800.46102
time 10800.46202
time 10800.46302
time 10800.46402
time 10800.46502
time 10800.46602
time 10800.46702
time 10800.46802
time 10800.46902
time 10800.47002
time 10800.47102
time 10800.47202
time 10800.47302
time 10800.47402
time 10800.47502
time 10800.47602
time 10800.47702
time 10800.47802
time 10800.47902
time 10800.48002
time 10800.48102
time 10800.48202
time 10800.48302
time 10800.48402
time 10800.48502
time 10800.48602
time 10800.48702
time 10800.48802
time 10800.48902
time 10800.49002
time 10800.49102
time 10800.49202
time 10800.49302
time 10800.49402
time 10800.49502
time 10800.49602
time 10800.49702
time 10800.49802
time 10800.49902
time 10800.50002
time 10800.50102
time 10800.50202
time 10800.50302
time 10800.50402
time 10800.50502
time 10800.50602
time 10800.50702
time 10800.50802
time 10800.50902
time 10800.51002
time 10800.51102
time 10800.51202
time 10800.51302
time 10800.51402
time 10800.51502
time 10800.51602
time 10800.51702
time 10800.51802
time 10800.51902

time	10800.52002	time	10800.56402	time	10800.60802
time	10800.52102	time	10800.56502	time	10800.60902
time	10800.52202	time	10800.56602	time	10800.61002
time	10800.52302	time	10800.56702	time	10800.61102
time	10800.52402	time	10800.56802	time	10800.61202
time	10800.52502	time	10800.56902	time	10800.61302
time	10800.52602	time	10800.57002	time	10800.61402
time	10800.52702	time	10800.57102	time	10800.61502
time	10800.52802	time	10800.57202	time	10800.61602
time	10800.52902	time	10800.57302	time	10800.61702
time	10800.53002	time	10800.57402	time	10800.61802
time	10800.53102	time	10800.57502	time	10800.61902
time	10800.53202	time	10800.57602	time	10800.62002
time	10800.53302	time	10800.57702	time	10800.62102
time	10800.53402	time	10800.57802	time	10800.62202
time	10800.53502	time	10800.57902	time	10800.62302
time	10800.53602	time	10800.58002	time	10800.62402
time	10800.53702	time	10800.58102	time	10800.62502
time	10800.53802	time	10800.58202	time	10800.62602
time	10800.53902	time	10800.58302	time	10800.62702
time	10800.54002	time	10800.58402	time	10800.62802
time	10800.54102	time	10800.58502	time	10800.62902
time	10800.54202	time	10800.58602	time	10800.63002
time	10800.54302	time	10800.58702	time	10800.63102
time	10800.54402	time	10800.58802	time	10800.63202
time	10800.54502	time	10800.58902	time	10800.63302
time	10800.54602	time	10800.59002	time	10800.63402
time	10800.54702	time	10800.59102	time	10800.63502
time	10800.54802	time	10800.59202	time	10800.63602
time	10800.54902	time	10800.59302	time	10800.63702
time	10800.55002	time	10800.59402	time	10800.63802
time	10800.55102	time	10800.59502	time	10800.63902
time	10800.55202	time	10800.59602	time	10800.64002
time	10800.55302	time	10800.59702	time	10800.64102
time	10800.55402	time	10800.59802	time	10800.64202
time	10800.55502	time	10800.59902	time	10800.64302
time	10800.55602	time	10800.60002	time	10800.64402
time	10800.55702	time	10800.60102	time	10800.64502
time	10800.55802	time	10800.60202	time	10800.64602
time	10800.55902	time	10800.60302	time	10800.64702
time	10800.56002	time	10800.60402	time	10800.64802
time	10800.56102	time	10800.60502	time	10800.64902
time	10800.56202	time	10800.60602	time	10800.65002
time	10800.56302	time	10800.60702	time	10800.65102

time	10800.65202	time	10800.69602	time	10800.74002
time	10800.65302	time	10800.69702	time	10800.74102
time	10800.65402	time	10800.69802	time	10800.74202
time	10800.65502	time	10800.69902	time	10800.74302
time	10800.65602	time	10800.70002	time	10800.74402
time	10800.65702	time	10800.70102	time	10800.74502
time	10800.65802	time	10800.70202	time	10800.74602
time	10800.65902	time	10800.70302	time	10800.74702
time	10800.66002	time	10800.70402	time	10800.74802
time	10800.66102	time	10800.70502	time	10800.74902
time	10800.66202	time	10800.70602	time	10800.75002
time	10800.66302	time	10800.70702	time	10800.75102
time	10800.66402	time	10800.70802	time	10800.75202
time	10800.66502	time	10800.70902	time	10800.75302
time	10800.66602	time	10800.71002	time	10800.75402
time	10800.66702	time	10800.71102	time	10800.75502
time	10800.66802	time	10800.71202	time	10800.75602
time	10800.66902	time	10800.71302	time	10800.75702
time	10800.67002	time	10800.71402	time	10800.75802
time	10800.67102	time	10800.71502	time	10800.75902
time	10800.67202	time	10800.71602	time	10800.76002
time	10800.67302	time	10800.71702	time	10800.76102
time	10800.67402	time	10800.71802	time	10800.76202
time	10800.67502	time	10800.71902	time	10800.76302
time	10800.67602	time	10800.72002	time	10800.76402
time	10800.67702	time	10800.72102	time	10800.76502
time	10800.67802	time	10800.72202	time	10800.76602
time	10800.67902	time	10800.72302	time	10800.76702
time	10800.68002	time	10800.72402	time	10800.76802
time	10800.68102	time	10800.72502	time	10800.76902
time	10800.68202	time	10800.72602	time	10800.77002
time	10800.68302	time	10800.72702	time	10800.77102
time	10800.68402	time	10800.72802	time	10800.77202
time	10800.68502	time	10800.72902	time	10800.77302
time	10800.68602	time	10800.73002	time	10800.77402
time	10800.68702	time	10800.73102	time	10800.77502
time	10800.68802	time	10800.73202	time	10800.77602
time	10800.68902	time	10800.73302	time	10800.77702
time	10800.69002	time	10800.73402	time	10800.77802
time	10800.69102	time	10800.73502	time	10800.77902
time	10800.69202	time	10800.73602	time	10800.78002
time	10800.69302	time	10800.73702	time	10800.78102
time	10800.69402	time	10800.73802	time	10800.78202
time	10800.69502	time	10800.73902	time	10800.78302

time 10800.78402
time 10800.78502
time 10800.78602
time 10800.78702
time 10800.78802
time 10800.78902
time 10800.79002
time 10800.79102
time 10800.79202
time 10800.79302
time 10800.79402
time 10800.79502
time 10800.79602
time 10800.79702
time 10800.79802
time 10800.79902
time 10800.80002
time 10800.80102
time 10800.80202
time 10800.80302
time 10800.80402
time 10800.80502
time 10800.80602
time 10800.80702
time 10800.80802
time 10800.80902
time 10800.81002
time 10800.81102
time 10800.81202
time 10800.81302
time 10800.81402
time 10800.81502
time 10800.81602
time 10800.81702
time 10800.81802
time 10800.81902
time 10800.82002
time 10800.82102
time 10800.82202
time 10800.82302
time 10800.82402
time 10800.82502
time 10800.82602
time 10800.82702
time 10800.82802
time 10800.82902
time 10800.83002
time 10800.83102
time 10800.83202
time 10800.83302
time 10800.83402
time 10800.83502
time 10800.83602
time 10800.83702
time 10800.83802
time 10800.83902
time 10800.84002
time 10800.84102
time 10800.84202
time 10800.84302
time 10800.84402
time 10800.84502
time 10800.84602
time 10800.84702
time 10800.84802
time 10800.84902
time 10800.85002
time 10800.85102
time 10800.85202
time 10800.85302
time 10800.85402
time 10800.85502
time 10800.85602
time 10800.85702
time 10800.85802
time 10800.85902
time 10800.86002
time 10800.86102
time 10800.86202
time 10800.86302
time 10800.86402
time 10800.86502
time 10800.86602
time 10800.86702
time 10800.86802
time 10800.86902
time 10800.87002
time 10800.87102
time 10800.87202
time 10800.87302
time 10800.87402
time 10800.87502
time 10800.87602
time 10800.87702
time 10800.87802
time 10800.87902
time 10800.88002
time 10800.88102
time 10800.88202
time 10800.88302
time 10800.88402
time 10800.88502
time 10800.88602
time 10800.88702
time 10800.88802
time 10800.88902
time 10800.89002
time 10800.89102
time 10800.89202
time 10800.89302
time 10800.89402
time 10800.89502
time 10800.89602
time 10800.89702
time 10800.89802
time 10800.89902
time 10800.90002
time 10800.90102
time 10800.90202
time 10800.90302
time 10800.90402
time 10800.90502
time 10800.90602
time 10800.90702
time 10800.90802
time 10800.90902
time 10800.91002
time 10800.91102
time 10800.91202
time 10800.91302
time 10800.91402
time 10800.91502

time 10800.91602
time 10800.91702
time 10800.91802
time 10800.91902
time 10800.92002
time 10800.92102
time 10800.92202
time 10800.92302
time 10800.92402
time 10800.92502
time 10800.92602
time 10800.92702
time 10800.92802
time 10800.92902
time 10800.93002
time 10800.93102
time 10800.93202
time 10800.93302
time 10800.93402
time 10800.93502
time 10800.93602
time 10800.93702
time 10800.93802
time 10800.93902
time 10800.94002
time 10800.94102
time 10800.94202
time 10800.94302
time 10800.94402
time 10800.94502
time 10800.94602
time 10800.94702
time 10800.94802
time 10800.94902
time 10800.95002
time 10800.95102
time 10800.95202
time 10800.95302
time 10800.95402
time 10800.95502
time 10800.95602
time 10800.95702
time 10800.95802
time 10800.95902
time 10800.96002
time 10800.96102
time 10800.96202
time 10800.96302
time 10800.96402
time 10800.96502
time 10800.96602
time 10800.96702
time 10800.96802
time 10800.96902
time 10800.97002
time 10800.97102
time 10800.97202
time 10800.97302
time 10800.97402
time 10800.97502
time 10800.97602
time 10800.97702
time 10800.97802
time 10800.97902
time 10800.98002
time 10800.98102
time 10800.98202
time 10800.98302
time 10800.98402
time 10800.98502
time 10800.98602
time 10800.98702
time 10800.98802
time 10800.98902
time 10800.99002
time 10800.99102
time 10800.99202
time 10800.99302
time 10800.99402
time 10800.99502
time 10800.99602
time 10800.99702
time 10800.99802
time 10800.99902
time 10801
time 10801.01
time 10801.02
time 10801.03
time 10801.04
time 10801.05
time 10801.06
time 10801.07
time 10801.08
time 10801.09
time 10801.1
time 10801.11
time 10801.12
time 10801.13
time 10801.14
time 10801.15
time 10801.16
time 10801.17
time 10801.18
time 10801.19
time 10801.2
time 10801.21
time 10801.22
time 10801.23
time 10801.24
time 10801.25
time 10801.26
time 10801.27
time 10801.28
time 10801.29
time 10801.3
time 10801.31
time 10801.32
time 10801.33
time 10801.34
time 10801.35
time 10801.36
time 10801.37
time 10801.38
time 10801.39
time 10801.4
time 10801.41
time 10801.42
time 10801.43
time 10801.44
time 10801.45
time 10801.46
time 10801.47

time 10801.48
time 10801.49
time 10801.5
time 10801.51
time 10801.52
time 10801.53
time 10801.54
time 10801.55
time 10801.56
time 10801.57
time 10801.58
time 10801.59
time 10801.6
time 10801.61
time 10801.62
time 10801.63
time 10801.64
time 10801.65
time 10801.66
time 10801.67
time 10801.68
time 10801.69
time 10801.7
time 10801.71
time 10801.72
time 10801.73
time 10801.74
time 10801.75
time 10801.76
time 10801.77
time 10801.78
time 10801.79
time 10801.8
time 10801.81
time 10801.82
time 10801.83
time 10801.84
time 10801.85
time 10801.86
time 10801.87
time 10801.88
time 10801.89
time 10801.9
time 10801.91
time 10801.92
time 10801.93
time 10801.94
time 10801.95
time 10801.96
time 10801.97
time 10801.98
time 10801.99
time 10802
time 10802.01
time 10802.02
time 10802.03
time 10802.04
time 10802.05
time 10802.06
time 10802.07
time 10802.08
time 10802.09
time 10802.1
time 10802.11
time 10802.12
time 10802.13
time 10802.14
time 10802.15
time 10802.16
time 10802.17
time 10802.18
time 10802.19
time 10802.2
time 10802.21
time 10802.22
time 10802.23
time 10802.24
time 10802.25
time 10802.26
time 10802.27
time 10802.28
time 10802.29
time 10802.3
time 10802.31
time 10802.32
time 10802.33
time 10802.34
time 10802.35
time 10802.36
time 10802.37
time 10802.38
time 10802.39
time 10802.4
time 10802.41
time 10802.42
time 10802.43
time 10802.44
time 10802.45
time 10802.46
time 10802.47
time 10802.48
time 10802.49
time 10802.5
time 10802.51
time 10802.52
time 10802.53
time 10802.54
time 10802.55
time 10802.56
time 10802.57
time 10802.58
time 10802.59
time 10802.6
time 10802.61
time 10802.62
time 10802.63
time 10802.64
time 10802.65
time 10802.66
time 10802.67
time 10802.68
time 10802.69
time 10802.7
time 10802.71
time 10802.72
time 10802.73
time 10802.74
time 10802.75
time 10802.76
time 10802.77
time 10802.78
time 10802.79

time 10802.8
time 10802.81
time 10802.82
time 10802.83
time 10802.84
time 10802.85
time 10802.86
time 10802.87
time 10802.88
time 10802.89
time 10802.9
time 10802.91
time 10802.92
time 10802.93
time 10802.94
time 10802.95
time 10802.96
time 10802.97
time 10802.98
time 10802.99
time 10803
time 10803.25
time 10803.5
time 10803.75
time 10804
time 10804.25
time 10804.5
time 10804.75
time 10805
time 10805.25
time 10805.5
time 10805.75
time 10806
time 10806.25
time 10806.5
time 10806.75
time 10807
time 10807.25
time 10807.5
time 10807.75
time 10808
time 10808.25
time 10808.5
time 10808.75
time 10809
time 10809.25
time 10809.5
time 10809.75
time 10810
time 10810.25
time 10810.5
time 10810.75
time 10811
time 10811.25
time 10811.5
time 10811.75
time 10812
time 10812.25
time 10812.5
time 10812.75
time 10813
time 10813.25
time 10813.5
time 10813.75
time 10814
time 10814.25
time 10814.5
time 10814.75
time 10815
time 10815.25
time 10815.5
time 10815.75
time 10816
time 10816.25
time 10816.5
time 10816.75
time 10817
time 10817.25
time 10817.5
time 10817.75
time 10818
time 10818.25
time 10818.5
time 10818.75
time 10819
time 10819.25
time 10819.5
time 10819.75
time 10820